The Dissertation Committee for Arley Frances Muth Certifies that this is the approved version of the following Dissertation:

Salinity and pH variations in the nearshore Arctic Ocean: Implications for benthic species physiology and biodiversity

Committee:

Kenneth H. Dunton, Supervisor

Amber Hardison

Amanda Kelley

James McClelland

Andrew Esbaugh

Salinity and pH variations in the nearshore Arctic Ocean: Implications for benthic species physiology and biodiversity

By

Arley Frances Muth

Dissertation

Presented to the Faculty of the Graduate School of The University of Texas at Austin
in Partial Fulfillment
of the Requirements
for the Degree of

Doctor of Philosophy

The University of Texas at Austin

August 2020

Abstract

Salinity and pH variations in the nearshore Arctic Ocean: Implications for benthic species physiology and biodiversity

Arley Frances Muth Ph.D.

The University of Texas at Austin, 2020

Supervisor: Kenneth H. Dunton

Benthic communities are formed by species-specific tolerances to environmental factors and further shaped by biological interactions that inhibit or enhance post-settlement processes. Abiotic conditions affect species differently, and one example of this in the marine world is the influence of ocean water carbonate chemistry on calcifying organisms. Crustose coralline algae (CCA) are dominant space occupiers, ecosystem engineers that often shape community structure are early responders to water chemistry changes, and are prevalent benthic species in the Stefansson Sound Boulder Patch. The Boulder Patch is located off the north coast of Alaska and receives large pulses of freshwater each spring from the Sagavanirktok River, reducing salinities to less than five on the benthos in certain locations. Continuous pH, temperature and salinity data (including under-ice data) revealed seasonal variability and the influence of the Sagavanirktok River runoff, which caused short (3-5 week) pulses of highly buffered pH (>8), low A_T (<1900 μmEq L^{-1}) and low salinity (<5) waters into the Boulder Patch. Through manipulative laboratory experiments we noted that low salinity waters (10) negatively affected CCA physiology and likely drive their distributions within the Boulder Patch, which range from 77% cover to completely absent on rock substrata at nearshore sites where river runoff is prevalent during break-up in spring. Samples were collected and analyzed for algal and

invertebrate species and biomass when CCA were present and absent, with a specific focus on the effects on population densities of the Arctic endemic kelp, *Laminaria solidungula,* an important foundation species. Areas with CCA had significantly higher densities of *L. solidunugla* adults (4.72 m^{-2}) than the site without CCA (0.36 m^{-2}). Experiments with early life history stages of *L. solidungula* raised in culture showed that low salinities (10) prevented recruitment. However, during winter, when early microscopic stages are present in the Boulder Patch, salinity levels are consistently high (32). These results point to other post-recruitment processes affecting the distribution of *L. solidungula*. In our system, CCA outcompeted turf and fleshy algal and other invertebrate species, creating more habitable space for kelp recruitment. This competitive interaction facilitates *L. solidungula* recruitment and survival and highlights the importance of abiotic factors in structuring benthic marine communities. The role of CCA in facilitating recruitment of a major foundation species and its susceptibility to low salinity events is critical to our understanding of this complex benthic ecosystem.

Table of Contents

List of Tables

List of Figures

List of Supplementary Materials

Introduction

The Stefansson Sound Boulder Patch is a unique environment within the Beaufort Sea because of glacially deposited boulder and cobbles that create hard substrate. The boulders and cobbles harbor a biodiverse algal, invertebrate and fish community, different from the flora and fauna present in the sediments that dominate the benthos of much of Stefansson Sound. Through years of monitoring permanent sites within the Boulder Patch, specific patterns have been observed concerning species distributions. Inshore sites, closer in proximity to the mouth of the Sagavanirktok River, have reduced densities of the Arctic endemic kelp, *Laminaria solidungula*, are devoid of crustose coralline algae, but higher coverage and densities of the red algal species *Phycodrys rubens* and the branching bryozoan *Eucratea loricata* are seen when compared to off-shore sites. This body of work was designed to build on previous work that characterized the ecological importance of *Laminaria solidujgula*, species distributions within the Boulder Patch, and highly seasonal environmental variability of salinity, temperature and light. Through deployment of environmental sensors (namely pH sensors), observational and experimental field studies and laboratory experiments, we now have a better understanding of the role that pH, salinity and carbonate chemistry have in influencing benthic species and resultant biological interactions that further shape nearshore assemblages.

High-frequency pH time-series of the nearshore Arctic Ocean Reveals Pronounced Seasonality

High-frequency measurements of pH and associated carbonate chemistry parameters are critical for understanding annual and long-term climate variability affecting near-shore Arctic systems. Two years of continuous pH, salinity and temperature data from the central Beaufort Sea coast of Alaska in Stefansson Sound, revealed a strong seasonal effect. Instruments were

deployed in 4.5-6 m of water at two sites, one located within ~3.5 km of the Sagavanirktok River Delta, and the other, ~9 km seaward. At the innermost site, short-term pH variability in late spring and summer was attributed to freshwater inputs from Sagavanirktok River runoff. Interestingly, Sagavanirktok River water is highly buffered, increasing nearshore seawater pH during times of increased river flow (up to 8.66), despite experiencing extremely low salinity values during these periods (0.19). The pH values at the outer site were less affected by freshwater input, although biological (heterotrophy) and chemical (ice formation) processes dominated during the winter months, driving pH to 7.47 under stable salinity and temperature values during the 8-mo period of ice cover (~ 33 and -1.8 ºC). These long-term physicochemical measurements reveal the natural, but critical influence of river inputs on the pH of nearshore waters. This work established baseline pH data and allowed for the calculations of other carbonate chemistry parameters that affect calcifying species. Information gathered during these deployments was applied to two laboratory experiments, exploring physiological repercussions of the intense seasonality of pH and salinity in the near-shore Arctic.

*Physiological responses of an Arctic crustose coralline alga (*Leptophytum foecundum*) to variations of salinity*

Coralline algae are the world's most distributed algal group and can be found from tropical reefs, polar regions, and also extreme depths. Their calcium carbonate thallus makes them susceptible to ocean acidification, which has recently increased interest in these species. Arctic crustose coralline algae (CCA) persist in an environment of high seasonal variability. In addition to anthropogenic seawater chemistry changes (ocean acidification), calcifying organisms in the Arctic face naturally low pH ocean water and high magnitude freshwater pulses in the spring. Data from 2016-2018 pH sensor deployments revealed interesting trends of higher

pH values during times of reduced salinity (ice "break-up" period). Also, previous work has documented the absence of CCA at the near-shore sites that are exposed to lower salinity from Sagavanirktok River runoff. The effects of salinity on the CCA *Leptophytum foecundum* were observed through a series of laboratory and field experiments in Stefansson Sound, Alaska. Laboratory experiments demonstrated through varying parameters (photosynthetic yield, pigments, and calcium carbonate dissolution), that salinity (treatments of 10, 20 and 30), independent of pH, affected *L. foecundum* physiology and dissolution. These experiments also revealed that *L. foecundum* was tolerant to a salinity down to 20, as individuals in the 20 and 30 salinity treatments were not significantly different for any of the parameters tested. Ultimately, spatially and temporally varying salinity regimes determined distribution of CCA in the nearshore Arctic. These results have implications for CCA populations near freshwater sources, and highlight the importance of salinity and total alkalinity in CCA physiology. In addition to implications for CCA population persistence, the loss of CCA at the inshore sites may also affect algal interactions and epilithic biodiversity.

*Life history stage tolerance to seasonal variability in light and salinity in an Arctic kelp (*Laminaria solidungula*)*

The Arctic endemic kelp species *Laminaria solidungula* is an important contributor to near-shore food webs of the Arctic. This perennial species is adapted to living and thriving in environmental conditions that change annually. *Laminaria solidungula* persists through seasons of high river input, which reduces salinity, and increased sedimentation from the rivers reduces light. We surveyed adult populations and found that areas in close proximity (3.5 km) to a freshwater input with increased turbidity exhibited lower densities (0.36 ± 0.44 m^{-2}) than further offshore sites (4.72 ± 1.51 m^{-2}). Culture experiments manipulating light (10, 20 and 40 umol

photons m^2 s^{-1}) and salinity (10, 20, 30) were used to observe the significance of these factors interactively and separately on microscopic sporophyte production and survival. Ultimately, cultures in the low salinity treatment were unable to produce sporophytes regardless of light level, but the highest light level (40 umol photons m^2 s^{-1}) did produce the highest sporophyte densities (0.37 ± 0.08 mm^{-2}). Additional salinity experiments emphasized the susceptibility of early microscopic stages (zoospores and gametophytes) to low salinity levels (10) as they were not able to produce sporophytes. However, microscopic sporophytes were able to survive low salinity conditions (10). Current light and salinity seasonal variations recorded in the Boulder Patch fall within the tolerance levels of *L. solidungula* microscopic stages. Although *Laminaria solidungula* has acclimated to extreme salinity and light variations, vulnerability of microscopic stages to reduced salinity can affect future population persistence as the timing or magnitude of freshwater input to the Arctic Ocean changes. The current conditions of the nearshore allow for *L. solidungula* microscopic and adult stages to persist, and population density differences may be driven by other factors, such as adult survivorship and species interactions.

Benthic community facilitation and competition in an Arctic kelp bed

Environmental gradients within the Boulder Patch affect the physiology and ability of species to persist on a small scale. From previous work (see Chapter 2), it is known that changes in salinity and total alkalinity (A_T) affect the distribution of CCA, and these species play important roles in structuring epilithic assemblages. Algal and invertebrate species were quantified at an inshore site devoid of CCA and an offshore site with CCA present. CCA coverage, *Laminaria solidungula* densities, and algal and invertebrate species and biomass were recorded for each site. In general, the inshore site without CCA had more algal and invertebrate biomass than the offshore site. CCA covered 77.5% ($\pm$ 3.8) of the rock surfaces at the offshore

site, and although overall invertebrate and red algal biomass was lower at this site, kelp densities were significantly higher (4.72 ± 1.51 m^{-2}) compared to the inshore sites without CCA (0.36 ± 0.44 m^{-2}; $t_{24.51}=3.34$, $p<0.01$). Kelp recruits (< 1 cm) were quantified at each site, and the inverse pattern was seen compared to adult kelp densities: 14 recruits were found on six of the cobbles collected at the inshore site and only three recruits were found on one cobble collected at the offshore site where CCA are present. When recruits were found at the inshore site, they were attached to algal or invertebrate species, not rock, as high algal and invertebrate biomass prevented epilithic attachment. Recruits at the offshore site with CCA were able to recruit to the CCA and the rocks, creating a more permanent hold and potentially increasing survivorship to adult individuals. Environmental factors within the Boulder Patch can affect kelp population persistence, but through salinity and light experiments (see Chapter 3), we see that kelp density patterns in the Boulder Patch are not driven by these factors alone. CCA inhibit the overgrowth of fleshy algae and branching invertebrates which in turn enhances kelp survivorship. This relationship creates an indirect susceptibility of *L. solidungula* to carbonate chemistry and salinity changes. *Laminaria solidungula* may have acclimated to survive in the variable salinity regimes of the nearshore Arctic (see Chapter 3), but CCA have not (see Chapter 2) and the loss of CCA in these systems will likely affect *L. solidungula* persistence. This work highlights the importance of species-specific responses to environmental conditions and the resultant biological interactions (positive or negative) that shape benthic systems.

Chapter 1: High-Frequency pH Time-Series Reveals Pronounced Seasonality in Arctic Coastal Waters

ABSTRACT

The accelerated rate of climate change in the Arctic Ocean occurs in conjunction with a system known for its extreme seasonal variability. Here, we present two years of continuous pH, salinity, and temperature data from the north Arctic coast of Alaska from instruments deployed in a kelp bed at 4.5-6 m depths in Stefansson Sound. At the innermost site, which receives freshwater runoff from the nearby Sagavanirktok River, short-term pH variability in late spring and summer produced pH values up to 8.67. The pH values of the deeper offshore site were less affected by freshwater input, although biological (heterotrophy) and chemical (ice formation) processes dominated during the winter months, driving pH down to 7.47 during the 8-mo period of ice cover. These long-term physicochemical measurements reveal the natural but critical influence of changing river inputs on the pH of Arctic nearshore waters which support highly productive communities and subsistence fisheries.

INTRODUCTION

High-latitude systems are most impacted by climate change as reflected by elevated sea surface temperature (SST), increases in freshwater input, a 30% decrease in summer ice extent, and higher susceptibility to ocean acidification (Zhang 2005, Fabry et al. 2009, Morison et al. 2012, Meier et al. 2014). Ocean acidification (OA), a process caused by an increase in atmospheric CO_2 that is subsequently absorbed by the world's oceans, has decreased ocean pH values below pre-industrial levels (0.1 units; Wickett and Caldiera 2003, Raven et al. 2005). As CO_2 dissolves into seawater, carbonic acid forms, releasing hydrogen ions into the ocean and decreasing pH.

OA has been shown to have complex, non-linear impacts on marine organisms across taxa (Kroeker et al. 2010), with polar organisms particularly sensitive to low pH conditions (Kelley & Lunden 2017). Acidification rates are governed by physicochemical processes that vary widely from region to region (Bates et al. 2014), making it difficult to predict future changes in areas that are data-limited, especially in polar regions. CO_2 is more soluble in high-latitude, colder oceans, and prolonged periods of time dominated by heterotrophy (respiration) further increase CO_2 partial pressure (pCO_2) within the water column that decreases ocean pH (Fabry et al. 2009). In the Arctic, this process is exacerbated by large amounts of freshwater input, decreasing nearshore salinities and total alkalinity (A_T; Mathis et al. 2015).

To date, most pH and carbonate chemistry data reported from the Arctic Ocean are low-resolution and consist primarily of discrete ship-based bottle sampling efforts that are concentrated during periods of lower ice cover from late spring to autumn (Bates et al. 2009, Mathis et al. 2012, Mathis et al. 2015). Freshwater input from ice melt and river runoff (Chierici & Fransson 2009, Yamamoto-Kawai et al. 2009), localized upwelling (Mathis et al. 2012), and anthropogenic CO_2 uptake (Bates et al. 2009) contribute to regional and temporal instances where waters are undersaturated with respect to aragonite. Low saturation levels of aragonite (Ω_{arag}), the most commonly reported calcium carbonate mineral, have direct repercussions on the ability of marine calcifying organisms to survive past their larval stages (Gangstø et al. 2008, Dupont et al. 2010, Büdenbender et al. 2011, Diaz-Pulido et al. 2012).

Individual tolerance to environmental shifts and species ability to acclimate creates species- and region- specific responses to changing pH regimes. Recent work has suggested that an organism's exposure to varying pH levels may determine its response and resilience to corrosive conditions (Frieder et al. 2014, Takeshita et al. 2015, Kapsenberg and Cyronak 2019),

similar to that reported for marine fauna in response to increased ocean temperatures, where species that live in highly variable environments (i.e., edge of distributions, estuaries, intertidal etc.) have the ability to persist in stressful abiotic conditions. Current records of high-frequency, continuous pH data have allowed researchers to identify patterns in natural systems on both temporal and spatial scales (Hofmann et al. 2011, Kapsenberg & Cyronak 2019).

At the land-sea interface, carbonate chemistry is highly dynamic, mainly due to biophysical forcing that is absent in the open ocean (Carstensen & Duarte 2019). Drivers of pH variability in marginal seas is a result of seasonal freshwater input and photosynthesis and respiration, which can act on multiples scales (hourly, daily and seasonal; Miller et al. 2018). Many nearshore marine environments are directly influenced by riverine waters which in turn affects Ω_{arag} values as these waters have higher A_T values than ice melt (Schneider et al. 2007, Cooper et al. 2008), which can have low A_T, particularly fjord-sourced freshwater (Evans et al. 2014).

While the Arctic Ocean receives ~11% of the world's freshwater run-off, it only contains ~1% of the world's ocean volume (McClelland et al. 2012), underscoring the impact that freshwater flux can have in the Arctic nearshore. Furthermore, most of this freshwater is released during a short period each spring, causing drastic changes to nearshore water composition and chemistry. The Sagavanirktok River, which is the second largest river draining the North of Alaska (1.6 km^3 annual discharge; McClelland et al. 2014), originates in the Brooks Range and empties into Stefansson Sound. This intense, seasonal burst of freshwater to the nearshore marine ecosystem likely plays an important role in structuring biological communities due to its direct impact on seawater physicochemical processes.

High-quality pH data is important for understanding the severity and magnitude of future impacts of OA on the carbonate dynamics of nearshore environments. The goal of this study was to capture high frequency, interannual pH measurements at two nearshore sites in the Beaufort Sea that differ in their proximity to a major river system. Our data includes under-ice measurements, which are difficult to capture during the eight-month period of continuous ice cover. Spatial placement of sensors in varying proximity to freshwater input allowed for comparisons to be made between areas of differing water masses (marine dominated vs. seasonal freshwater influenced). This seasonally dynamic region of the inner shelf and coast is an important foraging area for thousands of migrating waterfowl and many species of anadromous fish that are critical resource for native Inupiat subsistence hunters. It is also undergoing rapid transformation in response to regional climatic warming. We measured pH, salinity, temperature and A_T from discrete water samples and estimate aragonite saturation levels (Ω_{arag}) to further understand water chemistry effects on calcifying organisms. To our knowledge, this is the first high-frequency biennial time-series of pH data from the Arctic Ocean.

METHODS

Study Sites and Background

Sea-Bird (Satlantic) SeaFETs and SBE 37-SM MicroCATs C-T (P) were deployed July 2016-July 2018 at two sites within the Boulder Patch, Stefansson Sound, Alaska (Fig. 1.1); Site E1 (70º18.8665 N, 147º44.0413 W; 5 m depth) and site DS-11 (70º19.3248 N, 147º34.8816; 6.5 m depth). Sensors were embraced with Styrofoam collars that were attached to benthic weights and suspended in the water column (~1 m from the bottom) allowing the sensor to maintain an upright, yet flexible position to resist transport by deep-draft ice. Sensors deployed 4 August 2016 to 25 July (DS-11) and to 30 July (E-1) 2017, recorded values hourly (average of 20

samples per frame with one burst). The 2 August 2017 to 16 July 2018 deployments recorded values every two hours to increase battery life for the year-long deployment (same settings as 2016 deployments). The two sites varied in proximity to the Sagavanirktok River, the second largest river draining the North of Alaska (McClelland et al. 2014). We expected these placements would reflect the marked spatial and temporal gradients in salinity and carbonate chemistry moving from inner shelf at the Sagavanirktok River Delta to the outer shelf of the open Beaufort Sea.

Calibration and pH data processing

Water samples were collected via SCUBA by hand using a van Dorn water sampler proximate to each sensor at deployment and retrieval (temporally aligned with sensor sampling time at the top of the hour). Samples were immediately fixed with saturated $HgCl_2$ (75 µL in 250 mL for pH and 37.5 µL for 125 mL for A_T), and stored at 4°C until analysis (Dickson et al. 2007). Spectrophotometric pH was measured at 25ºC for 2016 deployment samples and 20ºC for 2017 retrieval and deployment samples using *m*-cresol purple sodium salt, dye content 90% (Sigma-Aldrich; spectrophotometric method, Dickson et al. 2007). An automated open cell Gran titration system (ASALK2; Apollo SciTech) was used to measure A_T (SOP 3b, Dickson et al. 2007). The in-situ temperature of the seawater samples were recorded using the SeaFET's thermistor. Single-point calibration method was used to calculate in situ pH_T (total hydrogen ion scale, CO_2Calc, (Robbins et al. 2010)), following Bresnahan et al. (2014) using constants from Dickson & Millero (1987). Due to field logistical constraints, water samples were collected at the time of deployment in 2016, which did not allow for adequate conditioning of the electrodes. A post-retrieval visual inspection of the data clearly demonstrated a stabilization in pH values within ~48 hours of deployment. Thus, a single-point calibration was applied 48 hours from the

time the water sample was initially collected, when pH stabilization had clearly taken place (Fig. 1.S1). For the 2017 datasets, the sensors were already conditioned at deployment and a single point calibration was applied at the time the water samples were taken.

Ω_{arag} values were calculated for each dataset using pH, salinity, and temperature values, and estimated A_T from several discrete water samples taken throughout the Boulder Patch in July 2018 (n=13; CO_2Calc, USGS). A_T was measured using the techniques described above and regressed against salinity values ($y=31.032x + 1653.3$; $r^2=0.61$; Fig. 1.S2). Temperature and salinity values were plotted against the freeze point line and any values that fell below the freeze point line were not included in the analysis (Fig. 1.S3).

Estimated pH Uncertainty

pH error estimates were measured for each site by taking a single point calibration measurement upon retrieval to allow comparisons between the value taken by the sensor and the analytical measurement of the discrete water sample. Reference sea water samples collected during sensor retrieval (~1 year) were used to calculate pH uncertainty over the year-long deployment for the 2016-2017 dataset. New sensors were deployed in 2018, and although reference samples were not collected, several pH (NBS) values were measured during sensor retrieval. In order to estimate a conversion factor between pH_{NBS} and pH_T, spectrophotometric pH was measured at 25ºC from a certified reference material (CRM, Dickson Laboratory, UC Scripps, Batch 171) that was diluted with deionized water to create five salinity samples (33.43, 20, 15, 10, 5). pH_T was calculated for the serial salinity dilution using spectrophotometric pH measured at 25ºC, in conjunction with the A_T, temperature and salinity of each sample. A calibrated PRO DSS YSI sonde (same model used in original field measurements) was then used to measure pH_{NBS} for each salinity sample created. Although there is greater error associated

with the data sonde (pH ± 0.01), this calibration protocol allowed the use of the pH_{NBS} values to estimate sensor error (pH_{NBS} + 0.118 = pH_T; Table 1.S1).

Statistics

All abiotic factors, pH, salinity and temperature and calculated Ω_{arag}, were analyzed by averaging each factor for each month of deployment for the 2016-2017 and 2017-2018 deployment periods for each site (4 groups). Due to unequal sample sizes and non-normal data distributions, the non-parametric statistical test Kruskal-Wallis was used to compare years and sites. Significant results were additionally followed by a Dunn test to use pairwise comparisons in order to see what factor (site or year) was driving the significant differences in values. All statistics were run using R version 1.2.1335.

RESULTS

We collected continuous pH data over two annual periods on the Beaufort Sea coast. These 12-mo periods were characterized by a confluence of interacting factors including sea ice coverage, low water temperature, low A_T freshwater and intense seasonal variability. Coastal ocean pH, salinity, and temperature followed seasonally distinct transitions that were related to four main events: summer open water, fall freeze-up, winter ice cover, and spring freshet. Freeze-up was defined as an icepack of nine-tenths or "very close pack" (Arctic Data Integration Portal, AOOS.org). For 2016, freeze-up was estimated as 4-6 November and 26-28 October for 2017. Peak discharge of the Sagavanirktok River predictably occurs in late May and early June (McClelland et al. 2014).

pH Time-series

For the 2016-2017 deployment, pH values varied ~0.87 pH units at E-1, and ~0.9 pH units at DS-11 (Table 1.1). pH values varied little following instrument deployment in early August, but anomalous spikes in fall 2016 were likely associated with changes in the physicochemical environment with the freezing of coastal waters (Fig. 1.2A), as freeze-up dates corresponded to increases in pH. Both sites showed a slight decrease in pH from November 2016 through February 2017 and subtle increases in pH were observed from March until break-up at E-1; Fig. 1.2A). Unfortunately, the SeaFET at DS-11 lost power on 28 February, 2017 and at E-1 on 4 July, 2017, compromising our ability to capture the effect of the spring freshet on pH values in 2017 at DS-11, as peak discharge was 22 July 2017. Both sites showed a unique pH spike in the fall of 2016 (Fig. 1.2A), but these spikes were not seen in 2017 (Fig. 1.2B). Clear shifts in average pH values were seen between ice-covered and open water regimes; pH was generally lower during the ice-covered period (see Table 1.1). DS-11 averaged 7.97 ($\pm$0.001) during months of open water and 7.92 ($\pm$0.002) when ice was present. E-1 values were 8.00 ($\pm$0.000) during the open water period and 7.95 ($\pm$0.001) under the ice.

The August 2017 – July 2018 deployment revealed annual variation in pH values of ~1 pH unit at E-1 and ~0.76 at DS-11 (Table 1.1). Two weeks after instrument deployment, a distinct drop in pH from ~8 to ~7.6 began in mid-August at offshore site DS-11 (Fig. 1.2B). Following ice formation in late October, pH continued to decrease at DS-11 until the spring freshet in May. In contrast to the August 2016 – July 2017 data, DS-11 recorded much lower pH values during the ice-covered period. On 18 June 2018, the freshwater input signal from break-up at inshore site E-1 was coincident with a substantial increase in pH and a steep drop in salinity from 32 to near zero (Figs. 1.2B, 1.3B), but the drop in salinity at DS-11 in early July (32 to 22),

was insufficient to trigger a pH change. Similar to 2016-2017, under-ice pH for 2017-2018 values were lower than open water averages, and pH values differed between periods of open water, and ice-cover, and break-up for each site (Table 1.1). Results from a Kruskal-Wallis test indicated significant differences of pH among site/year groups (Kruskal-Wallis chi-squared$_3$ = 12.54, p-value = 0.01). Post hoc pairwise comparisons showed that mean pH values at DS-11 (2016-17) and E-1 (2016-2018) were significantly different than the mean pH value at DS-11 in 2017-2018 ($p<0.001$; Fig. 1.S4).

Estimated pH Uncertainty

Deployment error values were likely affected by the length of the year-long deployments. August 2016 – July 2017 uncertainty estimates were 0.042 for E-1 and 0.046 for DS-11. August 2017 – July 2018 error values were 0.085 for E-1 and 0.028 for DS-11. The higher error values for E-1 during the second deployment year could be attributed to our use of a data sonde to measure pH. However, we applied the same methods described above to convert pH_{NBS} to pH_T for DS-11 and obtained a low (0.028) error value. Conditions at DS-11 were much more stable at the time of retrieval and this may have affected error calculations (see Fig. 1.2B).

Temperature and Salinity Time-series

Ranges in temperature (E-1: 8.95°C; DS-11: 7.96°C) and salinity (E-1:15.28; DS-11: 12.58) were similar between sites in 2016-2017 (Figs. 1.3B and 1.4B, Table 1.1). However, in 2017-2018, salinities differed drastically between sites during peak freshwater input (temperature range E-1: 11.59°C; DS-11: 10.96°C; salinity range E-1: 34.01; DS-11: 12.08; Figs. 1.3 and 1.4, Table 1.1). These patterns illustrate the dynamic conditions of this nearshore estuarine environment but also highlight the need for long-term monitoring. We found no significant

differences in salinity between mean values for sites and years because of the naturally high variance that is characteristic of estuarine systems (temperature: Kruskal-Wallis chi-squared$_3$ = 0.75894, p-value = 0.8593; salinity: Kruskal-Wallis chi-squared$_3$ = 1.2105$_3$, p-value = 0.7505; Fig. 1.S2).

Influence of Salinity on pH

The Sagavanirktok River had a significant effect on water composition and chemistry at both sites. Salinity and pH exhibited marked relationships that highlighted the seasonal influence of freshwater input into these coastal systems. Annually, distinct salinity and pH relationships were visible before and after freeze-up for both sites (Figs. 1.5 and 1.6). These relationship regime shifts were seen in all years and signaled a change between ice covered stabilized ocean water and ocean water mixed with freshwater from the Sagavanirktok River. Generally, the relationship showed lower pH_T and higher salinity values after freeze-up and higher pH with lower salinity levels prior to freeze-up (Figs. 1.5 and 1.6). The inverse relationship between pH and salinity (high pH associated with lower salinity values) was also visible during break-up at E-1 in 2018, where low salinity values (near 0) were associated with an increase in pH (Fig. 1.2B).

Estimated Ω_{arag} Time-series

Estimated Ω_{arag} levels ranged from 0.88 to 4.93 at E-1 and 0.89 to 4.79 at DS-11 for the 2016-2017 deployment, with values near equilibrium (Fig. 1.7A, Table 1.1) for much of the ice-covered period at both sites. Peaks in Ω_{arag} corresponded to peaks in pH (Fig. 1.2). The 2017-2018 dataset exhibited greater Ω_{arag} variability between sites than 2016-2017 (Fig. 1.7B), and this was also reflected in other parameters (see Figs. 1.2-1.4, Table 1.1). E-1 2017-2018 Ω_{arag}

fluctuated from 0.08 to 4.89 and 0.33 to 1.66 at E-1. Lowest values for both sites were reached during the spring freshet in July 2018. Annual mean levels compared between sites and years were significantly different (Kruskal-Wallis chi-squared$_3$ = 18.4929, p-value = 0.00). Post hoc pairwise comparisons show that the DS-11 2017-2018 deployment was significantly different than all other site and year deployments (Fig. 1.S4). We found that low Ω_{arag} (associated with periods of high pH) corresponded with low salinity and A_T, highlighting the critical role that salinity and associated A_T values play in carbonate chemistry that is independent of pH.

DISCUSSION

Nearshore pH, A_T and other carbonate chemistry parameters have been reported for the Arctic Ocean (Mathis et al. 2011), but the data reported here are the first to include multi-year, continuous measurements in the nearshore environment. Our measurements show the relatively large comparative spatial effect of a major freshwater source on pH as driven by salinity. Depth and location within pycnocline stratification layers can lead to values that may not represent the water column in offshore deeper environments (Miller et al. 2019). Measurements often include only surface waters that are heavily influenced by atmospheric exchange and varying freshwater sources (e.g., river run-off or ice melt; Yamamoto-Kawai et al. 2009, Tank et al. 2012). Our data captured conditions near the seabed and are representative of the water that is affecting the epilithic assemblages of the Arctic, near-shore benthic communities. These data also highlight the importance of understanding how freshwater sources can affect ocean carbonate chemistry on regional scales.

General Seasonal Patterns

Seasonal variability in pH, temperature and salinity corresponded to distinct time periods associated with open water, freeze-up, ice cover, and the spring freshet (Figs. 1.2-1.4, and 1.8). These distinct seasonal separations have been reported previously (Weingartner et al. 2017), and our results corroborate the patterns reported, albeit in higher frequency. In general, as nearshore waters transition from open water to ice cover with the onset of freezing temperatures and shorter days, salinity levels increase, and water temperature and pH values decrease (Fig. 1.8). Following ice formation, pH values continue to decrease slowly until light begins to penetrate the ice cover in late in early spring with increasing day-length and solar inclination. The initial decrease in pH may be driven by sediment respiration and water column heterotrophy that produces high pCO_2 levels. However, ice formation alone has been shown to increase pCO_2 in the absence of biological processes (DeGrandpre et al. 2019). In spring, the large pulse of freshwater runoff often creates a stratified water column in June, which in shallower inshore areas results in freshwater conditions that can extend completely to the bottom for several days (as occurred at E-1 in 2018). In deeper offshore areas, wind can facilitate mixing as ice retreats, sometimes causing moderate drops in salinity before the onset of full open-water conditions and a well-mixed water column.

In contrast to other nearshore polar ecosystems, we did not observe a sudden increase in pH that typically signals the onset of seasonal primary productivity in early summer. In the nearshore Antarctic, a rapid increase in pH at the beginning of the austral summer results from phytoplankton blooms that increase pH by 0.3 – 0.4 units compared to stable wintertime values (Kaspenberg et al. 2015). While there appears to be a small increase in pH during the transition from spring to summer at E-1 in both years, this pattern was not observed at DS-11 in 2018. One

potential cause for the lack of a pH increase at DS-11 in 2018 may be related to low light levels caused by turbid ice (Dunton 1990). Benthic light levels at DS-11 averaged only 0.142 µmol photons m^2 s^{-1} ± 0.021 15 June through 15 July 2018 (Dunton et al. 2020). Prolonged ice cover in 2018 likely dampened any primary production pulse and subsequent increase in pH for the deeper station (DS-11).

Annual Variations and Anomalies

Despite seasonal and annual patterns seen over the 2-year deployment, annual and spatial variations occurred between sites and years. In 2016, pH increases were observed at E-1 and DS-11 (Fig. 1.2B) during freeze-up in the fall. The reason for these pH increases is not clear. It is highly unlikely that amplitude anomalies were driven by an increase in primary production, since the fall period is characterized by a turbid water column, which combined with low sun angles, produce very low irradiance levels (Oct through Nov 2016 averages; E-1 0.059 µmol photons m^2 s^{-1} ± 0.011, DS-11 0.039 µmol photons m^2 s^{-1} ± 0.006; Dunton et al. 2020). Since increased pH levels were observed at both sites around the same period as freeze up, the higher values could be a result of brine formation and water column turnover that disturbs the bottom and increases turbidity (Chierici et al. 2011). Weingartner et al. (2017) also reported that conductivity sensors fail during this time period, and speculated that that increases in turbidity obstructed the sensors. A similar pH anomaly was seen in the Canadian Arctic within days of freeze-up, and the sudden increase in pH was attributed to increases in A_T and dissolved inorganic carbon (DIC) in conjunction with thermochemical reactions from temperature changes (Duke 2019).

The 2017-2018 pH dataset exhibited different patterns than in 2016-2017 at both sites. The pH anomalies that occurred freeze up in fall 2016 did not occur in fall 2017; pH also

increased dramatically at E-1 in association with the June freshwater pulse from the Sagavanirktok River. At DS-11, a dramatic decrease in pH from ~8.0 to 7.6 occurred mid-August 2017 (Fig. 1.2B). The lack of continuous baseline data in nearshore Arctic areas suggest a possible sensor error for the low pH values at DS-11, but the DS-11 2017-2018 uncertainty was the lowest (0.028) of all datasets. In addition, similar pH values (7.6 and below) were continuously recorded in Kaktovik Lagoon, Alaska, during the ice-covered months of 2018-2019, (Beaufort Lagoon Ecosystems LTER Core Team 2020), further corroborating our results. These low pH values could be the result of shallow, ice-covered waters dominated by heterotrophy and high pCO_2 values since the ice creates a closed system with no atmospheric mixing. The marked difference during the 2017-2018 deployment was constrained by each site's distance from the Sagavanirktok River, where the strong drop in salinity at E-1 in June 2018 was temporally synced with an increase in river discharge. The depth of the pycnocline also played a role in how each site was influenced by salinity. The shallower site (E-1; ~4.5 m) has a higher potential for the benthos to be completely exposed to freshwater (as seen in 2017-2018) during the spring freshet, while the deeper site (DS-11; ~6 m) is more likely to be buffered by marine waters.

Salinity and temperature did not significantly differ between sites or deployment years when averaged, but there were clear, distinct spatial and temporal patterns (Figs. 1.3 and 1.4). For the 2016-2017 deployment, salinity was similar between the offshore (21.93 to 34.51) and nearshore sites (19.07 to 34.35); but both sites experienced lower salinity values during the 2017-2018 deployment (offshore 12.71 to 34.86, nearshore 0.19 to 34.02). In addition to lower salinity values, maximum temperatures (9.04°C) were higher in the 2017-2018 dataset compared to the 2016-2017 period (6.08°C). Historical temperature data from these sites show that the

maximum temperatures at the offshore site were less than 7.5°C from August 2011 to July 2017, but temperatures at the nearshore site had climbed to 10°C in 2013 and 2016 (Bonsell & Dunton 2020).

There was a distinct temporal separation in the relationship between salinity and pH that occurred before and after freeze up from both sites in 2016-2017 (Fig. 1.5). Separations were seen in 2017 as well, although not as distinct as in fall 2016 (Fig. 1.6). In general, pH increased as freshwater from the Sagavanirktok River increased (Fig. 1.2B). Although a number of processes (wind, storms, freeze-up, break-up, and freshwater pulses) can drive these water mass changes, the separations likely represent a shift from a period of run-off from the Sagavanirktok River (lower salinity, higher pH vs. higher salinity, lower pH) to a stable, ice-covered period dominated by PML waters that are continually upwelled and transported onto the inner shelf under the ice.

Seasonal variability of the nearshore Arctic creates carbonate chemistry regimes that are unique and ephemeral, spatially and temporally. Although salinity levels dropped with freshwater input, pH levels increased. The Sagavanirktok River is classified as a mountain stream (Craig & McCart 1975), which drains limestone deposits. This pattern is not specific to the Sagavanirktok River outflow. Arctic river alkalinities are increasing due to changes in precipitation, permafrost depth, groundwater flow and vegetation coverage (Drake et al. 2018), and our data illustrate the connectivity of this riverine input with the Arctic nearshore system.

Estimated Ω_{arag} Time-series

Ω_{arag} levels calculated from the nearshore Arctic dataset reveal values less than 1.5 at both the inshore and offshore sites that remained relatively constant under the ice (Fig. 1.7). Similar Ω_{arag} ranges were reported for the Antarctic, but increases in pCO_2 and subsequent

decreases in pH drive lower Ω_{arag} while A_T values remain constant (Kapsenberg et al. 2015). Similar trends were seen in Ischia, Italy when drastic increases pCO_2 caused lower $\Omega_{calcite}$ (Kroeker et al. 2013). In contrast, our Ω_{arag} levels decreased when A_T and salinity levels dropped due to freshwater input from the Sagavanirktok River (Figs. 1.4-1.6). Biological processes (CO_2 production), may have driven low Ω_{arag} levels at the offshore site (DS-11) for the 2017-2018 deployment, as well as ice formation leading to increased pCO_2 and decreased pH values (DeGrandpre et al. 2019; Fig. 1.2B). Low Ω_{arag} levels were not observed during the winter months of 2017-2018 at inshore site E-1, which showed drastic decreases in Ω_{arag} levels during the freshet (Fig. 1.7B). The nearshore Arctic region's susceptibility to OA and low Ω_{arag} levels are amplified by the additional alterations from freshwater influence (low A_T) and the biological processes that create naturally lower ocean pH waters. It is important to note that CO_2SYS does not consider calcium (Ca) within freshwater sources in the calculation of Ω_{arag} levels.

The concentration of dissolved Ca in the Sagavanirktok River is almost twice as high as other nearby Arctic rivers (Rember and Trefry 2004). Average Ca values for the Sagavanirktok River are 24.48 mg L^{-1}, compared to the lower Kuparuk (10.43 mg L^{-1}) and the Colville (13.67 mg L^{-1}) as noted by Stieglitz et al. (2007), but still much lower than ocean Ca values (~ 400 mg L^{-1}; Perry et al. 2001). Ω_{arag} levels may be underestimated, especially during times of high amounts of freshwater influence (i.e., the freshet). Decreased salinity and A_T values during break-up result in Ω_{arag} levels below equilibrium (Fig. 1.7).

Conclusions

We documented annual pH ranges of 1.0 pH units at the inshore site (E-1) in 2017-2018, a variation much larger than recorded in the Antarctic (0.40 and 0.42; Kapsenberg et al. 2015). Lower latitude locations tend to have less pH variation (Hofmann et al. 2011; Kapsenberg et al.

2017), but with some exceptions (up to 1.4; Hofmann et al. 2011). pH ranges may be greater in the nearshore Arctic due to the number of biotic and abiotic factors influencing water chemistry. Ice thickness can influence ocean-atmospheric exchange (Sievers et al. 2015), and light can drive pH upward (photosynthesis) or downward (respiration), especially in shallow environments (Matson et al. 2014; this study). Biologically-driven pH systems are common in temperate kelp forests and coral reefs where primary production is relatively high (Hoffman et al. 2011), and similar pH seasonal variabilities were seen in Antarctica as well (Kapsenberg et al. 2017). Environments seasonally covered in ice experience biologically driven pH changes under the ice (respiration; Matson et al. 2014), atmospheric exchange during open water periods (Sievers et al. 2015), and if near a freshwater source, salinity and total alkalinity decreases during the spring (Yamamoto-Kawai et al. 2009), all of which affect ocean pH and carbonate chemistry, creating very dynamic systems with seasonal and annual variability.

Nearshore Arctic environments harbor highly productive communities, critical for maintaining ecologically important species. Our data provides the setting for the evaluation of future changes in the carbonate chemistry of nearshore Arctic systems and highlights the importance of daily, interannual and decadal variability in deciphering the complex relationships between salinity, temperature, and pH. These data also show the importance of long time series to detect rapid change in nearshore systems in response to changes in regional climate. Future studies should focus on the effects of seasonal and annual variations in salinity and pH characteristic of these environments and the effects they have on associated biological communities. The adaptations made by benthic species to tolerate such rapid shifts in salinity and pH are not fully understood, yet it is important to our understanding of ecosystem resilience.

TABLES

Table 1.1 pH, temperature, salinity and Ω_{arag} levels for both sites and years. Means are x ± SE (standard error)

	E-1		DS-11	
	August 2016 - July 2017	August 2017 - July 2018	August 2016 - July 2017	August 2017 - July 2018
pH range	7.83 to 8.70	7.67 to 8.67	7.79 to 8.69	7.47 to 8.23
open water period average (SE)	8.00 (> 0.000)	8.02 (> 0.000)	7.97 (0.001)	7.65 (0.004)
ice-covered period average (SE)	7.95 (0.001)	7.93 (0.001)	7.92 (0.002)	7.51 (0.006)
break-up period average (SE)	sensor failure	8.14 (0.029)	sensor failure	7.50 (0.002)
temperature range (°C)	-1.87 to 7.08	-1.86 to 9.73	-1.88 to 6.08	-1.91 to 9.05
salinity range	19.07 to 34.35	0.01 to 34.02	21.93 to 34.51	22.78 to 34.86
Ω_{arag} level range	0.88 to 4.93	0.08 to 4.89	0.89 to 4.79	0.33 to 1.66

FIGURES

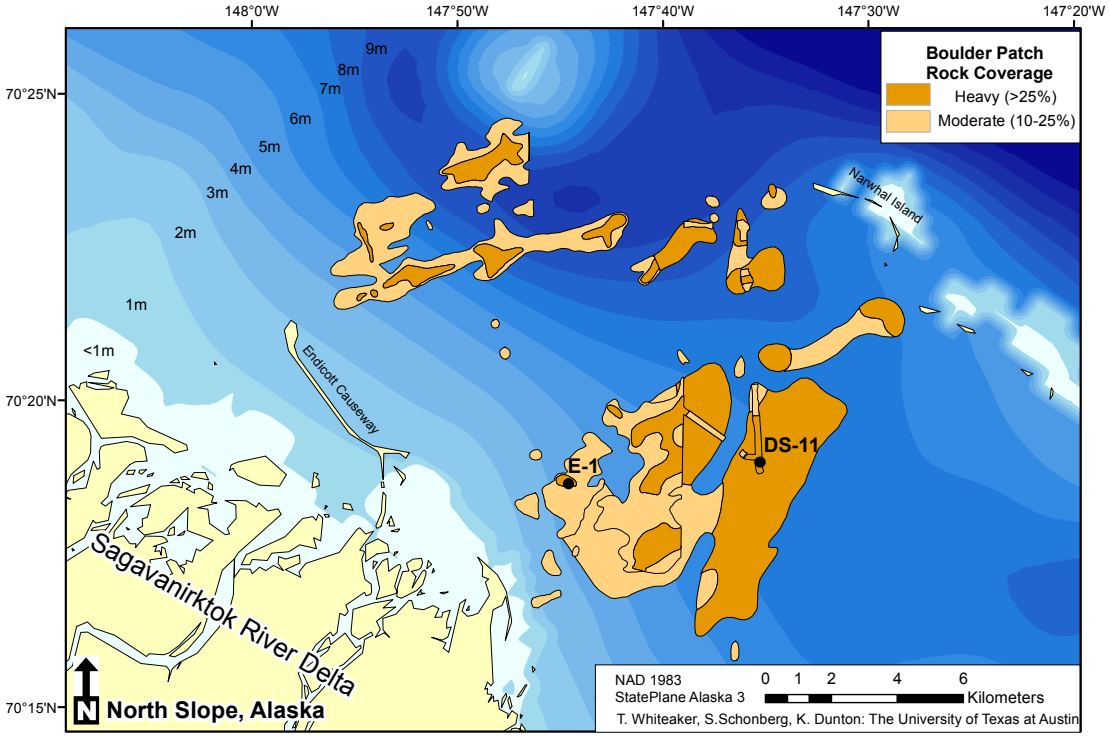

Figure 1.1 The Stefansson Sound Boulder Patch and instrument deployment sites. E-1 (4.5 m; inshore) and DS-11 (6 m; offshore), differed in proximity to the Sagavanirktok River, creating different salinity and chemistry regimes (adapted from Dunton et al. 2018).

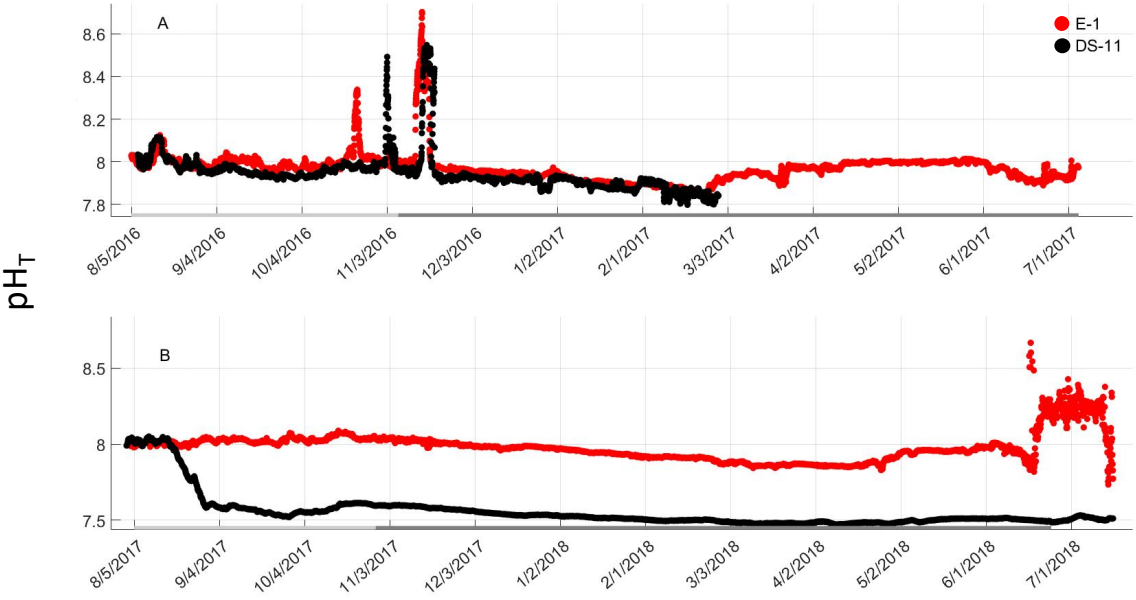

Figure 1.2 Continuous pH_T values for sites DS-11 (black) and E-1 (red). (A) 2016-2017 deployment, (B) 2017-2018 deployment, X-axis bars represent open water (light gray) and ice covered (dark gray).

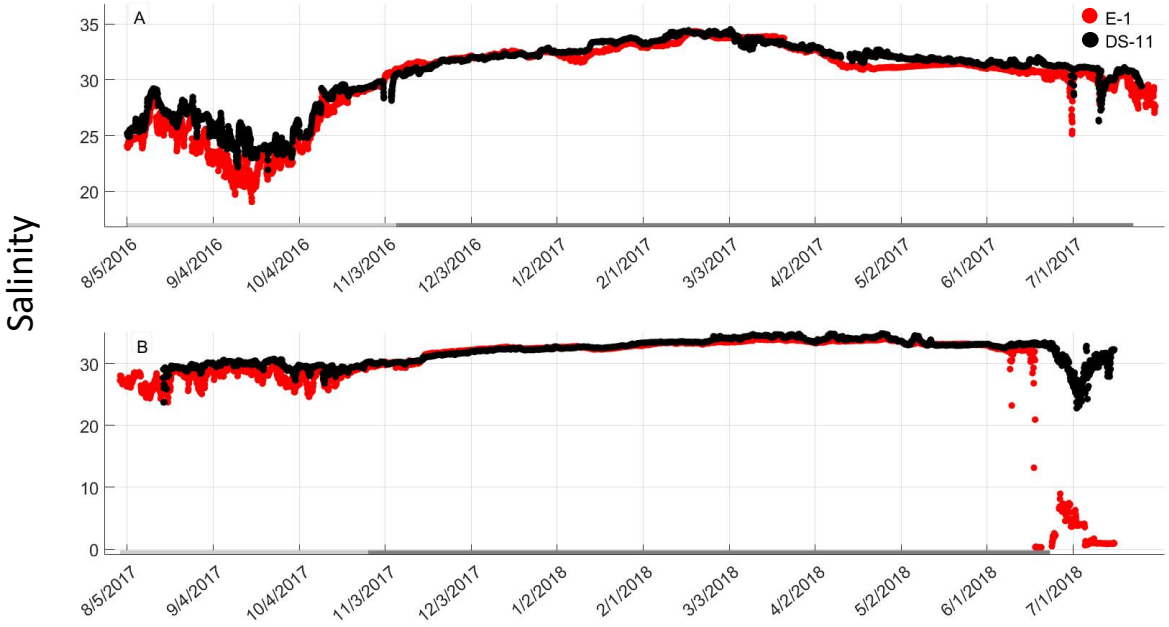

Figure 1.3 Continuous pH_T values for sites DS-11 (black) and E-1 (red). (A) 2016-2017 deployment, (B) 2017-2018 deployment, X-axis bars represent open water (light gray) and ice covered (dark gray).

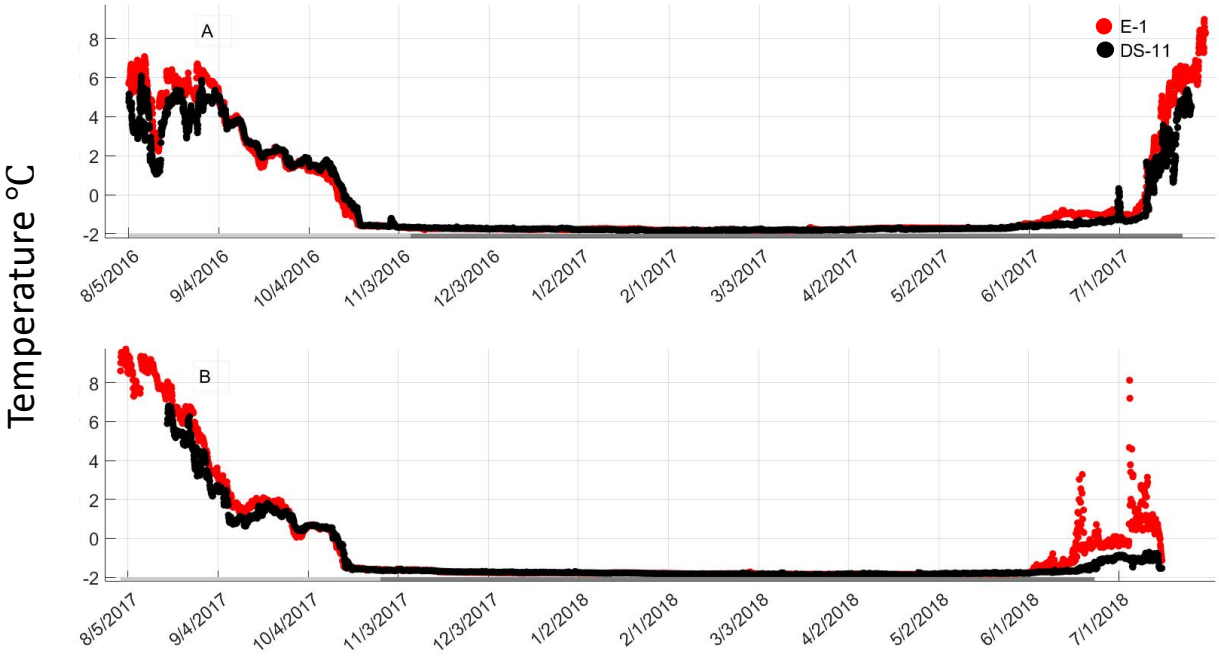

Figure 1.4 Continuous temperature values for sites DS-11 (black) and E-1 (red). A) 2016-2017 deployment B) 2017-2018 deployment. X-axis bars represent open water (light gray) and ice covered (dark gray).

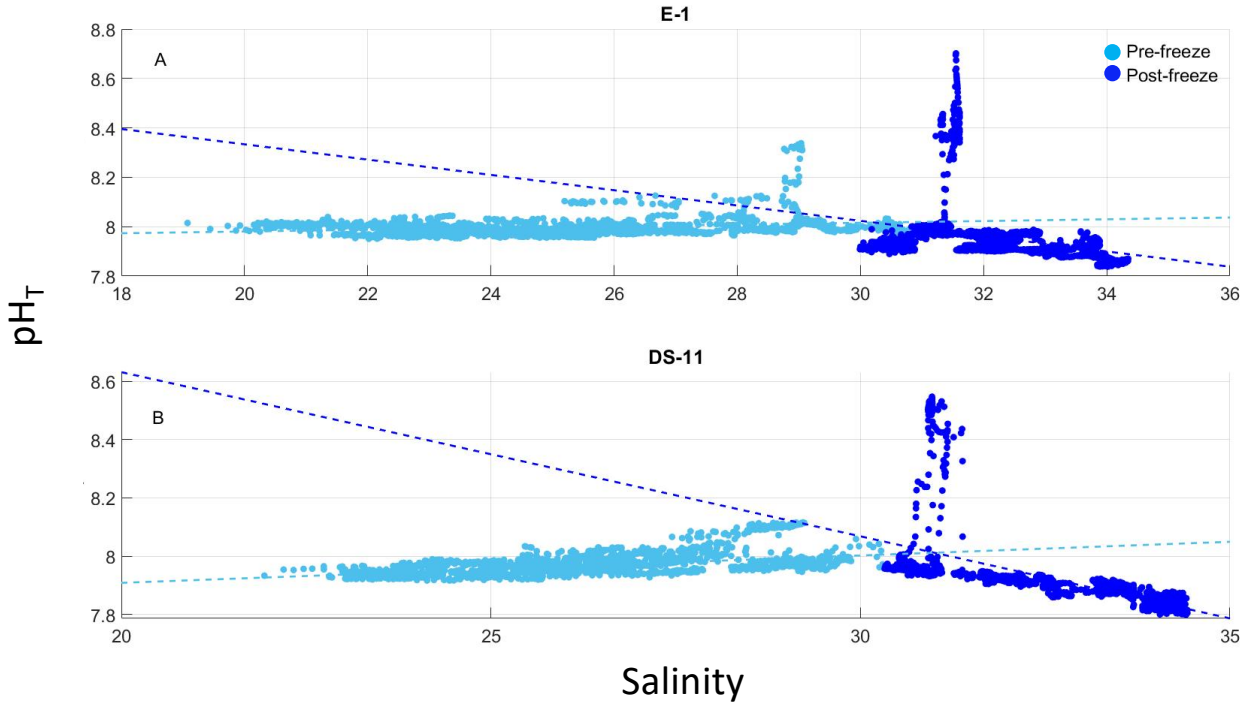

Figure 1.5 Salinity vs. pH_T relationships for 2016-2017 deployments separated by pre-freeze (light blue circles) and post-freeze (dark blue circles) time frames. Freeze-up was estimated to occur Nov. 4-6, 2016 at both sites a) E-1 and b) DS-11. Dotted lines represent general trendlines of the pre-freeze and post-freeze salinity and pH relationships.

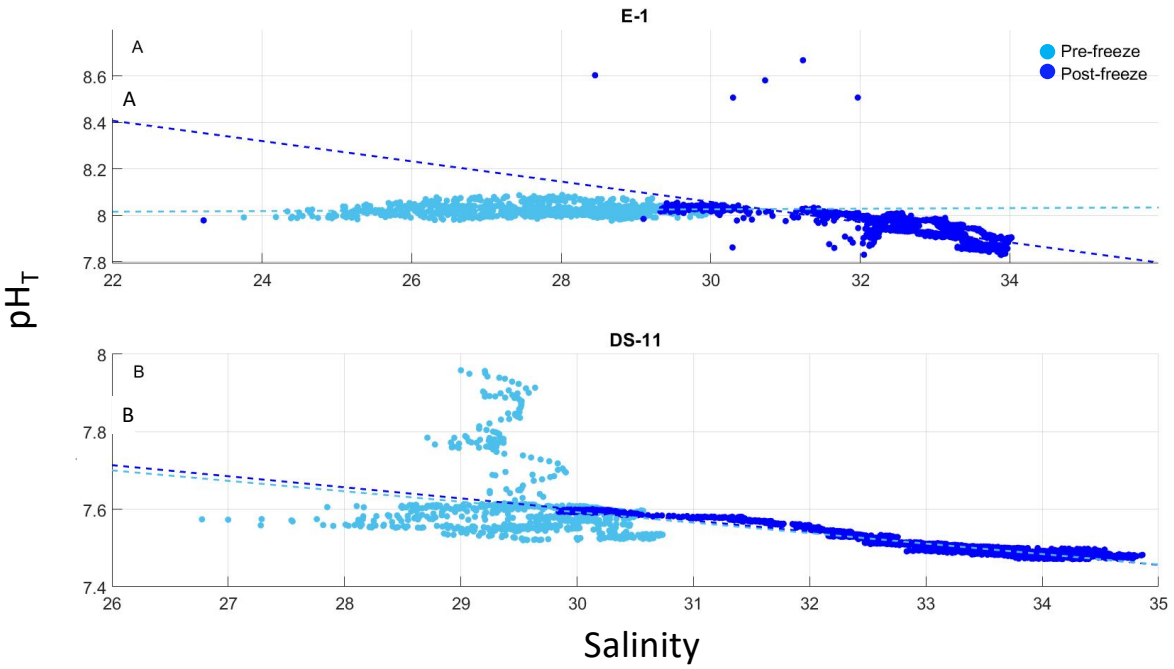

Figure 1.6 Salinity vs. pH_T relationships for 2017-2018 deployments separated by pre-freeze (light blue circles) and post-freeze (dark blue circles) time frames. Freeze-up was estimated to occur Oct. 26-28, 2017 at both sites a) E-1 and b) DS-11. Dotted lines represent general trendlines of the pre-freeze and post-freeze salinity and pH relationships.

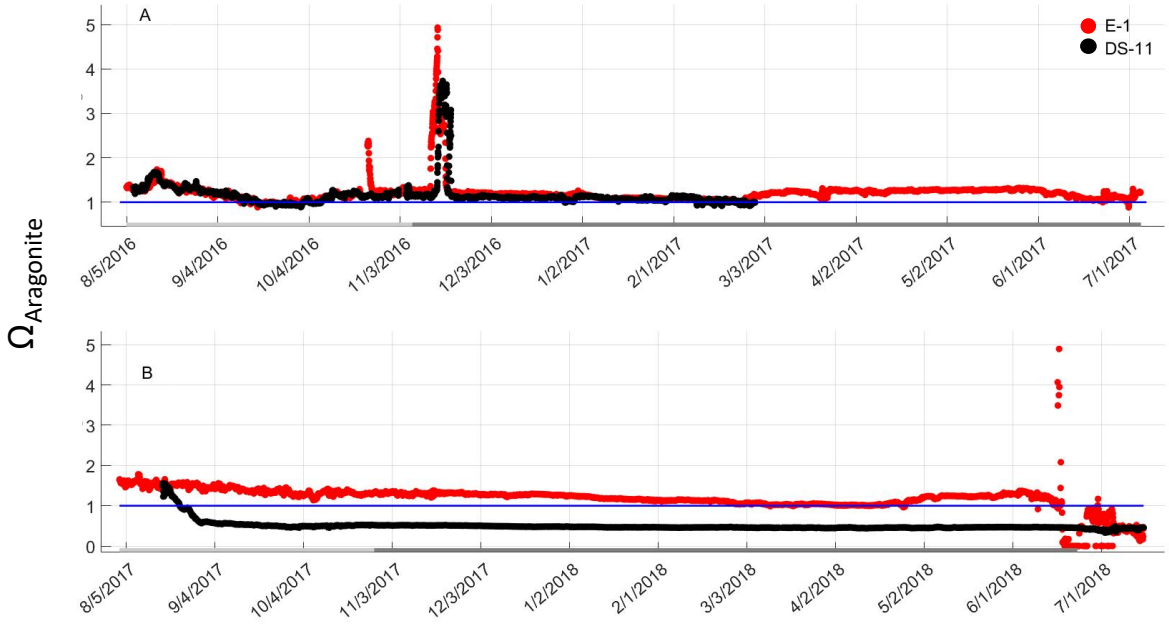

Figure 1.7 $\boldsymbol{\Omega}_{arag}$ levels for E-1 (red) and DS-11 (black) for 2016-2017 (A) and 2017-2018 (B). The blue line represents equilibrium with respect to aragonite ($\boldsymbol{\Omega} = 1$). Values less than one favor dissolution while values above the line favor precipitation of aragonite. X-axis bars represent open water (light gray) and ice covered (dark gray).

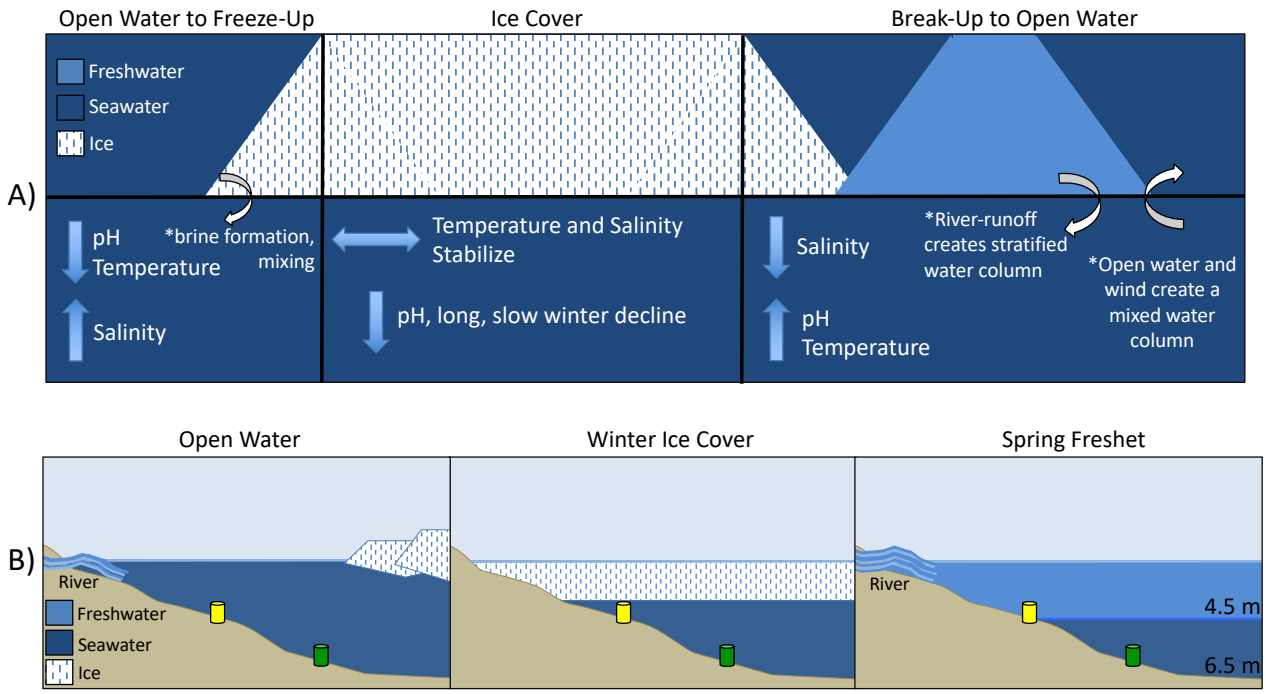

Figure 1.8 (A) Generalized seasonal changes of abiotic factors (temperature, salinity, pH) as ocean conditions transition from open water to freeze-up, ice cover, ice break-up and the spring freshet back to open water conditions. Biological processes (e.g. respiration) are likely responsible for the slow winter decline in pH during ice-covered months, although other physico-chemical processes may alter pH values. (B) Seasonal patterns of water column stratification in relation to depth of the site and sensor.

SUPPLEMENTARY MATERIAL

Table 1.S1 Carbonate chemistry parameters for pH NBS to pH_T conversions. The mean of the average difference values were used to estimate pH_T values from pH_{NBS} values. (pH_{NBS} + 0.118 = pH_T)

	Salinity	Total Alkalinity	pH Total	Temperature	pH (NBS) #1	pH(NBS) #2	Difference pH Total and pH (NBS) #1	Difference pH Total and pH (NBS) #2	Average Difference	pCO2 out (µatm)	HCO3 out (µmol/kgSW)	CO3 out (µmol/kgSW)	CO2 out (µmol/kgSW)	ΩCa out	ΩAr out
Sample 1	33.8	2216.53	7.98	25.57	8.09	8.06	0.106	0.076	0.091	151.7	1780.5	171.9	9.6	4.14	2.60
Sample 2	20.1	1382.63	8.09	25.19	8.18	8.11	0.092	0.022	0.057	84.4	1137.3	94.6	5.8	2.41	1.43
Sample 3	15.1	1248.10	8.14	25.17	8.17	8.23	0.030	0.090	0.060	71.8	1038.1	83.5	5.1	2.18	1.25
Sample 4	9.8	1043.33	8.14	25.08	8.28	8.28	0.142	0.142	0.142	67.1	898.5	59.8	4.9	1.60	0.89
Sample 5	5.2	1000.45	7.98	25.10	8.19	8.26	0.206	0.276	0.241	107.6	920.8	35.5	8.1	0.96	0.52

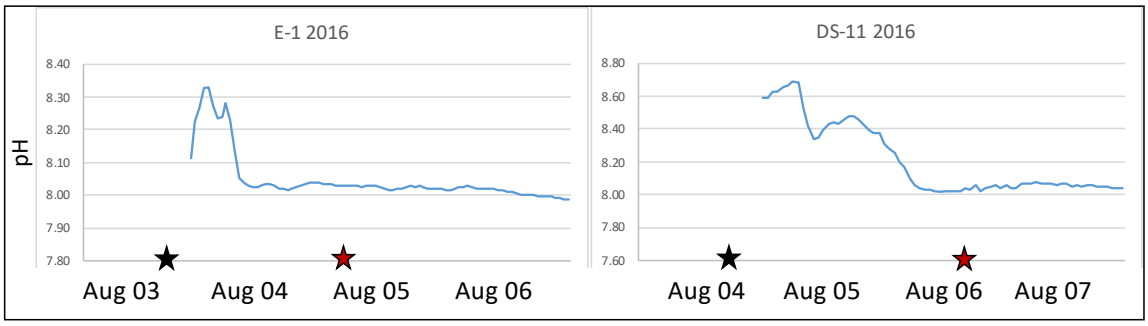

Figure 1.S1 Initial 72 hrs of 2016 deployments at E-1 and DS-11. After 48 hrs, pH values stabilized, and discrete water samples taken the day of deployment were applied to values taken 48 hrs after deployment when values had stabilized. E-1: 19:00 UTC Aug 03, 2016, applied to 19:00 UTC Aug 05, 2016 data point. DS-11: 16:00 UTC Aug 04, 2016 applied to 16:00 UTC Aug 06, 2016 data point. Black stars represent water samples taken and red stars represent the data point the calibration was applied to.

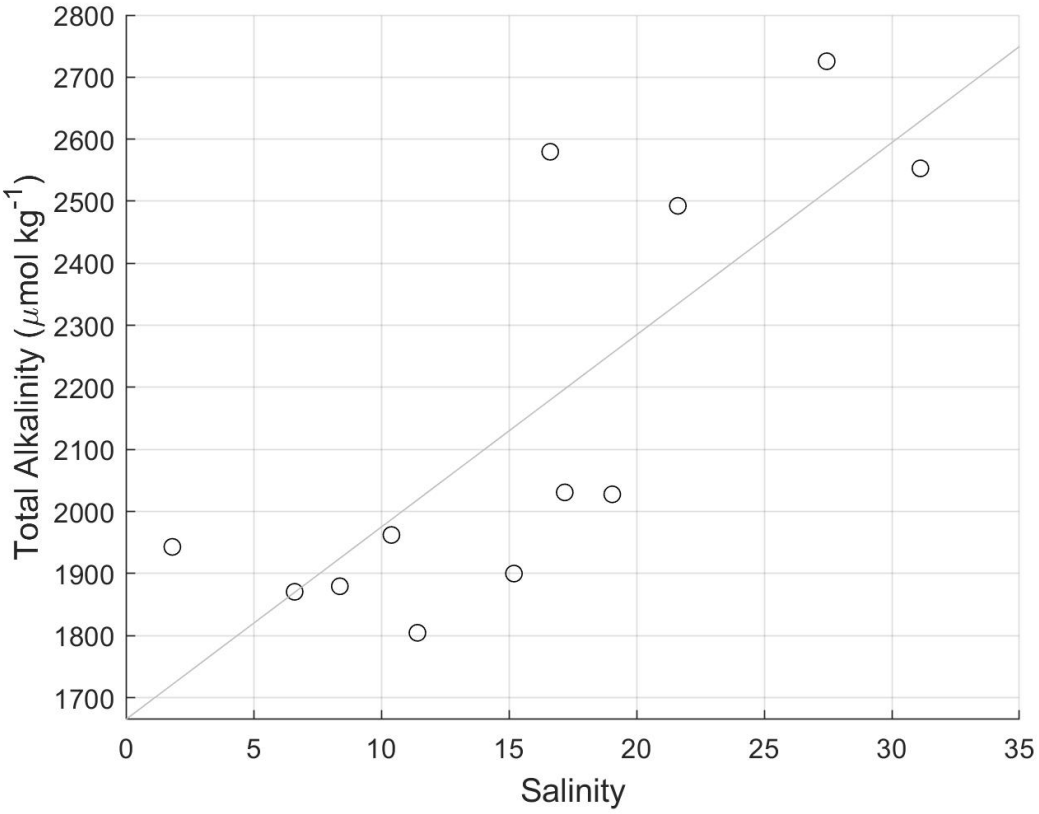

Figure 1.S2 Relationship between salinity and A_T from discrete water samples within the Boulder Patch taken July 2018. A_T=31.032*salinity + 1653.3; r^2=0.61.

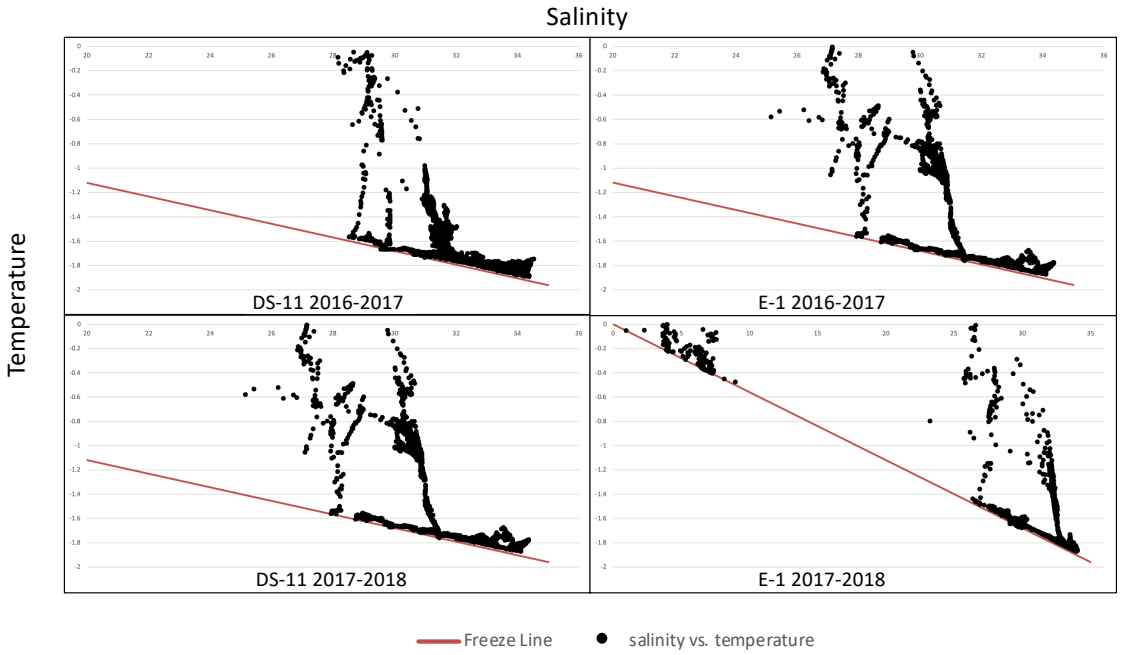

Figure 1.S3 Salinity vs. temperature data plotted against the freeze line of saltwater. Plots were used to identify and remove data values that fell beneath the line.

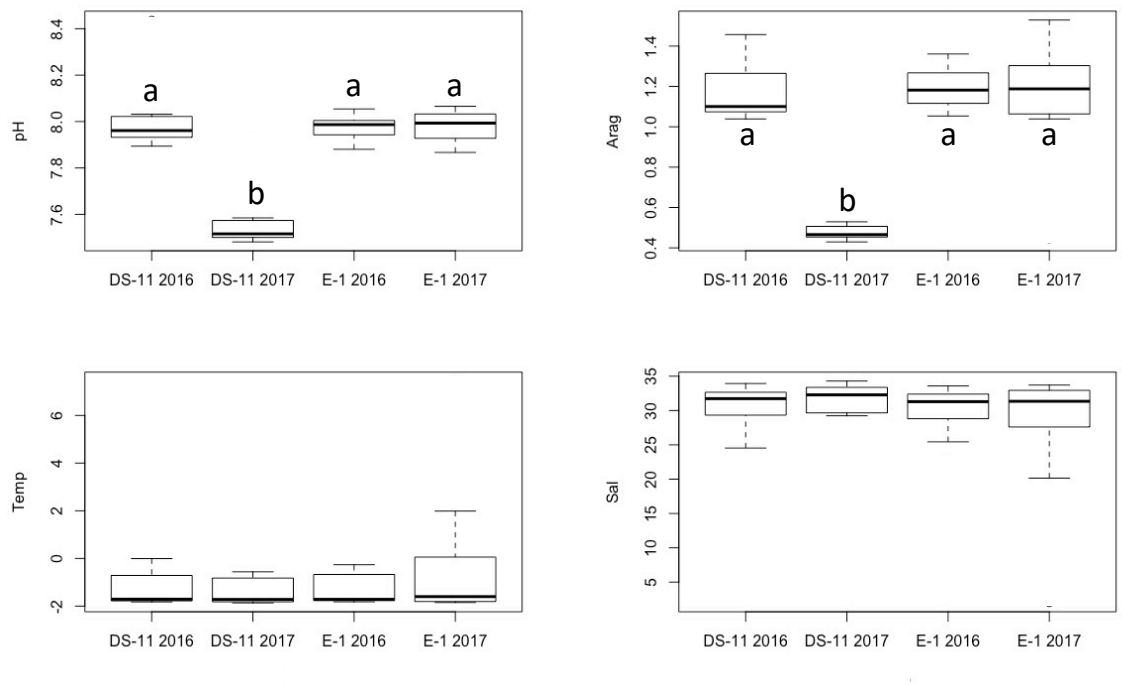

Figure 1.S4 Boxplots of average pH, $\mathbf{\Omega}_{arag}$ levels, temperature, and salinity for each site (E-1 and DS-11) for each deployment year (2016, 2017). Different letters denote mean values that are significantly different ($p < 0.05$).

Chapter 2: Physiological responses of an Arctic crustose coralline alga (*Leptophytum foecundum)* to variations in salinity

ABSTRACT

In the Beaufort Sea, Arctic crustose coralline algae (CCA) persist in an environment of high seasonal variability defined by naturally low pH ocean water and high magnitude freshwater pulses in the spring. The effects of salinity on the CCA *Leptophytum foecundum* were observed through a series of laboratory and field experiments in Stefansson Sound, Alaska. We found that salinity (treatments of 10, 20 and 30), independent of pH, affected *L. foecundum* physiology based on measurements of three parameters: photosynthetic yield, pigmentation, and calcium carbonate dissolution. Our experimental results revealed that *L. foecundum* individuals in the 10-salinity treatment exhibited lower photosynthetic efficiency, higher thallus dissolution and increased pigment loss, while those in the 20 and 30-salinity treatments were not significantly different for these three parameters. Reciprocal *in situ* transplants and recruitment patterns between areas dominated by CCA and areas where CCA were absent illustrated that inshore locations receiving large pulses of freshwater were not suitable for CCA persistence. Ultimately, spatially and temporally varying salinity regimes affected distribution of CCA in the nearshore Arctic. These results have implications for epilithic benthic community structure in subtidal areas near freshwater sources and highlight the importance of salinity in CCA physiology.

INTRODUCTION

Calcification of marine organisms is of broad and current interest in ocean climate change studies. Lower pH levels, driven by carbon dioxide (CO_2) uptake into ocean water, causes a reduction in calcium carbonate (and other forms e.g., aragonite and calcite) saturation levels, leading to decreased calcification rates of species. At high latitudes, aragonite saturation levels ($\mathbf{\Omega}_{arag}$) are low (~2) when compared to ocean averages (~3.5) or low latitude values (~4; Gangstø et al. 2008, Jiang et al. 2015) due to processes such as freshwater input, rapid seasonal ice melt, upwelling, cold water temperatures, and relatively high respiration rates from decomposition of organic matter (Mathis et al. 2015a). In the Arctic Ocean, natural factors in addition to anthropogenic factors have the potential to decrease aragonite saturation levels below natural variations ($\mathbf{\Omega}_{arag}$ 3.5-0.8) by 2025 (Mathis et al. 2015).

Decreased rates of productivity, growth, and net calcification have been shown to occur when coralline algal species are exposed to lower than ambient pH conditions for short time periods (~21 days; Diaz-Pulido et al. 2012, McCoy 2013, Büdenbender et al. 2015). CCA species are often the first species affected by lower pH because they precipitate magnesium calcite, which is about 20% more soluble than aragonite (Kamenos et al. 2008). In a study of natural CO_2 vents in Italy, decreased local pH levels lead to the disappearance of coralline species near the vents while turf algal biomass increased 60%, including certain invasive species (Hall-Spencer et al. 2008).

Low salinities also decrease calcification rates and slow productivity in CCA species (King and Schramm 1982). Schoenrock et al. (2018) saw decreased calcification rates, photosynthetic efficiency, and density in *Lithothamnion glaciale* in southwest Greenland as waters became more brackish in fjord environments. Marine invertebrates are also susceptible to freshening waters, as juvenile oysters cultured under decreased salinity and pH conditions

showed increased rates of mortality, but low salinities alone had the most impact (Dickinson et al. 2012).

Within the Arctic Beaufort Sea, a diverse benthic community attaches to boulders and cobbles in an area known as the Boulder Patch (for a detailed description of the Boulder Patch, Stefansson Sound, Alaska see Dunton et al. 1982, Wilce and Dunton 2014). Three kelp species (*Laminaria solidungula*, *Saccharina latissima* and *Alaria escuelenta*) and various red algal species (e.g., *Phycodrys fimbriata* and *Coccotylus truncatus*) are common on rock surfaces (Wilce and Dunton 2014). CCA species, including *Leptophytum foecundum* and *Leptophytum lavae*, cover an average of 77% of the hard substratum in some areas and are completely absent in others (Konar and Iken 2005; A. Muth pers. obs.). Benthic surveys in the Boulder Patch show patterns of decreasing CCA coverage with proximity to inshore areas with consequent increases in red algal biomass with no CCA present at the innermost sites (Bonsell & Dunton 2020). Data from salinity, temperature, and pH sensors deployed July 2016 to July 2018 in the Boulder Patch exhibit patterns of lower salinity in association with higher pH at the inshore site vs. the offshore site (Muth et al. 2020a). Sites closest to the freshwater source, the Sagavanirktok River, reach low (<5) salinity levels near the benthos during the ice break-up period, however, this low salinity water is alkaline, and pH levels increase during these pulses (Muth et al. 2020a).

The mechanisms and environmental conditions that prevent CCA persistence at the inshore locations are the subject of this paper, which seeks to specifically explain the role of salinity on CCA physiology and distribution. The unique characteristics of the high alkalinity and pH levels of the Sagavanirktok River allow for a study of the influence of salinity on CCA populations, independent of pH. In general, low salinity waters (<10) have higher pH levels than high salinity (>30) waters within the Boulder Patch. We hypothesize that seawater chemistry

conditions influence CCA distributions and that parameters that vary with salinity (e.g., A_T), affect CCA physiology and net calcification rates. Laboratory experiments were used to focus on short-term changes to CCA physiological mechanisms in response in alterations in water chemistry. Field studies allowed for real time, long-term observations of recruitment and persistence in natural conditions.

METHODS

Study site and CCA species

Within the Boulder Patch, Stefansson Sound, Alaska, there are varying distributions of CCA, and the most striking of these patterns is between an inshore site, located near the mouth of the Sagavanirktok River (E-1) and an offshore site (DS-11; Fig. 1.2). The substrate of cobbles and boulders at the offshore site is covered by *Leptophytum foecundum* (Wilce and Dunton, 2014), while CCA is absent at the inshore site. Salinity measurements throughout the study area from past years have shown that salinity can drop to 15-20 at both sites, but can reach as low as 0 at the inshore site (Muth et al. 2020a, Bonsell & Dunton 2020; Fig. 2.1). Total alkalinity (A_T) is often lower in fresh and brackish waters, which reduces pH buffering capacities and results in lower pH values, leading to dissolution of the calcium carbonate skeletons of calcifying organisms. However, recently collected continuous pH_T for the Boulder Patch show consistently higher pH values at the inshore site (values > 8), even though A_T values decreased with lower salinity measurements as expected (Muth et al. 2020a). The site with low salinity, high pH, and low A_T are where CCA are absent (Muth et al. 2020a). For this study, mesocosm experiments were conducted to observe if changes in salinity and A_T, with a constant pH, could drive dissolution and/or lower photosynthetic efficiency in the CCA *L. foecundum.*

Laboratory Manipulative Experiment

Culture conditions

Cobbles (5-25 cm in length and width) were collected in July 2016 at DS-11 (Fig. 2.1), wrapped in damp paper towels, and kept in separate plastic bags to prevent any damage to the coralline crust during transport. Corallines were then packed in a cooler within layers of Techni-Ice packs, and shipped overnight to the University of Texas Marine Science Institute (UTMSI) and kept at 0°C until experiments began 15 February 2017. *Leptophytum foecundum* cobbles were cultured within a cold room, complete darkness at three salinities (10, 20 and 30) and ambient environmental conditions (complete darkness and 0°C water temperatures). A no-specimen 30-salinity control treatment was also monitored to determine the effect of the medium on water chemistry, since we used nearby Gulf of Mexico water for the culture medium. Salinity treatments were chosen to represent three salinity regimes that these corallines experience throughout the year: 30 (Beaufort Sea waters predominate under stable open water conditions under the ice), 20 (mixing of offshore marine and near coastal waters), and 10 (brackish waters replace bottom saline marine waters during flooding events; Fig. 2.1).

Samples (four cobbles in each tank, one tank per salinity treatment) were stored at a salinity of 30, placed in salinity treatments (1 L of medium) for 5 weeks, after which all samples recovered at 30 (control treatment) for 5 weeks. To replicate field conditions, samples placed in low salinity (20 and 10 treatments) were placed in the control after 5 weeks for ecological relevance. Growth media was created using Gulf of Mexico (GOM) offshore water (low nutrient concentrations). Distilled water was added to achieve the salinity treatment levels. By diluting seawater to create salinity treatments, the ion concentrations are diluted as they would be with the input of freshwater, this ensures natural ion changes are kept constant and this method most

closely mimics natural conditions (Kirst 1989). All treatments were supplemented with Provasoli's Enriched Seawater, ensuring sufficient supply of macro- and micro-nutrients (20 mL L^{-1}). Media was replaced weekly, and water quality parameters (pH_{NBS}), temperature, salinity) were recorded before and after each water change using a data sonde (YSI 6920V2-2). Water samples were also taken before and after each water change so that total alkalinity (A_T) measurements could be undertaken (values were log transformed to meet ANOVA assumptions of normality and equal variances).

Photosynthetic efficiency

Samples were monitored weekly for photosynthetic efficiency, dark-adapted yield values (F_v/F_m) using a pulse amplitude modulation (PAM) fluorometer (Walz, diving-PAM). Initial baseline measurements were taken before cobbles were placed in salinity treatments. Three areas per cobble (n=4 cobbles for each salinity treatment) were measured for yield values each week at the same location on the cobble and time of day (Measuring Light Intensity 7, Saturation Intensity 0.8, Saturation Pulse Width 8, Gain 7 and Damping 2).

Calcium carbonate calcification

Calcium carbonate calcification was estimated by measurement of A_T when the culture medium was first replaced (initial) and from the media after one week (final) in the experimental tanks. An automated open cell Gran titration system (ASALK2; Apollo SciTech) coupled to a temperature-controlled water bath was used to measure A_T (Lonthair et al.2017) at 0°C. A_T values were combined with temperature, pH and salinity measurements to estimate aragonite saturation levels ($\boldsymbol{\Omega}_{arag}$; $\boldsymbol{\Omega} = [Ca^{2+}]\,[CO_3^{2-}] \,/\, [CaCO_3]$ solubility) using the software program CO_2SYS. Saturation levels equal to one are at equilibrium, greater than one favors precipitation, and less than one favors dissolution.

Visual pigmentation

To measure changes in visual pigmentation, cobbles were photographed before salinity treatments commenced, when placed in the recovery salinity treatments, and at the end of the experiment. Cobbles were photographed in the same position at each time point with a Nikon D7200, with each photograph containing a ruler for scale. Photographs were then analyzed using ImageJ to estimate pigmented CCA area at each time point for comparison among treatments.

In situ field experiments

Adults

To observe natural effects of abiotic factors and spatial changes in carbonate chemistry on *L. foecundum in situ*, we performed reciprocal transplants between the inshore (E-1) and offshore site (DS-11). Both sites differ considerably with respect to their hydrographic characteristics (Muth et al. 2020a), with the inshore site (E-1) characterized by periods of extremely low salinities in late spring and early summer (0-20), while salinities at the offshore site (DS-11) rarely fall below 22, with values up to 35 (Fig. 2.1). Cobbles (5-25 cm in length and width) from offshore (n=6), with CCA present, were photographed and transferred to the inshore site and remained on the seabed from July 2016 – July 2017. Cobbles were retrieved and kept in covered buckets in ambient seawater during transit to the laboratory on Endicott Island, Alaska. In addition to the transplanted cobbles, control cobbles from each site were also collected for quantum yield value comparison in July 2017. In the laboratory, all cobbles with CCA present were measured for dark-adapted yield using PAM fluorometry (same methods as above).

Recruits

Fibercement tiles (10 x 10 cm) were retrieved from DS-11 and E-1 (Fig. 2.1) following a 12-month deployment (July 2016 deployment) on the seabed. Tiles were attached to weighted

PVC pipes with cable ties, ~3 cm from the seafloor to avoid burial by sediments. Tiles/samples were wrapped in damp paper towels and kept in separate plastic bags to prevent any damage to the recruits. Tiles were then packed in a cooler within layers of Techni-Ice packs, shipped overnight to the University of Texas Marine Science Institute (UTMSI), and kept at 0°C.

Density and area of CCA recruits were quantified and compared between sites, using a uniform grid, density of CCA individuals was counted for 50 FOV per tile at 40x. Pictures were taken at 40x, capturing 5 individuals per tile, and ImageJ was used to analyze the area of the recruits from both sites.

Statistics

Manipulative laboratory experiment parameters were compared by calculating differences in A_T and pH in new media and week-old media, using 2-way ANOVAs (salinity treatment and treatment*recovery period), and values were log transformed in order to meet test normality and equal variance assumptions. Tukey HSD tests were used for post hoc comparisons. F_v/F_m among treatments were compared using repeated measures 2-way ANOVAs (salinity and time) during salinity treatments and following the placement of all cobbles in recovery conditions. Changes in visual pigmentation were compared using 2-way ANOVAs (salinity treatment and treatment/recovery period), and ANOVAs were used to compare recruit size (values were square root transformed in order to meet ANOVA assumptions of normality and equal variances) and density between sites. All statistics were run using R Version 3.3.1.

RESULTS

Culture Conditions

Salinity treatments remained consistent over the 5-week treatment period (Table 2.S1).

pH values decreased in all treatments, including the control, over each week (start pH 8.06 ± 0.02, end pH 7.84 ± 0.02; Table 2.S1), but the changes did not differ among treatments or between periods (treatment/recovery; 2-way ANOVA: period F_1=0.004, p=0.949; salinity treatment F_4=1.07, p=0.388; interaction F_4=0.661, p=0.623).

Manipulative Laboratory Experiments

Photosynthetic Efficiency

Photosynthetic yield (F_v/F_m) values differed between the 10-salinity treatment and the 20- and 30- salinity treatments (Fig. 2.2; Repeated measures 2-way ANOVA: salinity F_1=23.60, p<0.001, time F_5=44.33, p =?, salinity*time F_5=5.47, p<0.001). Baseline yield values were 0.40, 0.45, and 0.43 for the 10-, 20- and 30-salinity treatments, but at week five, values dropped to 0.26 in the 10-salinity treatment while the values for the 20- and 30-salinity treatment remained similar and higher (0.34 and 0.33). After cobbles were placed in a recovery salinity of 30, the previous salinity treatments did not affect yield values, however yield values for all treatments did decrease initially and then recovered over time (Fig. 2.2; Repeated measures 2-way ANOVA: salinity F_1=0.50, p=0.49, time F_4=56.88, p<0.001, salinity*time F_4=2.14, p=0.07).

Calcium Carbonate Parameters

Discrete water samples analyzed for A_T fluctuations each week of the experiment, measuring the initial and final A_T of the medium each week and calculating the difference ($A_{T\ Final} - A_{T\ Initial}$). These values showed an increase in A_T in the 10-salinity treatment compared to the control and salinity of 20- and 30-salinity treatments during the 5-week period (Fig. 2.3 and Table 2.1; 2-way ANOVA period F_1=5.39, p=0.027; treatment F_4=6.39, p<0.001; interaction F_4=4.50, p=0.006; Tukey HSD 10-20 p=0.03, 10-30 p=0.004, 10-control p<0.001;Fig. 2.3, Table

2.1). Since the experimental containers had lids and were closed systems, an increase in A_T can only be derived from dissolution of the calcium carbonate thallus of the CCA. Treatment media aragonite saturation levels of the media used for each treatment (Table 2.2), showed that only the 10-salinity treatment was undersaturated with respect to aragonite, meaning the process of dissolution was favored (Ω_{arag} = 0.5 +/- 0.1; dissolution favored at $\Omega_{arag} < 1$). The 20- and 30-salinity treatment media were above equilibrium (1.0 +/- 0.2) and 1.6 +/- 0.1 respectively (precipitation/calcification favored at $\Omega_{arag} > 1$). Dissolution did not differ between salinities with respect to A_T changes (Fig. 2.3, top panel). Samples placed in a recovery salinity of 30 showed no significant differences in A_T (Tukey HSD $p>0.05$).

Visual pigmentation

The cobbles in the 10-salinity treatment lost significantly more pigmented area (8.06 % lost) during the treatment period (Fig. 2.3, lower panel; 2-way ANOVA: period $F_1=4.4$, $p=0.046$; salinity treatment $F_3=15.56$, $p<0.001$, interaction $F_4=5.92$, $p=0.024$) while the 20- and 30-salinity treatment cobbles remained unaffected and lost little to no pigmentation throughout the experiment (0.25 % gain and 0.15% loss respectively; Fig. 2.3, lower panel). Once placed in the recovery treatment of 30 salinity, loss of pigmented areas slowed in the 10-salinity treatment (1.96 % loss; Fig. 2.3, bottom panel, recovery period). As seen in all parameters measured (F_v/F_m, A_T changes, pigmentation changes), *L. foecundum* was affected when immersed in stressful conditions (salinity = 10), but was able to recover when returned to the 30 salinity treatment.

Field Experiments

Adults

Photosynthetic Efficiency and Pigmentation

Field transplants with adult CCA showed high amounts of variability. Yield (F_v/F_m) values did not differ significantly between pigmented areas of the control and transplanted cobbles (transplanted 0.45 ± 0.01, control 0.43 ± 0.01, n = 6, ANOVA $F_{1,34}$=2.79, p=0.103). Non-pigmented or dead areas (found only on the transplanted cobbles) had yield values as high as pigmented areas (0.40 ± 0.04) which we attributed to endolithic algal species living within the calcium carbonate structure. Green tinted areas had higher yield values than the control cobbles (0.53 ± 0.02). Overall, transplanted cobbles from the offshore to the inshore site lost pigmentation (Fig. 2.4, a-d). However, the percent lost (23.03% ± 15.0%) was highly variable among individuals.

Recruits

Size and Density

Recruit size and density were compared between the offshore and near-shore sites. Recruits were present at both sites, but were significantly larger at the offshore site (Fig. 2.4, e and f; offshore 12.89 ± 1.91 mm^2, inshore 1.35 ± 0.209 mm^2; ANOVA $F_{1,78}$=64.91, p<0.001). Densities of CCA recruits were significantly higher offshore (density 9.02 ± 3.76 per cm^2 offshore, 1.16 ± 0.40 per cm^2, inshore; ANOVA $F_{1,14}$=7.02, p=0.01).

DISCUSSION

Arctic coralline algae survive in an environment of high seasonal variability and extreme salinity changes (Figs. 2.1 and 2.S1; Bonsell and Dunton 2020). Within the Boulder Patch in Stefansson Sound, CCA distributions vary from dominant benthic space holders to complete

absence. The discharge of the Sagavanirktok River waters into Stefansson Sound drives changes in seawater chemistry that affect CCA and their ability to persist. Other environmental factors, such as temperature and light, vary between the two sites studied and could also influence CCA distributions. For this study we focused on salinity to ascertain if freshwater input can influence CCA physiology. Laboratory experiments with *L. foecundum* demonstrated their sensitivity to low salinity. Reciprocal transplants between offshore station DS-11 and inshore station E-1 revealed a loss of CCA cover at E-1. These results corroborate field observations of the absence of CCA in areas in close proximity to the mouth of the Sagavanirktok River.

Effects of water chemistry on Leptophytum foecundum

Results from manipulative laboratory experiments illustrated that *Leptophytum foecundum,* the dominant CCA species in the Boulder Patch (Wilce and Dunton, 2014), was able to tolerate salinities to 20 without any measured physiological impacts (Figs. 2.2 and 2.3). However, at a salinity of 10, CCA experienced reduced photosynthetic efficiency, decreased visual pigments and increased calcium carbonate dissolution (Figs. 2.2 and 2.3). Interestingly, all parameters (F_v/F_m, pigmentation and A_T) recovered rapidly once specimens were placed in a recovery salinity of 30. These results highlight that *L. foecundum* is likely very resilient to lower salinities and associated changes in carbonate chemistry. Similar resiliency has been seen in other sub-Arctic coralline species. Wilson and colleagues (2004) demonstrated a decreased in Fv/Fm at low salinities <15, but the corallines did not die and were able to recover, as in the current study (Wilson et al. 2004) As noted by Santelices et al. (2007), we expect that such acclimation is related to periods of stress that the algae experience naturally on an annual basis.

The significant ($p>0.05$) increase in A_T in the 10-salinity treatment (Fig. 2.3, Table 2.1) was driven by the $\mathbf{\Omega}_{arag}$ level, chemically favoring net dissolution of calcium carbonate

(aragonite). Dissolution of calcium carbonate is the main process that would affect A_T in closed mesocosm systems, especially under our culture conditions of cold temperatures and 24 h dark periods. Photosynthesis and respiration exchange neutrally charged compounds (CO_2 and O_2), which do not alter A_T. CCA precipitate magnesium calcite, which is around 20% more soluble than aragonite (depending on Mg content; Morse et al. 2006), therefore CCA are even more susceptible to dissolution when $\mathbf{\Omega}_{arag}$ levels are less than one.

We kept pH levels constant across salinity treatment media (Table 2.S1). pH did decrease in all treatments throughout the week (likely attributed to respiration, which increased pCO_2 thereby lowering pH), however, pH did not differ significantly among treatments ($p=0.388$) or between stress and recovery periods ($p=0.949$). Because pH levels were similar throughout all salinity levels, results of these experiments enable us to disentangle the effects of pH and salinity. We attribute the observed physiological effects to changes in salinity and associated parameters (e.g. A_T), but not to pH. These results are important and ecologically relevant in systems like the nearshore Arctic, where the higher alkalinity of river run-off drives pH upward to values greater than eight when compared to other freshwater sources and ice melt (Cooper et al. 2008, Semiletov et al. 2016). Although some river run-off has higher A_T than other freshwater sources, alkalinity levels are still lower than ocean water values (Table 2.1; Yamamoto-kawai and Tanaka 2005, Tynan et al. 2016, Muth et al. 2020a), and the increased pH of these waters does not ameliorate lower A_T with regard to $\mathbf{\Omega}_{arag}$ levels and calcium carbonate dissolution. These low salinity and alkalinity waters initially overlay dense ocean water, creating a stratified environment (Fig. 2.5) that eventually mixes. Heterotrophic processes during the dark ice-covered period drive down pH, causing the ocean water to have lower pH values than freshwater run-off (Muth et al. 2020a). The higher pH values of Alaska North Slope river waters

are not sufficient to offset the influence of low A_T values and the resultant $\mathbf{\Omega}_{arag}$ levels. Lower pH typical of Eurasian rivers (Cooper et al. 2008) and ice melt (Yamamoto-kawai and Tanaka 2005) would decrease $\mathbf{\Omega}_{arag}$ even more, exacerbating corrosive conditions for calcium carbonate secreting organisms.

Cobbles transplanted in the field were extremely variable in their response (pigmentation and photosynthetic efficiency) to environmental change (Fig. 2.4, a-d). During the period of transplant (July 2016- July 2017), salinity levels at the inshore site did not fall below 20, while the following year (2017-2018), salinity at the inshore site was near zero (Fig. 2.1). These annual variations and periods of low salinity likely affect mature CCA assemblages and CCA recruitment at inshore sites, while extreme low salinity events may prevent CCA establishment entirely. In addition to changes in salinity, other factors such as sedimentation could also influence CCA distributions (Wilson et al. 2004), and this could have affected *in situ* transplant experiment results.

Recruit size and density were significantly ($p< 0.05$) greater at the offshore site compared to the inshore site (Fig. 2.4, e and f). CCA recruitment observed onto settlement tiles at the inshore site shows that the absence of CCA at the inshore site is not related to propagule dispersal limitations (Bonsell and Dunton submitted). CCA propagules did reach the inshore site, but their size and density were reduced when compared to the offshore site. We hypothesize that persistence of adult communities is prevented by water chemistry changes associated with low salinity pulses at the inshore site. Other CCA species (*Lithothamnion glaciale*) have shown tolerance to low salinity conditions, but as in our mesocosm studies, these studies were conducted on mature individuals (Burdett et al. 2015). However, further studies are needed to quantify and observe other factors such as grazing (Wai & Williams 2006) and sedimentation

(Wilson et al. 2004) on recruitment.

During the years of this study (2016-2018), $\mathbf{\Omega}_{arag}$ levels were close to one for much of the year (Muth et al. 2020a), even at the offshore site where CCA cover the benthos. Gangstø et al. (2008) predicted that Arctic waters could reach $\mathbf{\Omega}_{arag} = 1$ levels by 2100, but our work has already documented these levels in arctic near-shore environments. It is important to note that corallines are composed of magnesium calcite, and this form of calcium carbonate is ~20% more soluble than aragonite (Kamenos et al. 2008). CCA species in the Boulder Patch survive at $\mathbf{\Omega}_{arag}$ ~1, but during the period of spring break-up (~4-5 weeks) salinity levels drastically drop (Fig. 2.S1), and this in turn affects $\mathbf{\Omega}_{arag}$ levels (Fig. 2.1). These events likely drive CCA distributional patterns in Stefansson Sound.

Ecological Implications

Predicted increases in freshwater input and the overall susceptibility of the Arctic to ocean acidification threaten to drastically change the carbonate chemistry of nearshore systems and their biological assemblages (Kelley and Lunden 2017). This study focuses on CCA physiology and the resultant distributions, but distributions and population dynamics also affect entire communities through species interactions (Kroeker et al. 2012).

Corallines are known to grow laterally rather than vertically when colonizing space, allowing them to cover the benthos (Airoldi 2000). However, the roles which corallines play in algal and sessile invertebrate succession vary drastically across communities. Studies have shown that corallines enhance biodiversity (Asnaghi et al. 2015) while other work has focused on the lack of further algal recruitment once coralline secure dominance (Bulleri et al. 2002). Johnson and Mann (1986) found *Phymatolithon* in Nova Scotia to suppress the recruitment of turf algal species. A similar pattern has been observed in the Boulder Patch in Stefansson Sound,

but some algal species possess the ability to recruit to CCA (*Laminaria solidungula* and *Rhodomela confervoides,* pers. obs,). The mechanism that allows for this recruitment is unknown, but slower growing crusts (e.g., *Lithothamnion phymatodeum*; Dethier and Steneck 2001) have shown resilience to turf overgrowth and shading. In Stefansson Sound, CCA appears to inhibit red algal occurrence but facilitates kelp recruitment (Chapter 4). The mechanism driving this pattern is not clear but as CCA cover varies, algal and invertebrate assemblages co-vary.

The susceptibility of CCA to variations in carbonate chemistry (reviewed in Nelson 2009) makes these species ideal sentinels as bioindicators of change in ocean chemistry in near-shore environments. Coral species in tropical zones have been used as ocean acidificationOA bioindicators (Fabricius et al. 2012) while sea-level rising has been estimated using CCA presence (Ortlieb et al. 1996). In the Arctic, freshwater inputs are expected to increase (Peterson et al. 2006), and few studies have considered the effects of decreased salinity in exacerbating the effects of anthropogenic OA (Schoenrock et al. 2018).

Seasonal, low salinity pulses, as seen in the Boulder Patch (Muth et al. 2020a) affect CCA recruitment and growth. As freshwater input into the Arctic Ocean increases, areas devoid of CCA could increase, causing changes in epilithic communities. CCA are conspicuous benthic species, and their presence and absence could serve as an effective tool for assessing water quality changes in the nearshore Arctic that will not only affect CCA, but also other marine calcifying organisms. Increased freshwater input is not unique to the Arctic, and this work highlights the importance of salinity in CCA physiology. More exploration into the functional role of CCA species is needed to fully understand ecological consequences should CCA densities decrease or disappear under future ocean conditions.

Acknowledgments:

This study was funded under BOEM Award Number M12AS00001 as part of the Continuation of the Arctic Nearshore Impact Monitoring in Development Area (cANIMIDA) Project and the BOEM Alaska Environmental Studies Program and STAR Fellowship Assistance Agreement no. FP917814 awarded by the U.S. Environmental Protection Agency (EPA). It has not been formally reviewed by EPA. The views expressed in this publication are solely those of Arley F. Muth and EPA does not endorse any products or commercial services mentioned in this publication. We thank J. Lonthair, C. McClure, K. Schoenrock, M. Fox, M. D. Johnson for help and advice on laboratory techniques. We are grateful to P. Gabrielson who sequenced the CCA species and C. Bonsell, J. Dunton, and T. Dunton for field and collection assistance and M. Mueller for GOM water collection.

TABLES

Table 2.1 A_T (μmEq L^{-1}) values of the culture medium at the beginning and end of each week during the experimental and recovery period (see Fig. 2.3). Values are means (±SE), n=5.

	Experimental Period		Recovery Period	
	Start Average	**Week-Old Average**	**Start Average**	**Week-Old Average**
Control	2512.82 (119.11)	2431.00 (117.11)	2771.72 (54.38)	2741.62 (50.55)
10	1208.04 (114.41)	1732.16 (63.10)	2719.36 (69.77)	2695.56 (47.42)
20	1870.68 (95.29)	1951.92 (71.55)	2734.06 (68.25)	2688.58 (55.60)
30	2550.00 (114.15)	2543.76 (77.73)	2691.54 (84.90)	2724.98 (29.49)

Table 2.2 Calculated carbonate chemistry parameters for media used to make salinity treatments in laboratory experiments. Bicarbonate (HCO_3), carbonate (CO_3) and aqueous carbon dioxide (CO_2) concentrations for each treatment are listed here. An **Ω** level greater than one favors precipitation and less than one favors dissolution, while one is at equilibrium with respect to aragonite. Values are means (± SE).

Salinity Treatment	HCO_3 (mmol $kgSW^{-1}$)	CO_3 (mmol $kgSW^{-1}$)	CO_2 (mmol $kgSW^{-1}$)	Ω_{arag}
10	1131.1 (107.2)	32.4 (9.3)	17.2 (3.1)	0.5 (0.1)
20	1711.8 (100.1)	64.9 (13.0)	21.7 (3.6)	1.0 (0.2)
30	2293.0 (65.9)	105.4 (2.4)	25.9 (1.1)	1.6 (0.1)

FIGURES

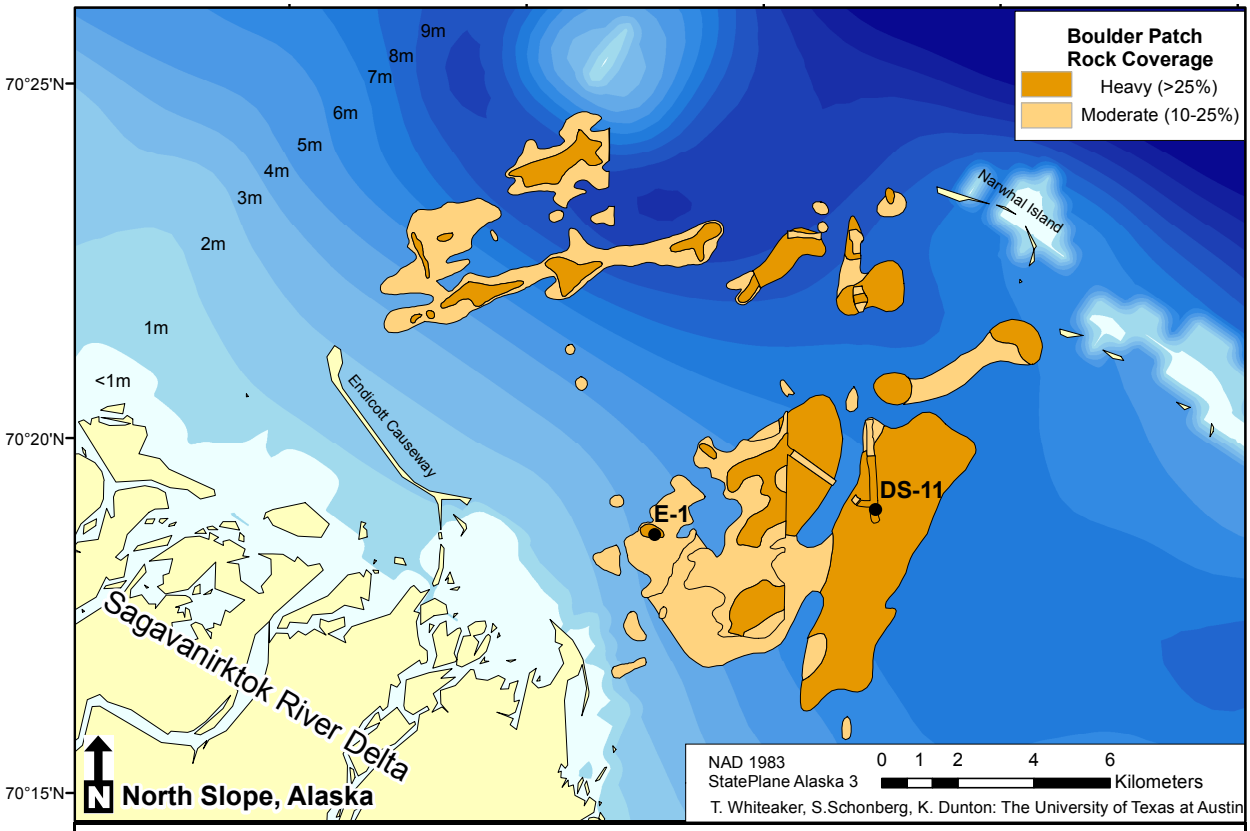

Site	E-1	DS-11
CCA	No CCA present	CCA present
Distance from the Sagavanirktok (km)	3.5	9
Depth (m)	4.5	6
Salinity (2016-2018)	0.0 - 34.0	21.9-34.8
Ω Arag (2016-2018)	0.1 - 4.9	0.3 - 4.8
*Transplants	Cobbles with CCA transplanted from DS-11	Cobbles with CCA transplanted to E-1

Figure 2.1 The Boulder Patch kelp bed community in Stefansson Sound, Alaska showing rock cover, site distances (km) from the Sagavanirktok River (Sag), and ranges of salinity and Ω_{arag} (Muth et al. 2020a).

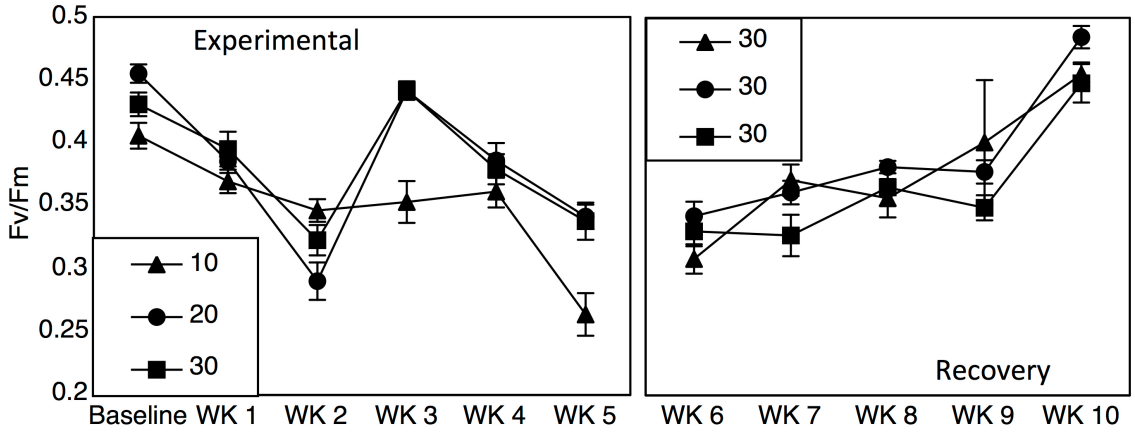

Figure 2.2 Fv/Fm values (± SE, n=3) across 5 weeks of salinity treatments (10, 20 and 30) and 5 weeks in a recovery treatment of 30.

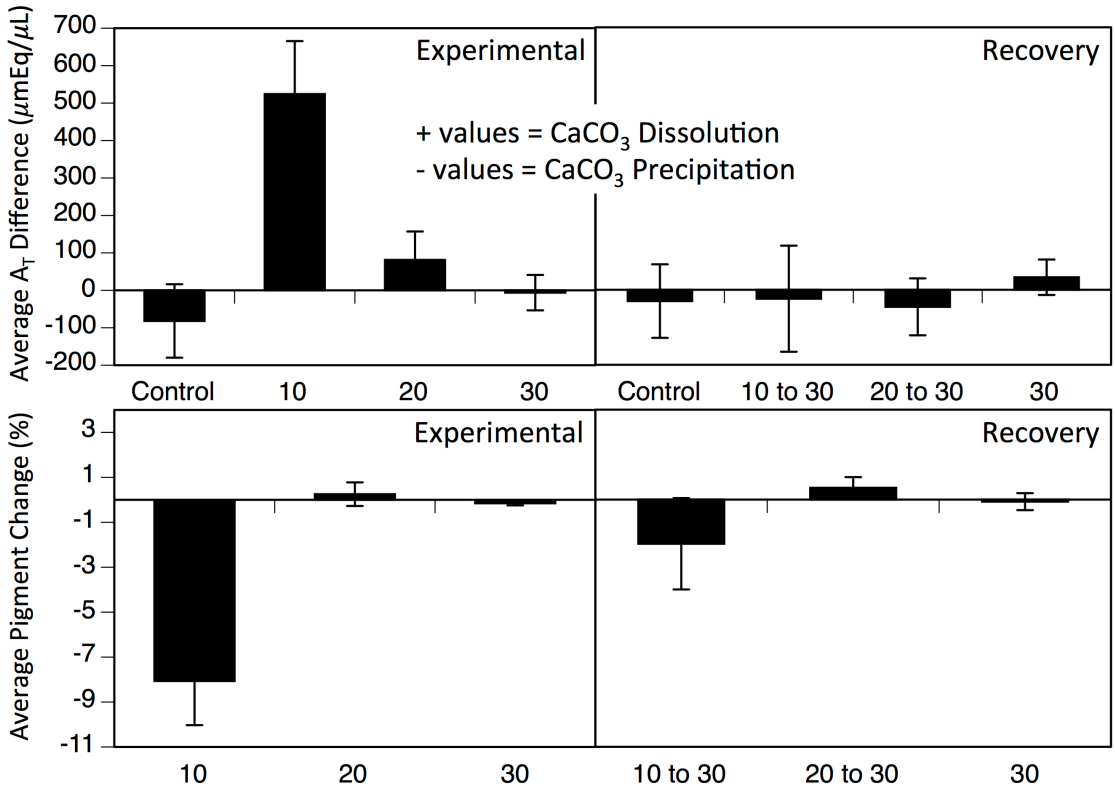

Figure 2.3 Top: Average weekly differences in A_T of the culture medium (+/- SE, n=4) over 5 weeks at varying salinities (10, 20, 30 and control without any cobbles) and 5 weeks of recovery, when all treatments were at a salinity of 30. Bottom: Average pigment loss over 5 weeks of salinity treatments (10, 20 and 30) and 5 weeks of recovery, when all treatments were at a salinity of 30. Values are means ±SE, n=5.

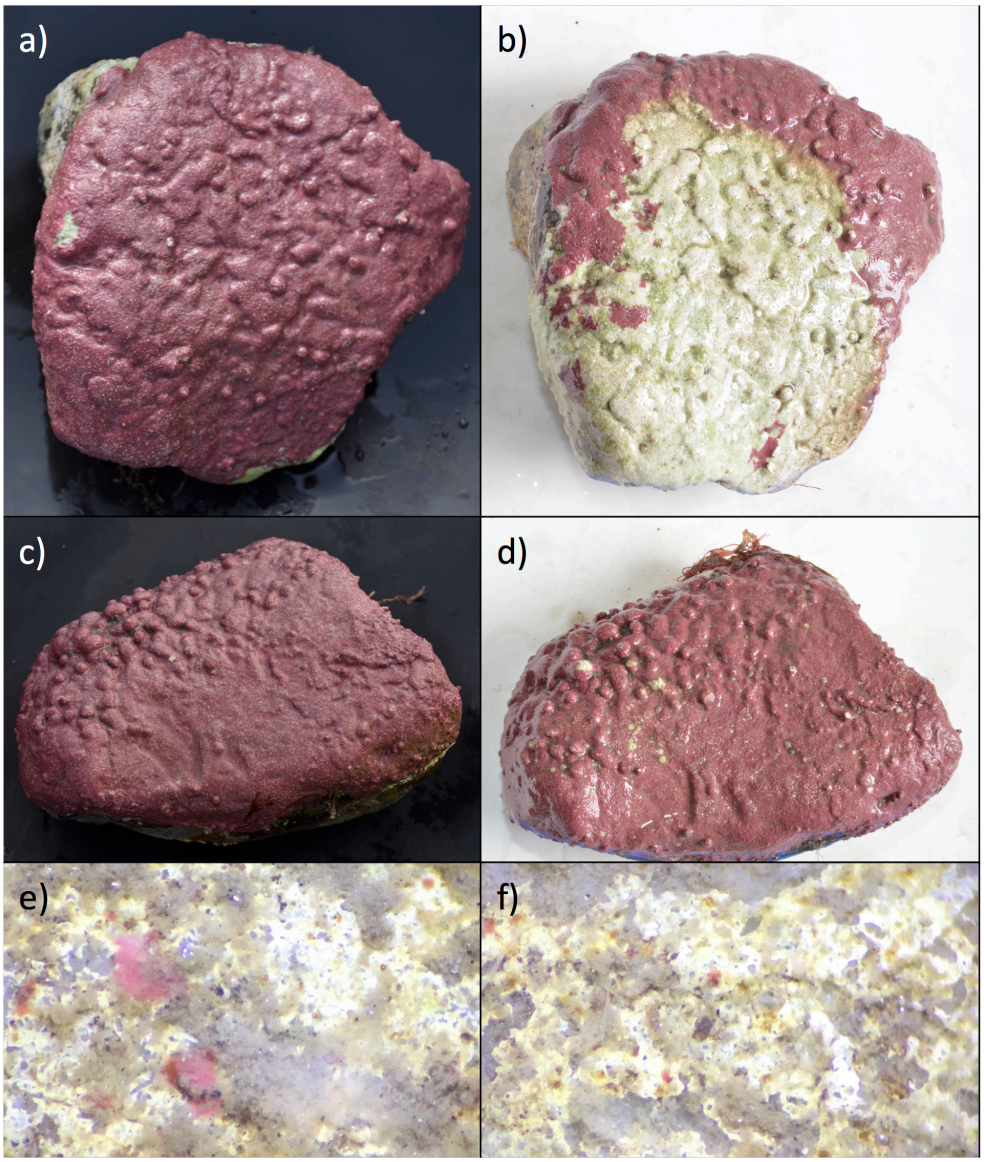

Figure 2.4 Examples of field experiments, transplanted cobbles and recruits from each site. (a) cobble from offshore site D-11 photographed in 2016 pre-transplant (b) same cobble as (a), photographed in 2017 following a 12-month transplant to inshore site E-1, showing high pigment loss (c) cobble from offshore site D-11 photographed in 2016 pre-transplant d) same cobble as (c), photographed in 2017 following a 12-month transplant to inshore site E-1, showing low pigment loss (e) one year recruits at the offshore site (DS-11) at 400x (f) one year recruits at the inshore site (E-1) at 400x.

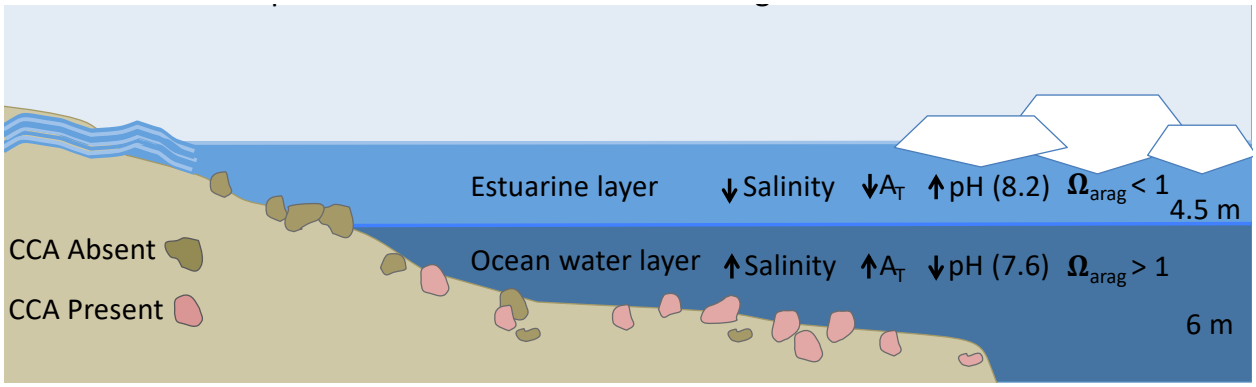

Saturation level of calcium carbonate (aragonite) $\mathbf{\Omega} = [Ca^{2+}]\,[CO_3^{2-}] / [CaCO_3]$ solubility

Total Alkalinity (A_T)= $2[CO_3^{2-}] + [HCO_3^-] + [OH^-] - [H^+]$

Figure 2.5 Conditions during ice break-up in the nearshore inner shelf region of the Beaufort Sea. Freshwater input from rivers peaks while remnant sea-ice reduces wave action and mixing, creating a stratified water column with a less dense brackish or estuarine water layer over cold, dense ocean water. Benthic regions within the freshwater layer experience low salinity and alkalinity conditions, driving down the aragonite saturation state, causing dissolution of the CCA populations. Lower salinity water (5-15) is characterized by lower A_T values (1900 μmEq L^{-1}) than ocean water (>30-salinity and 2400 μmEq L^{-1}). Lower A_T values decrease the numerator in the $\mathbf{\Omega}$ equation, depressing $\mathbf{\Omega}_{arag}$ levels. This process is independent of pH, as river water pH is higher than ocean water in many near-shore Arctic systems. As break-up continues, wind driven mixing occurs, creating a homogenous water column for the summer and ice-covered seasons.

SUPPLEMENTARY MATERIAL

Table 2.S1 Weekly start and end measurements of media salinity, pH and A_T for the experimental studies in culture.

					Treatment								Recovery						Averages			
	15-Feb	22-Feb	22-Feb	1-Mar	1-Mar	8-Mar	8-Mar	15-Mar	15-Mar	22-Mar	22-Mar	29-Mar	29-Mar	5-Apr	5-Apr	12-Apr	19-Apr	19-Apr	26-Apr	Treatment		Recovery
	w1 - start	w1 - end	w2 - start	w2 - end	w3 - start	w3 - end	w4 - start	w4 - end	w5 - start	w5 - end	w6 - start	w6 - end	w7 - start	w7 - end	w8 - start	w8 - end	w9 - start	w9 - end	w10 - start	w10 - end	Avg - start	Avg - end	Avg - start	Avg - end
Salinity																								
control	30.1	30	30.03	30.23	31.48	31.36	31.61	31.45	31.52	31.73	31.82	–	31.7	31.67	31.5	31.3	31.1	28.7	29.4	29.8	30.948	30.954	31.104	30.355
10	10.21	10.6	10.06	10.38	10.3	10.81	10.25	10.43	10.32	10.4	31.69	31.39	31.95	32.34	32.24	31.01	31.1	30.96	29.8	29.75	10.228	10.524	31.356	31.33
20	21.01	20.8	20.98	21.08	20.02	21.05	21.13	21.02	20.78	20.98	31.52	31.48	30.64	31.97	32.51	30.4	31.12	31	30.7	30.95	20.784	20.986	31.298	31.16
30	30.8	31	31	30.98	31.86	31.87	31.62	31.82	32.06	31.98	31.37	31.47	31.88	31.88	31.87	31.6	31.08	31.02	30.82	30.96	31.436	31.458	31.404	31.386
																					Treatment		Recovery	
AT																					Avg - start	Avg - end	Avg - start	Avg - end
control	24743	2459.8	2156	2144.2	2382.7	2394.8	2776.1	2307.3	2775	2848.9	2639.1	2821.2	2653.5	2649.3	2788.9	2773.6	2888.3	2599.6	2888.8	2864.4	2642.27	2586.31	2771.72	2741.62
10	12966	1565.1	972.6	1842.2	1525.6	1868.2	1326.6	1597.8	918.8	1787.5	2523.6	2569.8	2607.8	2619.2	2898.2	2796.4	2840	2809.6	2727.2	2682.8	1208.04	1732.16	2719.36	2695.56
20	18174	1768.7	1684.1	2027	1742.7	1905.5	2227.7	2185.9	1881.5	1872.5	2538.4	2492.9	2601.2	2639	2828.7	2777.8	2872.7	2788.5	2829.3	2744.7	1870.68	1951.92	2734.06	2688.38
30	24927	2428.8	2228.2	2397.8	2528.6	2529.4	2539	2526.1	2941.5	2836.7	2726.9	2673.6	2366.7	2652.7	2767.6	2804.5	2864.7	2780.5	2731.8	2713.6	2550	2543.76	2691.34	2724.98
																					Treatment		Recovery	
pH																					Avg - start	Avg - end	Avg - start	Avg - end
control	8.3	7.93	8.03	7.8	8.03	7.97	8.06	7.74	8.03	8.07	8.01	–	8.03	7.82	8.01	7.74	8.03	7.94	8.01	7.83	8.09	7.902	8.018	7.8325
10	8.49	8.01	8.01	7.9	8.04	8.04	8.03	7.87	8.02	7.94	8.03	7.73	8.06	7.98	8.03	7.58	8.03	7.85	8.05	7.8	8.118	7.952	8.04	7.788
20	8.44	7.92	8.07	7.85	8.03	7.89	8.04	7.78	8	7.79	8.05	7.85	8.02	7.81	8.01	7.65	8.03	7.8	8.08	7.8	8.116	7.846	8.038	7.782
30	8.3	7.74	8.02	7.93	8.05	7.81	8.07	7.65	8.01	7.76	8	7.92	8.01	7.78	8.02	7.71	8.03	7.95	8.09	7.82	8.09	7.778	8.03	7.836

Chapter 3: Life history stage tolerance to seasonal variability in light and salinity in an Arctic kelp (Laminaria solidungula)

ABSTRACT

The kelp *Laminaria solidungula* is an important foundation species in the circumpolar Arctic. One of the largest populations of *L. solidungula* in the Beaufort Sea occurs in Stefansson Sound, off the north coast of Alaska. We surveyed kelp populations in the Stefansson Sound Boulder Patch and found that sites in close proximity (3.5 km) to river input and increased turbidity exhibited lower densities (0.36 ± 0.44 m^{-2}) than offshore sites (4.72 ± 1.51 m^{-2}). Culture experiments with varying light and salinity conditions were used to observe the significance of these factors interactively and separately on microscopic sporophyte production and survival. Microscopic stages cultured in the low salinity treatment were unable to produce sporophytes regardless of light level; while the highest light level (40 µmol photons m^{-2} s^{-1}) produced the highest sporophyte densities (0.37 ± 0.08 mm^{-2}) at a salinity of 30. An additional experiment was used to assess the effects of salinity at each microscopic stage. EE arly 1N microscopic stages (zoospores and gametophytes) were not capable of producing 2N sporophytes at a salinity of 10, but microscopic 2N sporophytes were tolerant of this lower salinity. Current light and salinity seasonal variations recorded in the Boulder Patch fall within the tolerance levels of *L. solidungula* microscopic stages. Although *L. solidungula* sporophytes have apparently acclimated to extreme salinity (0-33) and light variations, the vulnerability of 1N microscopic stages to reduced salinity has the potential to affect future populations as the timing and magnitude of freshwater input to the Arctic Ocean changes.

INTRODUCTION

Brown seaweeds of the order Laminariales (kelps) play important roles in nearshore marine ecosystems by providing a food source and habitat through their physical structure (Steneck et al. 2002, Graham 2004). Over 100 species of kelp are distributed world-wide along temperate coastlines into high latitude polar regions (Druehl 1970). Although many kelp species play similar ecological roles, response to variations in environmental factors differ tremendously. Certain species can adjust timing of their growth and reproduction to when conditions are favorable (e.g., *Macrocystis*) while other species respond to specific extrinsic factors (i.e., daylight; *Pterygophora californica*; Reed et al. 1996) or possess endogenous rhythms that are linked to day-length (Lüning & Kadel 1993). These rhythms may be based on species adaptation to environmental fluctuations over long periods (temperature, Matson and Edwards 2007; nutrients, Dunton et al. 1982; light, Reed et al. 1996). Sentinel population biology theory (Harper 1977) stresses the importance of considering all life history stages when exploring adult population dynamics. Abiotic factors affecting adult kelp processes also affect reproductive success, and include temperature (Deysher and Dean 1986b, Matson and Edwards 2007, Muth et al. 2019), nutrients (Santelices and Ojeda 1984), light (Lüning and Dring 1979, Lüning 2018), and settlement densities of zoospores (Reed et al. 1991, Muth 2012). The ability to predict biotic and abiotic controls on all life history stages of kelp species is a critical step towards understanding population dynamics.

Kelps possess a diplohaplontic life history strategy for reproduction. Macroscopic 2N sporophytes release microscopic 1N zoospores (meiospores) that settle onto the substrate, undergo gametogenesis, form gametophytes and release 1N gametes. Male gametophytes produce and release spermatazoids that fertilize eggs protruding from female gametophytes.

Once fertilization occurs, a microscopic 2N sporophyte is produced (Fig. 3.1). Often, microscopic stages are more vulnerable to changes in environmental conditions (Deysher and Dean 1986a, reviewed in Graham et al. 2007, Harley et al. 2012, Muth et al. 2019), which ultimately affects adult population persistence (Graham et al. 2007).

Laminaria solidungula J.Agardh, is the only Arctic endemic kelp. Like many kelps, this species provides a source of carbon and habitat for benthic communities along the northern coasts of Alaska and Russia (Dunton and Schell 1987, Filbee Dexter 2019). Known as a "season anticipator" (Wiencke et al. 2006), *L. solidungula* optimizes annual light and nutrient variability by fixing carbon when light is available (summer), and producing new frond tissue during the dark winter period when nitrogen is available in nearshore Arctic waters (Dunton et al. 1982, Dunton & Schell 1986). As a perennial species with high biomass, it represents a foundation species in many parts of the Arctic (Dunton et al. 1982).

The Stefansson Sound Boulder Patch, located on the north coast of Alaska, is a defined area of rocky substrate composed of boulders and cobbles that creates a habitat for kelp populations (Fig. 3.2). The Boulder Patch is characterized by high floral and faunal diversity and is the basis of a diverse food web in an otherwise highly oligotrophic system (Dunton and Schell 1987; Dunton and Schonberg 2000; Wilce and Dunton, 2014). In Stefansson Sound, nearshore salinity and light levels differ drastically on both spatial and temporal scales (Dunton et al. 1992, Sellmann et al. 1992, Bonsell & Dunton 2018), but the effects of such variability on the population demographics of *L. solidungula* are not well understood. Since observations by divers over several years suggest that there are strong spatial differences in kelp density, we sought to first quantify these differences and secondly, examine the potential mechanisms that would affect kelp density and distribution within the Boulder Patch. To address the second

objective, we designed experiments to 1) quantify the effects of salinity and light separately and interactively on *L. solidungula* microscopic stages and sporophyte production and 2) overlay seasonal variability in light and salinity with corresponding life history stages.

METHODS

Site Overview

The Stefansson Sound Boulder Patch (Fig. 3.2) is a shallow shelf (less than 10 m depth) located near the mouth of the Sagavanirktok River. This area is unique from the sediment substrate of the Beaufort Sea because of the presence of boulders and cobbles that support a diverse and productive benthic community (Dunton et al. 1982). The benthic communities of the Boulder Patch are exposed to drastic seasonal variability, including ice-cover and low-light conditions during winter months and a large pulse of freshwater from the Sagavanirktok River that enters the sound every spring (Dunton et al. 1982, Bonsell & Dunton 2018). Throughout the Boulder Patch, *Laminaria solidungula* population densities vary, but kelp are present in nearly all areas with rock cover.

Boulder Patch Kelp Densities

To quantify *Laminaria solidungula* densities at three sites within the Boulder Patch, 0.05 m^2 photoquadrats were taken with a Nikon 1 AW1 waterproof digital camera in July and August 2016 and 2017. Photographs were taken in a spiral pattern around a central point at three sites: DS-11, E-1, and W-3 (Fig. 3.2). Rock cover within the Boulder Patch varies greatly (Fig. 3.2), and because kelp species need rock to recruit, photographs were taken when rock coverage was >75%. This process standardized rock cover among sites and allowed for direct comparisons of kelp densities among sites. *Laminaria solidungula* densities were quantified from photoquadrats

taken at three sites within the Boulder Patch (n values, E-1=36, DS-11=31, W-3=35). Individuals were counted only if the holdfast was present within the quadrat (overlying blades were not counted). Densities were compared using a Kruskal-Wallis rank sum test and a Dunn test for pairwise comparisons.

Salinity and Light Culture Experiment

Reproductive *L. solidungula* individuals were collected from Endicott Island, Alaska and shipped to the University of Texas Marine Science Institute in October 2017. Samples were kept at 0°C in aerated filtered seawater until experiments were initiated. Reproductive sori were placed between layers of damp paper towels, kept in darkness for 24 h, then placed in 10°C seawater to induce sporulation (7 Dec 2017; Fig. 3.1). After sporulation, 10 mL of the solution was placed in 50 x 10 mm Petri dishes. The zoospore solution remained in the dishes for 1 week to allow for maximum settlement. The medium was then replaced with offshore Gulf of Mexico (GOM) seawater (oligotrophic) and mixed with reverse osmosis (RO) water to attain salinity treatments of 10, 20 and 30. Provasoli's Enriched Seawater (PES) was added to ensure the availability of all micro and macro nutrients (20 mL L^{-1}). After settlement, dishes were divided into three light treatments (10, 20 and 40 µmol photons m^2 s^{-2}) within the three salinity treatments using shade cloth, creating nine salinity/light treatments. Each treatment was replicated 5 times. Medium was changed weekly. Dishes were kept at 0°C in a 10:14 light:dark regime.

Dishes were monitored weekly for microscopic stage development. Initial settlement densities were quantified (15 Dec 2017) to ensure all treatments initially had similar settlement. Gametophyte densities were quantified once (26 Jan 2018) and sporophyte densities over one

month (28 Feb, 16 Mar, and 27 Mar), to track any delays in sporophyte production. Each dish was observed under 400x magnification for 10 fields of view (FOV).

Densities at each stage (settlement and gametophytes) were compared using two-way ANOVAs among light and salinity levels. Sporophyte densities were compared using a repeated measures ANOVA (time, light, salinity, and light X salinity) to assess sporophyte densities over time. The interaction of light and salinity was not significant ($p=0.59$) and was removed from the model. All statistics were run using R Version 3.3.1.

Salinity and stage-specific culture experiment

Zoospores and Gametophytes

Kelps have a multi-stage, complex life history and we observed the effects of salinity on (1) settled zoospores, (2) the ability of gametophytes to produce sporophytes, and (3) survivorship of sporophytes. Sporulation from five reproductive *L. solidungula* individuals was induced (11 Feb 2019), and equal aliquots of zoospore solution (10 mL) were settled onto 18, 50 x 10 mm Petri Dishes. As described above, the zoospore solution was left on the dishes for one week to allow for maximum settlement (0°C, 40 µmol photons m^2 s^{-2}, 10:14 light:dark regime). After one week, all dishes were replaced with GOM seawater and varying amounts of RO water to create salinity treatments (10, 20, and 30) as well as 20 mL L^{-1} of PES. Settlement densities were quantified for all dishes to ensure similar starting densities (18 Feb 2019; 10 FOV at 400x).

At the conclusion of the first week, salinity treatments were initiated to observe the effects of salinity on zoospore development and sporophyte production (salinity treatments of 10, 20 and 30, n=3). Nine dishes were replaced with control solution (30-salinity) and left for further observation once gametophytes were mature. Dishes were monitored, and media changes occurred weekly. Once gametophytes (pre-egg development) were present, salinity treatments

were enacted on the remaining nine dishes (salinity treatments of 10, 20 and 30, n=3; 27 Mar 2019).Once sporophytes were present in the control treatments (6 May 2019), presence and absence of sporophytes was recorded for each treatment (100x, 20 FOV), which enabled us to document the effects of salinity on each stages' ability to successfully produce sporophytes and complete the recruitment process (Fig. 3.3a).

Sporophytes

Survivorship of microscopic sporophytes was quantified by assessing densities (50x, entire dish) for 12 dishes (11 May 2019), initiating salinity treatments (n=4; 10, 20 and 30), and measuring sporophyte density in each dish after one month (12 June 2019). The initial quantity and final quantity of sporophytes were used to calculate percent change in sporophyte densities, and to compare densities among salinity treatments. We used a one-way ANOVA to compare the percent change in sporophyte densities.

RESULTS

Boulder Patch Kelp Densities

Adult *LaminariaL solidungula* densities were significantly different among Boulder Patch sites (Kruskal Wallis chi-squared = 14.3023, $p<0.0001$), and pairwise comparisons showed that DS-11(4.72 ± 1.51 m^{-2}) differed from E-1(0.36 ± 0.44 m^{-2}) and W-3 (0.72 ± 0.48 m^{-2}; DS-11 x E-1 $p<0.001$, DS-11 x W-3 $p<0.001$, E-1 x W-3 $p=0.3603$; Fig. 3.4). Rock cover is greatest at DS-11, intermediate at W-3 and least at E-1. However, photoquadrat methods standardized rock cover among sites, and these results are independent of substrate changes.

Salinity and Light Culture Experiment

Zoospore settlement densities were not significantly different among salinity and light treatments and ranged from 0.79 to 1.45 zoospores mm^{-2} (2-way ANOVA, light vs. salinity $F_{3,41}$ = 0.3293, p=0.80; Table 3.S1, Fig. 3.5). Any differences in gametophyte or sporophyte densities are assumed to be a result of environmental conditions after settlement.

Gametophyte densities were significantly different among salinity treatments, however, there was no significant difference among light treatments or the salinity light interactions (2-way ANOVA, salinity $F_{2,41}$ = 21.67, p<0.001; Fig. 3.6). The low salinity treatment (10) had significantly lower densities (0.04±0.04) than the 20 (0.22±0.03) and 30 (0.42±0.04) treatments; light (p=0.41) and the interaction between light and salinity (p=0.61) did not have a significant effect. Gametophytes were not produced in the 20 and 40 umol photons m^{-2} s^{-1} light treatments, at a salinity of 10.

Sporophytes densities were quantified over one month; however, time was not significant (p=0.127). Sporophyte densities were significantly higher in the 40 umol photons m^{-2} s^{-1} light treatments than the 10 umol photons m^{-2} s^{-1} light treatment (p=0.007; Fig. 3.7, Table 3.S1), and densities in the 10-salinity treatment was significantly different (no sporophytes produced) than the 20 and 30 treatments (repeated measures ANOVA: light p=0.01, salinity p<0.001).

Salinity and stage-specific culture experiment

Zoospores and gametophytes

Zoospore densities did not significantly differ among treatments, ensuring that all treatments began with similar settlement densities (salinity: 10, 1.02 ± 0.27; 20, 1.53 ± 2.79; 30, 1.60 ± 0.31 zoospores mm^{-2}; one way ANOVA $F_{2,21}$=0.265, p=0.7691). Once zoospore densities were quantified, salinity treatments were placed within the dishes, and sporophyte

presence or absence was recorded after 11 weeks. Dishes exposed to salinities of 10 and 20 at the zoospore stage did not produce sporophytes, while dishes in the 30-salinity or control treatment were able to complete the fertilzation process and produce sporophytes (Fig. 3.3b).

After initial settlement counts, nine dishes were treated with the control treatment (30-salinity) and left until gametophytes developed. Once gametophytes developed (after five weeks), salinity treatments were enacted within the gametophyte dishes, and sporophyte presence or absence was recorded after six weeks (same date as the zoospore experimental dishes). Gametophytes exposed to the low salinity treatment (10) were unable to produce sporophytes, but gametophytes exposed to the higher salinity treatments (20 and 30) were successful in recruitment (Fig. 3.3b).

Sporophyte Survivorship

Survivorship of three-month-old sporophytes was compared among salinity treatments after a one-month exposure time. The sporophytes in the 10-salinity treatment had initial densities of 15.75 ($\pm$3.42) and after one-month averaged 22 ($\pm$4.06) sporophytes per dish. These changes represent a 62.48% increase in sporophytes, highlighting sporophyte survival and continued development in the low salinity treatment. Initial densities in the 20-salinity treatment were 17.75 ($\pm$2.62) and increased to 31.5 ($\pm$7.97) over one-month, a 74.53% increase in sporophytes. Although not significant ($F_{2,10}$=1.69, p=0.22), the salinity of 30 did have the highest percent increase (130.68%), starting at 18 ($\pm$4.81) and almost doubling to 37 ($\pm$5.21) sporophytes per dish.

DISCUSSION

Tolerance of kelp microscopic life history stages to environmental factors often determines species population persistence and distribution (Peteiro and Sanchez 2012, Muth et al. 2019). Low light and temperature tolerances of early life stages are critical adaptations for polar seaweeds (reviewed in Wiencke et al. 2006); however, nearshore Arctic species must tolerate extreme salinity variations as they are exposed to large freshwater inputs (Wiencke et al. 2006, McClelland et al. 2012). Results of this study highlight low light acclimation and disparate salinity tolerances for macro and microscopic stages of the kelp *L. solidungula*.

Laminaria solidungula Microscopic Stages

Laboratory culture experiments allowed the effects of light and salinity on sporophyte production to be quantified independently. *Laminaria solidungula* was cultured under replete nutrient regimes and settlement densities were very close to 1 mm^{-2} for both culture experiments (Fig. 3.5; Reed et al. 1991). Lower settlement densities resulted in lower gametophyte and sporophyte densities, but were high enough for successful fertilization and formation of sporophytes. Because settlement density did not differ among treatments from day one of both experiments, initial densities did not affect final results.

Light

Experiments found that zoospore and gametophyte maturation and the production of sporophyte timing was not delayed in low light treatment levels (10 and 20 umol photons m^{-2} s^{-1}), but final sporophyte densities were significantly ($p<0.001$) higher in the high light (40 umol photons m^{-2} s^{-1}) treatment compared to the low light treatment (Fig. 3.7). Ecologically, low light levels should not limit maturation rates as these stages are developing on the benthos under ice at extremely low light levels (< 2 umol photons m^{-2} s^{-1}; Dunton 1990) in their natural environment (Fig. 3.8). These results demonstrate low-light adaption in *L. solidungula* microscopic stages

compared to other kelps (see tom Dieck 1993, table 4). Differences in light affected sporophyte production, but did not prevent recruitment from occurring as demonstrated in the salinity treatments (Fig. 3.7). *Laminaria solidungula* sporophytes are incredibly shade-tolerant (Dunton & Jodwalis 1988, Dunton 1990), and this trait is shared among all life history stages (tom Dieck 1993).

Salinity

Low salinity (10) decreased gametophyte densities (Fig. 3.6) and prevented sporophytes from forming (Fig. 3.7). Treatments testing salinity and light interactions were initiated after an initial settlement period, and gametophyte development was negatively affected by lower salinities (Fig. 3.6). This made it difficult to ascertain if sporophyte production was affected by diminished gametophyte production or the salinity treatments. A second culture experiment that examined the effects of salinity on each stage independently allowed us to specifically identify the most vulnerable stages.

A second experiment tested salinity treatments at different life history stages and revealed that zoospores were the least tolerant stage to low salinities. When exposed to the 10 and 20 salinity treatments, zoospores were unable to mature to produce sporophytes (Table 3.S1). Gametophytes exposed to the 20 and 30 salinity treatments were able to complete the recruitment process, but as noted in the first experiment, the 10-salinity treatment did not yield sporophytes (Fig. 3.3b). Interestingly, sporophyte survivorship was not affected by salinity (Fig. 3.3b). Lower salinity levels (10 and 20) had smaller percent increases in sporophytes over one month than the salinity of 30 treatment, but all treatments gained sporophytes, and the differences in percent increase were not significant ($p=0.22$) among the three salinity regimes. *Macrocystis pyrifera (integrifolia)* in Chile required high salinity levels and low temperatures for

microscopic stage development, but adults were able to persist in less optimal conditions (Buschmann et al. 2004), similar to *L. solidungula* adults.

It is important to note that adults were only observed in field conditions, and microscopic stages were cultured in medium composed of ocean water from the Gulf of Mexico and reverse osmosis freshwater. CultureC media was prepared by diluting ocean water, keeping all ion ratios constant. This approach mimics seawater dilution from the addition of freshwater (Kirst 1989), but ion concentrations are different depending on source water values.

Development Times

A common observation in both laboratory experiments was that *L. solidungula* microscopic stages developed at a much slower rate than most other kelps (Reed et al. 1991, Muth et al. 2019). Using *Macrocystis pyrifera* as a reference, settlement is generally counted after 24 h, germination after 48 h, gametophytes after seven days and sporophytes within two-five weeks (Reed et al. 1991). *Laminaria solidungula* settlement required a week, after which we needed nearly three weeks to distinguish and count germinated zoospores. Gametophytes were generally seen after 6 weeks and sporophytes after 10 weeks. *Laminaria solidungula* from the Canadian Arctic had similar developmental times, but produced reproductive material earlier and zoospore release occurred later than the populations of the Boulder Patch (Roleda 2016). Delayed maturation exposes the more vulnerable macroscopic stages to unfavorable environmental conditions, but it appears that life history stages have acclimated to local seasonal patterns of salinity (Bonsell and Dunton 2020) and irradiance (Dunton and Bonsell 2018). The delay may also benefit populations growing vegetatively until conditions improve and *L. solidungula* gametophytes have been seen to survive 18-months in complete darkness (tom Dieck 1993).

Scaling up to Laminaria solidungula populations

Laminaria solidungula adult populations were present at all sites surveyed (E-1, W-3, DS-11; Figs. 3.2 and 3.4) even when standardized to less available substrate (i.e, rock cover; see Fig. 3.4). However, densities were seen to decrease with proximity to the Sagavanirktok River (E-1 and W-3; Fig. 3.4). These sites annually experience lower salinity and light levels (Fig. 3.8; Dunton et al. 2020 NCEI archive; Bonsell and Dunton 2018). Adult populations of *L. solidungula* in Kongsfjorden, Svalbard, were more tolerant to low salinities (5) than other kelp species also present in the Boulder Patch (*Alaria esculenta* and *Saccarina latissma*; Karsten 2007). The timing of low salinity events with increased ocean temperatures (spring) may ameliorate *L. solidungula* adult populations in the Boulder Patch (Fig. 3.8). As opposed to Antarctic seaweed species, warmer water temperatures may increase Arctic kelp acclimation rates to changes in salinity changes (Karsten 2007). The sub-Antarctic species, *Lessonia flavicans,* exhibited decreased salinity tolerance when combined with stressful temperature (9 vs. 5°C) and photoperiod (6:18 vs. 18:6) conditions (Mansilla et al., 2014). Alternatively, low temperatures (0°C) in culture conditions of this study may have exacerbated hyposaline stress of the microscopic stages; however, these temperature conditions represent natural conditions for this species.

Results from the salinity and light experiment do show trends of high light ameliorating hyposaline conditions in *L. solidungula* sporophyte production. Zoospores exposed to a medium with a salinity of 20 were able to consistently produce more sporophytes in the high light treatment (40 umol photons m^{-2} s^{-1}; Fig. 3.7). With warming temperatures and reduced sea ice, hyposaline conditions may be less detrimental to kelp gametophytes and sporophyte production if more light is present (Clark 2013). However, higher temperatures also increase

kelp respiration rates causing the individuals to enter into carbon deficits and affect productivity (Wiencke et al. 2006).

Variable salinities within the Boulder Patch have been shown to affect other seaweed species, notably crustose coralline algae (CCA; Muth et al. 2020b). Results from the laboratory experiments presented in this study demonstrate resilience of microscopic sporophytes to low salinities and suggest that other factors, such as post recruitment survival, are affecting *L. solidungula* distributions. Although 1N microscopic stages are vulnerable to low salinity levels, these stages occur during months of stable oceanic salinity levels (Fig. 3.8). Microscopic sporophytes showed resilience to low salinity levels, and this may be an acclimation of *L. solidungula*, given that microscopic sporophytes are likely present during spring break-up when salinity levels decrease (Fig. 3.8). Long-term in situ monitoring studies within the Boulder Patch have noted that CCA are absent at E-1 (Bonsell & Dunton 2020), the site closest to the Sagavanirktok River. This is likely driven by lower salinity levels, as seen in *Lithothamnion glaciale* in Greenland (Schoenrock et al. 2018), which may ultimately affect *L. solidungula* densities. Previous work has seen kelp deforestation after low salinity events (reviewed in Steneck et al. 2002), but in these cases all foliose algae were also affected. Within the Boulder Patch, sites without CCA have increased red algal biomass and lower *L. solidungula* densities (Bonsell & Dunton 2020, Muth Chapter 4).

Predictable Variability

Although Arctic near-shore environments experience high annual variability in abiotic factors, the variability is relatively similar among years (Dunton & Bonsell 2020). Changes in the amplitude or timing of seasonal variability could be detrimental to *L. solidungula* populations and other species acclimated to long-standing seasonal patterns. For example, changes in the

timing of break-up, delays in zoospore release, and an increase of freshwater input into the system could affect the overlapping of favorable environmental variables with microscopic stage development (i.e., low salinity pulses when 1N microscopic stages are present). *Laminaria solidungula* adults were present at the inshore site and showed resilience to low light and salinity levels. Kelp density was reduced at lower salinity sites, and it does not appear that salinity and/or light alone could cause these decreases, as microscopic sporophyte survival was not affected by low salinity levels. The loss of CCA at the inshore sites as a result of low salinity levels (Muth et al. 2020a), may decrease kelp densities through the loss of positive turf/canopy interactions (Barner & Muth 2020). Work to explore these interactions is ongoing and critical to understanding current *L. solidungula* distributions and how these populations may respond with regional climatic warming and large scale ice retreat in the western Arctic Ocean.

FIGURES

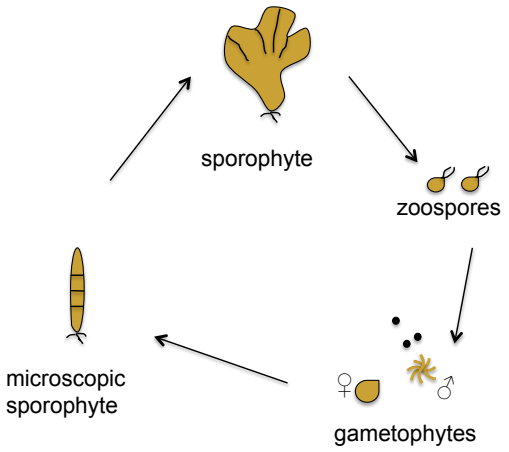

Figure 3.1 Generalized kelp life history. Macroscopic sporophytes (2n) release zoospores (1N) at a 50:50 sex ratio. Zoospores develop into male and female gametophytes, and the female egg is fertilized by the male spermatazoids, producing a microscopic sporophyte (2N).

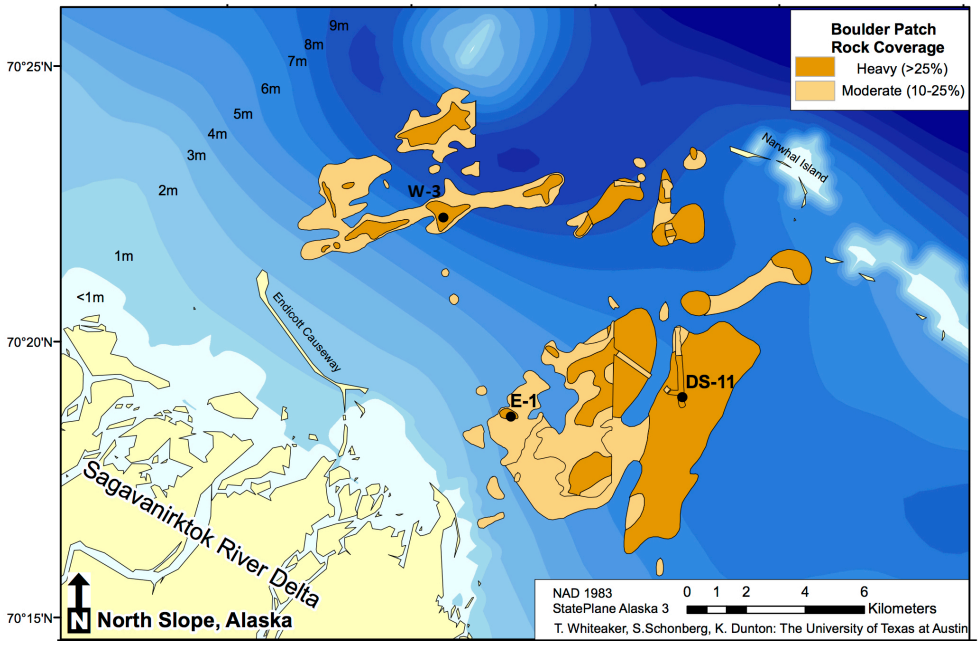

Figure 3.2 The Boulder Patch in Stefansson Sound. Rock cover is denoted by brown shading. Densities of *L. solidungula*were measured at E-1, W-3, DS-11. Adapted from from Bonsell and Dunton (2018).

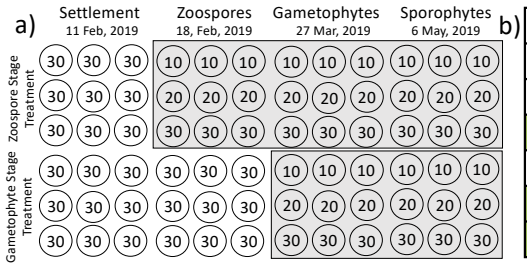

b)

Salinity Treatment	Stage	Sporophyte (y/n)
10	Zoospore	N
20	Zoospore	N
30	Zoospore	Y
10	Gametophyte	N
20	Gametophyte	Y
30	Gametophyte	Y

Figure 3.3 a) Experimental design for determination of salinity effects (at 10, 20, 30) on 1N microscopic zoospores and gametophytes and 2N sporophyte stages of *L. solidungula*. Gray shaded areas represent the stage and timing when salinity treatments were initiated. The Zoospore Stage treatment dishes received salinity treatments after settlement, once zoospores had attached and the Gametophyte Stage treatment received salinity treatments once gametophytes were. b) Overview of the presence and absence of microscopic sporophytes when salinity treatments (10, 20 and 30) were enacted at the zoospore or gametophyte stage. N (No) denotes treatments where sporophytes were not produced and Y (Yes) represents treatments with successful sporophyte production.

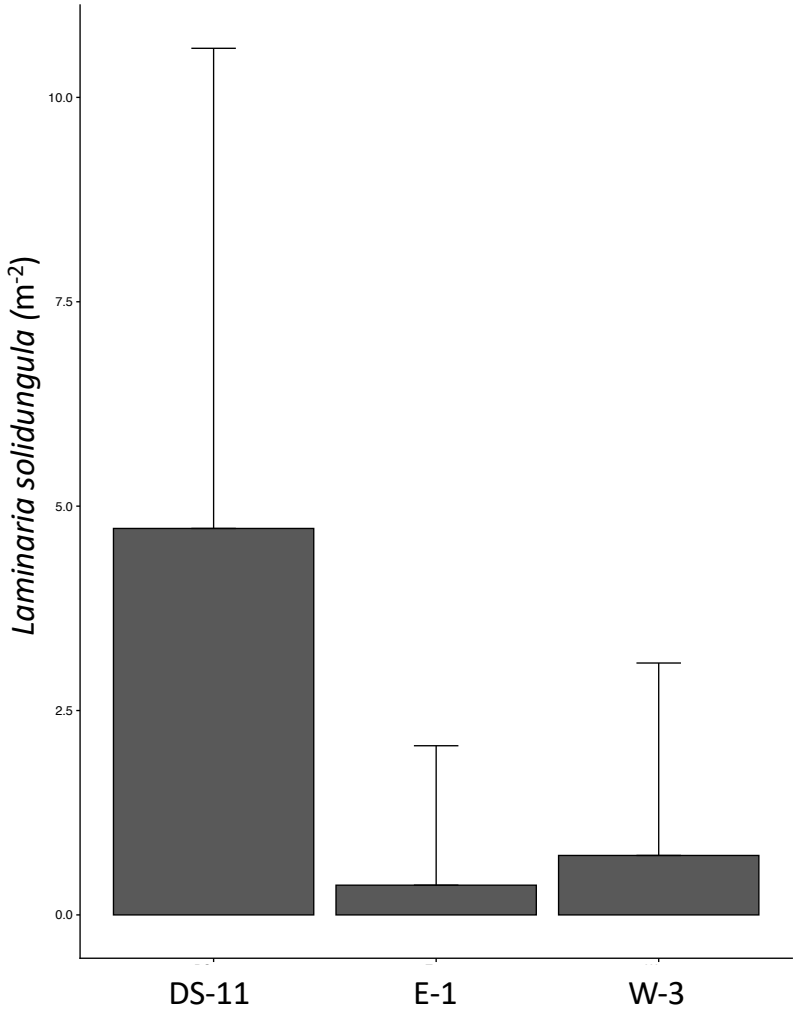

Figure 3.4 *Laminaria solidungula* densities (x ± standard deviation, n values DS-11=31, E-1=36, W-3=35) at DS-11, E-1, and W-3 within the Boulder Patch. Densities were quantified using photo quadrats and employed a standardized rock cover (75%) to minimize the effects of patchy hard substrate occurrence among sites.

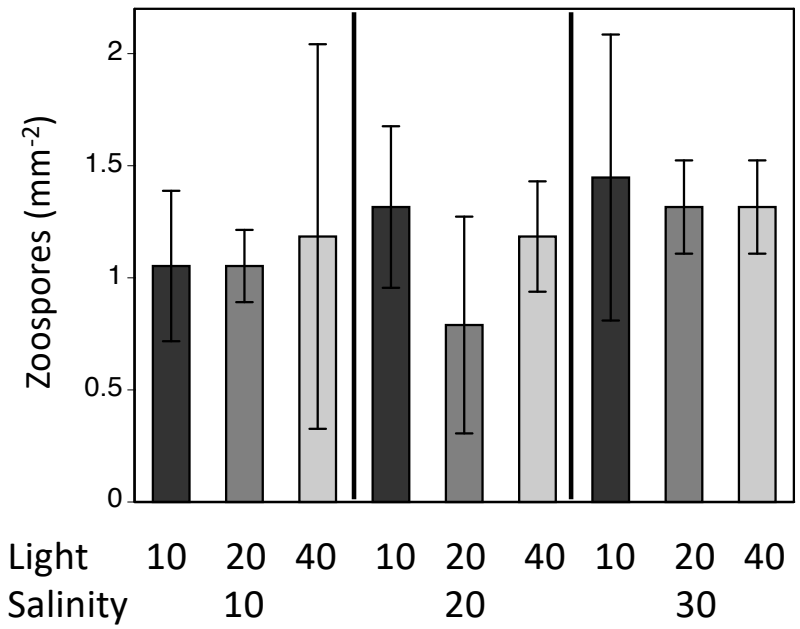

Figure 3.5 Zoospores mm^{-2} (x ± SE, n = 5) after a 1-week settlement period. There was no significant (p=0.80) difference among salinity or light treatments.

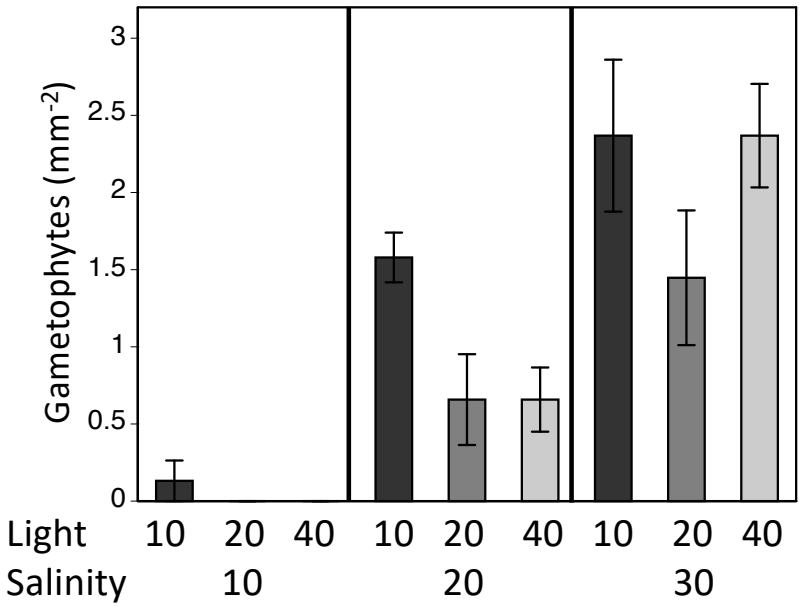

Figure 3.6 Gametophytes mm^{-2} (x ± SE, n = 5) Salinity treatments (10 vs. 20 10 vs. 30) were significantly different ($p<0.001$). Light ($p=0.41$) and salinity x light interaction ($p=0.61$)were not significant.

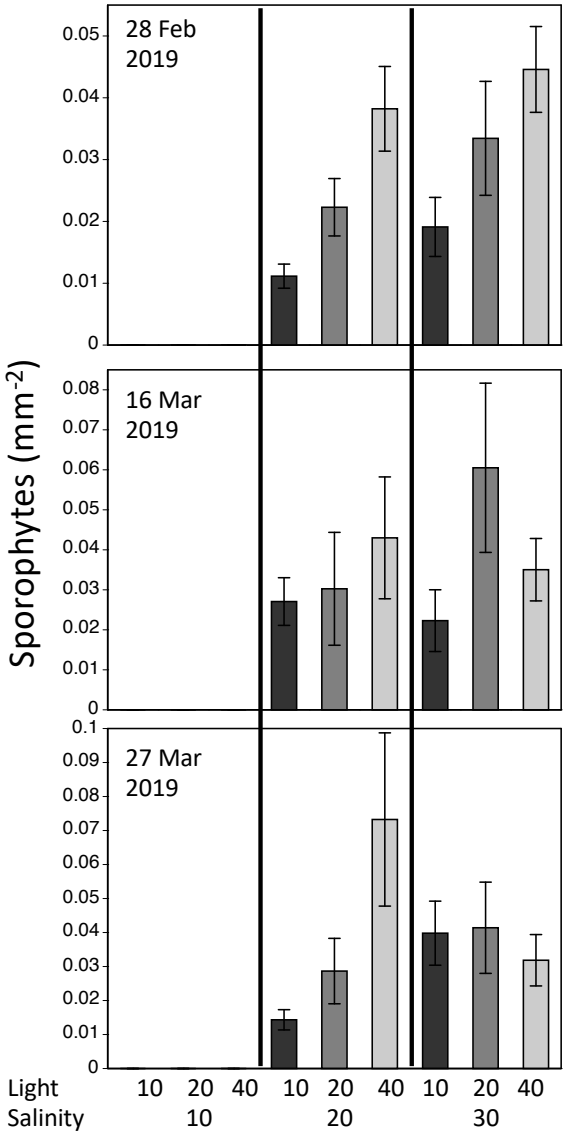

Figure 3.7 Sporophyte densities mm^{-2} (x ± SE, n = 5) from 28 Feb 2019 to 27 Mar 2019. Densities were significantly (p=0.007) lower in the 10 vs. 40 µmol photons m^{-2} s^{-1}. Sporophytes were not detected in the low salinity treatment (10), and densities were not significantly (p=0.65) different between the 20 and 30 treatments.

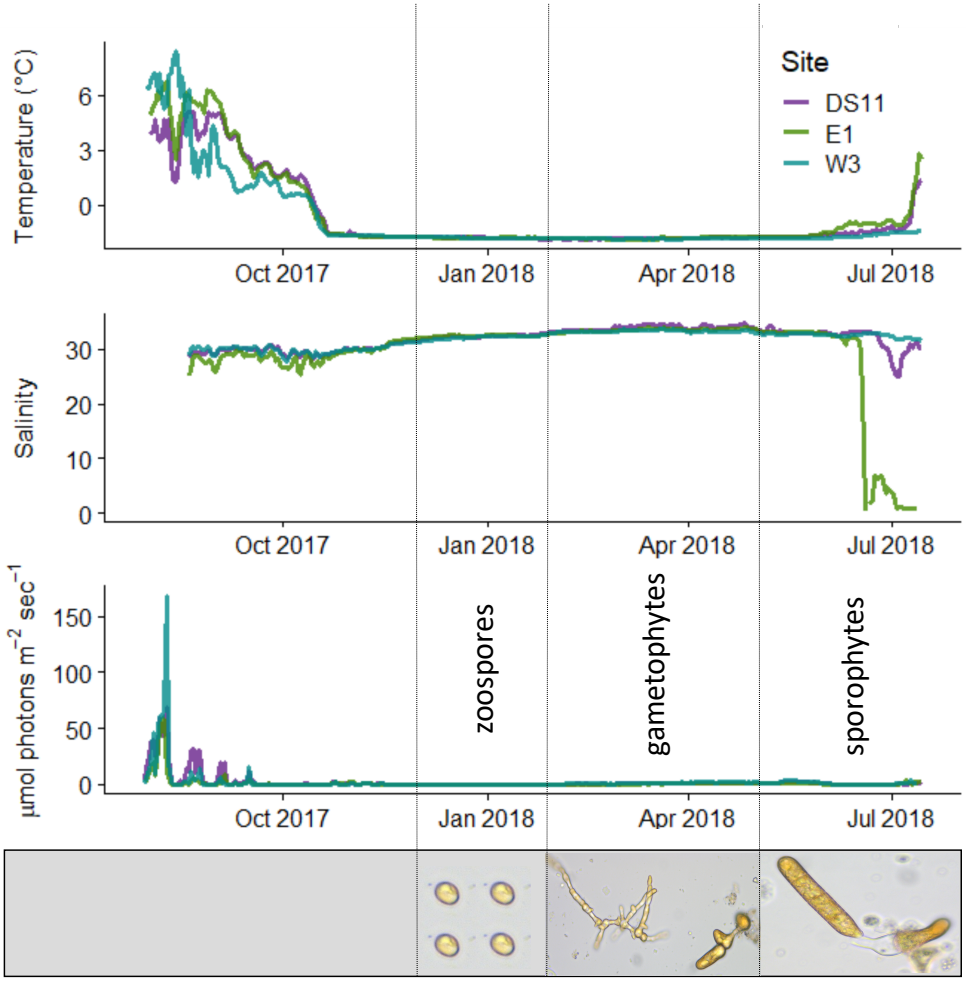

Figure 3.8 August 2017-August 2018 temperature (top), salinity (center) and light (bottom) for DS-11 (purple), E-1 (green), and W-3 (teal). Timing of *Laminaria solidungula* microscopic stage development along the annual patterns of light and salinity, highlight that zoospores and gametophytes are developing when ocean salinity levels are stable, and sporophytes are present when salinity becomes more variable. In addition, light levels are very low during all microscopic stage development. Adult populations are exposed to low salinity levels when temperatures are increasing, ameliorating osmotic stress and allowing rapid acclimation to the hyposaline conditions (data from Bonsell & Dunton 2020).

SUPPLEMENTARY MATERIAL

Table 3.S1 Treatments (salinity:10, 20, 30 and light: 10, 20, 40) and average densities for zoospores, gametophytes and sporophytes.

Salinity	Light (µmol photons m-2 s-1)	Zoospores (mm-2) 15 Dec 2017	Zoospores standard error	Gametophytes (mm-2) 26 Jan 2018	Gametophytes standard error	Sporophytes (mm-2) 28 Feb 2018	Sporophytes standard error	Sporophytes (mm-2) 16 Mar 2018	Sporophytes standard error	Sporophytes (mm-2) 27 Mar 2018	Sporophytes standard error
10	10	1.05263158	0.33546181	0.131578947	0.131578947	-	-	-	-	-	-
10	20	1.05263158	0.16115064	-	-	-	-	-	-	-	-
10	40	1.18421053	0.85778979	-	-	-	-	-	-	-	-
20	10	1.31578947	0.36034379	1.578947368	0.161150641	0.011146497	0.00195023	0.027070064	0.00595805	0.01433121	0.00297903
20	20	0.78947368	0.48345192	0.657894737	0.294219471	0.022292994	0.00464248	0.030254777	0.01410832	0.02866242	0.00962026
20	40	1.18421053	0.24616167	0.657894737	0.208044583	0.038216561	0.00684899	0.042993631	0.01523179	0.073248408	0.02547771
30	10	1.44736842	0.63785261	2.368421053	0.49232334	0.01910828	0.00477707	0.022292994	0.00771924	0.039808917	0.00942051
30	20	1.31578947	0.20804458	1.447368421	0.436397999	0.03343949	0.00921643	0.060509554	0.02115498	0.041401274	0.01341744
30	40	1.31578947	0.20804458	2.368421053	0.33546181	0.044585987	0.00694092	0.035031847	0.00780092	0.031847134	0.00755321

Chapter 4: Benthic community facilitation and competition in an Arctic kelp bed

ABSTRACT

Crustose coralline algae (CCA) are dominant space occupiers and ecosystem engineers in marine systems. They shape community structure and are early responders to water chemistry changes. In the Beaufort Sea, CCA distributions within an Arctic kelp bed community range from 77% cover of the substrate to complete absence. The patterns in cover provided an opportunity to better understand the role that CCA play in the structuring of marine epilithic communities in subtidal systems. We examined the composition of epilithic invertebrates, algal species and kelp density on cobbles with and without CCA. Cobbles without CCA were higher in algal species richness, algal and invertebrate biomass, and algal diversity than cobbles with CCA present. Areas with CCA had significantly higher densities of *L. solidunugla* adults (4.72 m^{-2}), an important contributor to nearshore Arctic communities, than the site without CCA (0.36 m^{-2}). CCA outcompeted turf and fleshy algal and other invertebrate species, creating more habitable space on the substrate for kelp recruitment. This competitive interaction facilitated *L. solidungula* recruitment and survival. This study demonstrates the positive interactions between kelp and CCA, highlighting the importance of facilitation by CCA for kelp recruitment and its indirect effects on community assemblages.

INTRODUCTION

Environmental factors affect persistence and distribution of individuals through species-specific resilience, acclimation and adaptation (Grime 1977). In addition to abiotic factors, biological processes (e.g., competition and facilitation) can further shape communities through species interactions (Beatty 1984, Miller 1994). Species interactions (positive or negative) are often driven by abiotic stressors in the environment, an ecological principle known as the Stress Gradient Hypothesis (SGH; Bertness & Callaway 1994). Intertidal marine zones exemplify these processes as species assemblages in the lower, less environmentally stressful intertidal zone are driven by competition (Lubchenco 1980) and species assemblages in the high intertidal zone are driven by resilience to stressful abiotic conditions and species facilitation (Farrell 1991, Bertness & Leonard 1997). Patterns of facilitation in abiotically stressful environments are not specific to intertidal zones and have also been observed in salt marshes (Bertness & Hacker 1994), high altitude plant communities (Callaway et al. 2002) and along other stress gradients in marine systems such as latitude (e.g., temperature, light etc.; Barner & Muth 2020).

Abiotic factors do not affect all species through similar physiological mechanisms at similar magnitudes. For example, marine heatwaves and increased ocean temperatures have been shown to decimate kelp populations (western Australia) and limit recruitment (eastern Pacific; Wernberg et al. 2015, Muth et al. 2019),, while turf species were able to tolerate these temperature shifts and ultimately dominate the benthos. In the Mediterranean, shifts in algal assemblages have been observed along pH and pCO_2 gradients (Kroeker et al. 2013). Turfs dominated in stressful conditions (low pH, high pCO_2), but crustose coralline algae (CCA) were lost from the system as water became more corrosive to calcium carbonate (Kroeker et al. 2013). CCA often are first to respond to carbonate chemistry changes as they precipitate magnesium calcite, which is more soluble than aragonite, the most commonly analyzed calcium carbonate

mineral (Gangstø et al. 2008, Diaz-Pulido et al. 2012, Mccoy & Kamenos 2015). In addition to seaweeds, acidic waters affect calcifying grazers that are important in shaping benthic communities.

Acidic waters pose a threat to calcifying herbivores (such as gastropods and urchins) and CCA, creating dominance of turf or fleshy seaweeds in systems with less grazing pressure and competition for space with CCA (reviewed in Harley et al. 2012). CCA are able to influence community structure by inhibiting or enhancing recruitment of sessile invertebrates and other algal species (reviewed in McCoy & Kamenos 2013). Therefore, CCA presence or absence in benthic assemblages can affect community structure, but depend on environmental conditions.

Benthic organisms that colonize nearshore Arctic environments must have the ability to acclimate to large seasonal changes in light (Sellmann et al. 1992, Bonsell & Dunton 2018), temperature, salinity, and pH (Sellmann et al. 1992, Dunton & Bonsell 2020, Muth et al. 2020a; Muth Chapter 1). Along the north Alaskan coast, glacially deposited boulders and cobbles provide the substrate needed for benthic communities (algae and invertebrates) to thrive and provide important energy sources for near-shore food webs (Dunton et al. 1982). Although many abiotic factors vary seasonally, benthic communities near Arctic rivers can experience wide variations in salinity (e.g. Muth et al. 2020a; Muth Chapter 1), which is typical for many estuaries, including the Arctic. Arctic rivers are particularly important source of freshwater to nearshore systems , which receive 11% of the world's freshwater run-off, but only contains 1% of the world's ocean volume (McClelland et al. 2012). Furthermore, most of this water is released during a short period each spring before/during break-up, causing drastic changes to the nearshore water composition and chemistry (Muth et al. 2020a; Chapter 1).

The Stefansson Sound Boulder Patch, located in the Alaska Beaufort Sea, is composed of boulders and cobbles and sustains a rich benthic community (Wilce & Dunton 2014). The Arctic endemic kelp species, *Laminaria solidungula* is a foundation species in this community and an important contributor to nearshore food webs (Dunton & Schell 1987). The Boulder Patch lies at the mouth of the Sagavanirktok (Sag) River, the second largest river draining the North Slope of Alaska (1.6 km^3 annual discharge; McClelland et al. 2014).

One of the most conspicuous floristic patterns in the Boulder Patch is the lack of CCA at the inshore sites near the Sag River Delta (Bonsell & Dunton 2020). The CCA species *Leptophytum foecundum* and *Leptophytum lavae* cover the substrate of cobbles and boulders at the offshore sites (Wilce & Dunton, 2014; P. Gabrielson, pers. comm.). These patterns are the result of rapid and drastic changes to nearshore waters that directly affect the physiology of these CCA species and their ability to persist (Muth et al. 2020b; Chapter 2). The goals of this study were to characterize algal and invertebrate communities of the Boulder Patch with and without CCA present. In addition, we documented how species interactions in the presence or absence of CCA affect population densities of *Laminaria solidungula*.

METHODS

Temperature, salinity, pH and Ω_{arag} saturation levels

Sea-bird (Satlantic) SeaFETs (pH total; pH_T) and SBE 37-SM MicroCATs C-T (P) (salinity and temperature) were deployed July 2016-July 2018 at two sites within the Boulder Patch, Stefansson Sound, Alaska (Fig. 4.1); nearshore site, E-1 (70º18.8665 N, 147º44.0413 W; 4.5 m depth) and offshore site DS-11 (70º19.3248 N, 147º34.8816; 6.5 m depth). Salinity, temperature and pH measurements were recorded hourly. For deployment and calibration

details, and calculation of Ω_{arag} levels in CO_2Calc using continuous pH_T, salinity, temperature, and total alkalinity, see Muth et al. (2020a) (Chapter 1).

Community Composition Analysis

In order to quantify algal and sessile invertebrate biomass and diversity, 15 cobbles (5-25 cm in length and width) were collected randomly along ordinal direction transects (180˚) at dive sites DS-11 and E-1 (July 2016; Fig. 4.1). Cobbles were transported to the laboratory on Endicott Island in coolers and immersed in seawater. In the laboratory, each cobble was analyzed for algal species present and biomass. Fleshy algal biomass was separated by species, and wet weights were recorded. Kelp recruits (> 3 cm) were quantified and recorded. After removal of all turf algae, cobbles were photographed using a Nikon D7200 and analyzed using ImageJ for crustose coralline algae (CCA) percent cover. Invertebrate species were identified to lowest taxonomic level, catalogued and preserved (90% ethanol) for further identification and biomass measurements at the University of Texas Marine Science Institute (UTMSI).

Biodiversity metrics were calculated and compared between sites for both turf and fleshy algal species and invertebrate species that were collected and weighed for biomass (Table 4.1, yellow-highlighted species). *Laminaria solidungula* was included in the list of total algal species present (Table 4.2), and densities were compared between sites. But *L. solidungula* was not included in biodiversity metrics as this species occurs on a larger scale and is not comparable to fleshy and turf species (Beatty 1984). Metrics used were 1) Species per site = total algal and invertebrate species identified at each site (all species listed in Table 4.1); 2) Species Richness = average number of species per cm^2 of substrate (highlighted species in Table 4.1); 3) Species Biomass = average mg of species biomass per cm^2 of substrate (highlighted species in Table 4.1);

4) Species Diversity – Shannon-Wiener Index (H') = average H' per cm^2 of substrate (highlighted species in Table 4.2); and 5) Species Evenness – Pilou Evenness (J) = average J per cm^2 of substrate (highlighted species in Table 4.1).

Biodiversity metrics were calculated using the *vegan* package in R. Algal biodiversity metrics were compared between sites using a non-parametric, zero-inflated regression, and a likelihood ratio test for species richness (due to count-like nature of the data). ANOVAs using cube root transformations for biomass and diversity and a logarithmic transformation for species evenness were used to compare biodiversity statistics between sites. Invertebrate species richness was compared between sites using a non-parametric, zero-inflated regression and a likelihood ratio test, while ANOVAs using a cube root transformation for biomass and square root transformations for evenness and diversity were used to compare biodiversity metrics between sites.

Kelp Densities

The density of mature *Laminaria solidungula* plants were quantified within the Boulder Patch using 0.05 m^2 photoquadrats acquired using a Nikon 1 AW1 waterproof digital camera in July and August 2016 and 2017 (Bonsell and Dunton 2020). Photographs were taken in a spiral pattern around a central point at sites DS-11 and E-1 (Fig. 4.2). Rock cover within the Boulder Patch varies greatly (Fig. 4.2), and kelp species require rock substrata for recruitment. Therefore, photographs were taken when rock coverage was estimated to be >75% within the 0.05 m^2 photoquadrats. This process standardized rock cover between sites and allowed for direct comparisons of kelp densities between sites. Individuals were counted only if the holdfast was attached within the quadrat. Densities of mature individuals and recent recruits <3 cm in

height were compared using a non-parametric, zero-inflated regression, and a likelihood ratio test in R.

RESULTS

Temperature, salinity, pH and Ω_{arag} levels

Nearshore Arctic abiotic parameters (temperature, salinity, pH and Ω_{arag} levels) were seasonally dynamic and exhibited different patterns among sites (Fig. 4.2). As sites varied in proximity to the Sagavanirktok River, we expected marked spatial and temporal gradients in salinity and carbonate chemistry moving from near shore of the Sagavanirktok River to offshore in the open Stefansson Sound. Temperatures ranged from 8.9°C (2016-2017) to 11.4°C (2017-2018) at the inshore site and from 7.9°C (2016-2017) to 10.9°C (2017-2018) at the offshore site (Table 4.2). Temperatures, much like other parameters measured, were stable during ice-covered periods and fluctuated during ice free periods (Fig. 4.2a). Salinity was also stable during the ice-covered periods, but ranges were larger for both sites during the 2017-2018 deployment (Table 4.2), with salinities decreasing to near zero during the strong spring 2018. At the inshore site, the salinity range was 15.3 (2016-2017) vs. 34.0 (2017-2018), and 12.6 (2016-2017) vs. 12.1 (2017-2018) at the offshore site. pH ranges were 0.87 and 1.0 for the inshore site and 0.9 and 0.76 for the offshore site for the 2016-2017 and 2017-2018 deployments, respectively (Fig. 4.2c). Temperature, salinity, pH values, and A_T estimates were used to calculate Ω_{arag}. Low salinity waters decreased Ω_{arag} with A_T values lower than in ocean water (Muth et al. 2020a; Fig. 1.S1). At the inshore site, when salinity values were low (<5), Ω_{arag} levels were near zero (Fig. 4.2). Low pH values (~7.6) for the ice-covered season at the offshore site also affected Ω_{arag} and during the 2017-2018 ice-covered period, Ω_{arag} levels remained around 0.5. In general, Ω_{arag}

levels were near equilibrium or undersaturated with respect to aragonite, even at the offshore site where CCA dominated the substrate (Fig. 4.2d).

Community Composition Analysis

Epilithic algae and kelp densities

Algal species identified from cobbles at sites E-1 and DS-11 included 12 species (Fig. 4.3, Table 4.1). The CCA species, *Leptophytum foecundum* and *L. lavae* were only found at the offshore site (DS-11), and fleshy species including *Ahnfeltia borealis, Chaetomorpha* sp., *Spacelaria plumosa* and *Ectocarpus siliculosus* were only found at the inshore site (E-1; Table 4.1). On average, offshore cobble CCA coverage was 77.5% $\pm$ 3.8, while CCA were absent on the inshore substrate (Fig. 4.3). Six algal species were weighed and used in biodiversity statistics for the offshore site, and ten were measured at the inshore site (Table 4.1; Fig. 4.3). Average algal richness, abundance (biomass) and diversity (H') cm^{-2} were both significantly higher at the inshore site, where CCA were absent (Table 4.3; richness Likelihood Ratio Test Chi $Square_2$=13.37, $p<0.001$; ANOVA abundance $F_{1,28}$=13.63, $p<0.001$, ANOVA diversity $F_{1,28}$=7.51, p=0.01). Evenness, although not significant, was higher at the offshore site (Fig. 4.4, Table 4.3; ANOVA evenness $F_{1,28}$=2.08, p=0.16).

Kelp juveniles (<3 cm) were slightly more prevalent at the inshore site (Likelihood Ratio Test Chi $Square_2$=5.25, p=0.07). We found three recruits on one cobble, while 14 recruits were found on six of the 15 cobbles analyzed at the inshore site. Densities of mature *Laminaria solidungula* plants were significantly greater at the offshore than the inshore site (Likelihood Ratio Test Chi $Square_2$=11.58, p=0.003). The offshore site had an average of 4.72 adults $\pm$ 1.5 m^2 versus 0.4 adults $\pm$ 0.4 m^2 at the inshore site (Fig. 4.5).

Invertebrates

Across both sites, twenty-nine invertebrate species were found, but only six of those species occurred at both sites (Table 4.1). Species richness, diversity and evenness were not significantly different between the offshore and inshore site (Table 4.3; richness Likelihood Ratio Test Chi Square$_2$=2.58, p=0.27; ANOVA diversity $F_{1,28}$=0.027, p=0.86; ANOVA evenness $F_{1,28}$=0.33, p=0.567; Fig. 4.5). However, invertebrate biomass was significantly higher at the inshore site (Table 4.3; ANOVA abundance $F_{1,28}$=15.16, p<0.001). The bryozoan *Eucratea loricata* and a barnacle, *Balanus crenatus,* dominated the invertebrate biomass at the inshore site, while the offshore site biomass was composed of bryozoans (*Eucratea loricata, Flustrella gigantea, Carbasea carbasea*) and hydrozoans (*Sertularia* spp.; Fig. 4.6).

DISCUSSION

Small-scale variations in environmental factors such as salinity, pH, and Ω_{arag} levels (Fig. 4.2) within the Stefansson Sound Boulder Patch drive CCA distributions (Muth et al. 2020b). Varying CCA coverage within the Boulder Patch allowed for observations and comparisons to be made of biological interactions in the presence and absence of CCA. Algal and invertebrate species were present at both sites (Table 4.2), but the communities differed in terms of composition, spatial distribution on the cobbles, and *Laminaria solidungula* densities. CCA distributions, driven by freshwater river input (Muth et al. 2020b; Chapter 2), influenced species distributions on the available substrate, occupying valuable space that *L. solidungula* was able to colonize. Thus, when CCA were present, *L. solidungula* densities were higher than when CCA was absent.

Abiotic Environment

Abiotic conditions exhibited strong seasonal variations (Fig. 4.2), and conditions diverged during the spring freshet (May and June) between the inshore and offshore site. The inshore site experienced a strong freshet-effect in June 2018, with salinity and Ω_{arag} levels falling near zero on the benthos (Fig. 4.2; Table 4.1). Sagavanirktok River run-off along with other North Slope rivers (Kuparak and Colville) have experienced increased freshwater input (1981-2010; Rawlins et al. 2019). Ever increasing annual pulses of waters with low salinity and low Ω_{arag} levels have the potential to expand their influence on nearshore Arctic benthic assemblages and change species assemblages. As noted in this study, inshore areas subject to low salinity waters were characterized by the loss of CCA and decreased kelp densities. Glacially fed rivers may continue to increase with warmer temperatures; however, recent climate models have predicted that the Arctic will receive more rainfall, and this could decrease run-off pulses from snow melt (Bintanja & Andry 2017), potentially decreasing spring freshwater plumes and increasing areas habitable by CCA.

Biotic Interactions

Annual riverine freshwater events likely prevent CCA from persisting at the inshore site (Muth et al. 2020b; Chapter 2), creating a major community shift in the benthic assemblage (Bonsell & Dunton 2020). These shifts were driven by species-specific tolerance to changes in salinity, followed by subsequent biological interactions that affected the species able to persist.

Algal Species

All algal species present at the offshore site were also found at the inshore site, except for CCA (Table 4.2). Species richness and diversity were significantly higher ($p=0.01$) at the inshore site, driven by species from all three algal divisions (Rhodophyta, Chlorophyta and Phaeophyta), although these additional species contributed minimal biomass to the inshore

assemblage (Fig. 4.4). Abundance was significantly higher at the inshore site ($p<0.001$), and this was mostly driven by red algal biomass (i.e., *Phycodrys fimbriata, Coccotylus truncates*, and *Dilsea socialis*; Fig. 4.4). Although fewer species composed a majority of the biomass at the inshore site, evenness between the sites was not significantly different ($p=0.16$). When CCA was present, few species (only *Laminaria solidungula* and *Rhodomela confervoides*) were observed to grow directly on the CCA, which is considered a competitive dominant algal species (Konar & Iken 2005). This limited space on the boulders where algae could attach and persist, limiting fleshy and turf algal biomass.

Laminaria solidungula densities were significantly higher at the offshore site than the inshore site ($p=0.003$; Fig. 4.5). Since quadrats were only taken when rock cover was over 75%, differences in rock cover at the sites did not affect the densities measured. Interestingly, kelp juveniles were slightly more abundant at the inshore site ($p=0.07$). This observation is important, as it points to post-settlement processes that affect kelp adults and survival. Kelp juveniles observed at the inshore site were attached to turf algae or within the *E. loricata* canopies, which are difficult substrates for long-term persistence (Burek et al. 2018). In contrast, recruits observed at the offshore site were attached to rock or CCA, which are suitable substrates for long-term persistence (cite). Low salinities have been shown to affect kelp mortality and decrease kelp populations (Karsten 2007); however, studies from the Boulder Patch revealed resilience of *Laminaria solidungula* to low salinities (<10) once microscopic sporophytes were formed (Muth et al. 2020c, Chapter 3). This observation further supports our hypothesis that *L. solidungula* densities are higher at the offshore site because of the prevalence of CCA, which can outcompete both turf algae and epilithic invertebrates, creating space for kelp recruitment.

Invertebrates

In contrast to the algal community, the invertebrate species differed greatly between sites, with only six of the 29 species found at both sites (Table 4.1). Species such as *Eucratea loricata* and *Balanus crenatus* dominated at the inshore site. These species have been reported to tolerate low salinities in the British Isles (Readman 2016, Readman & Hiscock 2016) and in shallow areas of Svalbard fjords (Kuklinski et al. 2005). Species richness, diversity and evenness were not significantly different between sites, but biomass was higher at the inshore site where CCA was absent, occupying space on the substrate and further decreasing suitable substrate for kelp recruitment.

Species interactions, the Stress Gradient Hypothesis, competition and facilitation

When CCA were present in the Boulder Patch, it was the main space occupier (Konar & Iken 2005, this study). A common pattern observed on offshore Boulder Patch cobbles showed that CCA occupied horizontal spaces and sessile invertebrates recruited and survived on the fringes of the CCA and other vertical areas of the cobbles, a pattern seen in other systems (Irving et al. 2004, Kuklinski 2009, Muth et al. 2017). Without CCA present, the bryozoan *E. loricata* was able to attach within other algal species and formed a dense canopy over the substrate (Readman & Hiscock 2016). This species was seen to cover much of the horizontal surfaces at the inshore site when CCA were absent (Figs. 4.3 and 4.6).

The absence of CCA clearly created different spatial assemblages on the substrates of the inshore and offshore sites (Fig. 4.3). As in the Stress Gradient Hypothesis, abiotic pressures (low salinity) may influence the species present at each site, and then biotic competition subsequently shapes species assemblages on the cobbles and boulders. The absence of CCA at the inshore site allowed space for higher abundance of turf and fleshy algae and invertebrates,

potentially limiting space for kelp recruitment and reducing the densities of mature *L. solidungula* (Fig. 4.7).

CCA, articulated corallines and other fleshy and turf algae are known to compete with kelps (Filbee-Dexter & Wernberg 2018). A recent metanalysis highlighted facilitative relationships between algal turf species and canopy forming species when abiotic stressors are increased, such as high latitude and intertidal areas (Barner & Muth 2020). This pattern of increased facilitation by primary producers aligns with the Stress Gradient Hypothesis (SGH; Bertness & Callaway 1994), and although competitive kelp-coralline interactions are seen worldwide, facilitation may be occurring more often than previously thought (Barner & Muth 2020).

Future Implications

The physiological susceptibility of CCA to variations in salinity (Schoenrock et al. 2018, Muth et al. 2020b; Muth Chapter 2) and carbonate chemistry (reviewed in Nelson 2009), allows CCA distributions have the ability to be used as bioindicators for ocean chemistry changes, such as pH and calcium carbonate saturation levels. Environmental sensors are expensive and logistically challenging to deploy, and although bioindicators do not record hydrographic data, monitoring CCA distributions may identify areas that are particularly beneficial for in-depth studies

Unlike previous studies, we did not see a community simplification, as salinity and Ω_{arag} levels decreased (Hall-Spencer et al. 2008, Kroeker et al. 2013), but algal and invertebrate shifts did occur (Table 4.2). When CCA were absent from the community, red algal and invertebrate biomass dominated rock surfaces and *L. solidungula* survivorship was reduced, likely attributable to unstable attachment surfaces and space competition with algal turfs and

invertebrates (Fig. 4.7). The reduction of *L. solidungula* is an important shift as *L. solidungula* is a foundation species of these Arctic cobble and boulder areas and is known to contribute to the Arctic nearshore foodwebs (Dunton & Schell 1987), more so than other fleshy and turf algal species. The interaction between kelp and CCA is also important for other ecosystems or areas affected by low salinities (fjords and estuaries) or areas with reduced Ω_{arag} levels (upwelling zones). Although kelps may tolerate lower pH, salinities, and Ω_{arag} levels than CCA, the loss of CCA from systems has the ability to indirectly negatively impact kelp populations (Fig. 4.7).

In addition, the assemblage shift we observed in the Boulder Patch is indicative of shifts that may occur as different processes (ocean acidification and increased freshwater input) create corrosive ocean water for CCA. Rather than relying on species-specific tolerances to changing ocean chemistry conditions, we can visualize how it will change with the small-scale variations we see within the Boulder Patch. The inshore site, lacking CCA, with reduced kelp densities and high algal and invertebrate turf cover could represent future benthic assemblages as conditions shift with climate change.

TABLES

Table 4.1 Invertebrate and algal species present on cobbles analyzed from E-1 (CCA Absent) and DS-11 (CCA Present). Species highlighted in yellow were analyzed statistically in calculations of species richness, biomass, diversity and evenness.

Invertebrates	**CCA Absent**	**CCA Present**
Bryozoa	*Eucratea loricata* unknown Bryozoan *Alcyonidium gelatinosum*	*Eucratea loricata* unknown Bryozoan *Flustrella gigantea* *Crisiidae* sp. *Carbasea carbasea*
Hydrozoa	*Lafornia maxima* *Abietinaria* sp. *Sertularia albimaris* *Bougainvillia* sp.	*Lafornia maxima* *Sertularia cupressoides* *Sertularia albimaris*
Polychaeta	*Nereimyra aphroditoides* *Exogone* sp. *Harmothoe imbricata*	unknown Nereis *Exogone* sp. unknown Serpulidae unknown Polydora unknown Spionidae
Demospongiae		*Haliclona rufescens* unknown demo sponge unknown glass sponge
Nematoda	unknown Nematoda	unknown Nematoda
Foraminifera		unknown Foramnifera
Polyplacophora		*Stenosemus albus*
Malacostraca	*Caprella* sp. *Atylus carinatus*	
Cirripedia	*Balanus crenatus*	
Ascidiacea	unknown Ascidian *Chelysoma* sp. *Dendrodoa aggregata*	
Algae	**CCA Absent**	**CCA Present**
Rhodophyta	*Phycodrys fimbriata* *Coccotylus truncatus* *Rhodomela confervoides* *Odonthalia dentata* *Dilsea socialis* *Ahnfeltia borealis*	*Phycodrys fimbriata* *Coccotylus truncatus* *Rhodomela confervoides* *Odonthalia dentata* *Dilsea socialis* *Leptophytum foecundum* *Leptophytum lavae*
Chlorophyta	*Chaetomorpha* sp.	
Ochrophyta	*Laminaria solidungula* *Sphacelaria plumosa* *Ectocarpus siliculosus*	*Laminaria solidungula*

Table 4.2 Temperature, salinity, pH and Ω_{arag} ranges for the inshore (E-1) and offshore (DS-11) sites for each deployment.

	E-1		DS-11	
	August 2016 - July 2017	August 2017 - July 2018	August 2016 - July 2017	August 2017 - July 2018
temperature range (°C)	-1.87 to 7.08	-1.86 to 9.73	-1.88 to 6.08	-1.91 to 9.05
salinity range	19.07 to 34.35	0.01 to 34.02	21.93 to 34.51	22.78 to 34.86
pH range	7.83 to 8.70	7.67 to 8.67	7.79 to 8.69	7.47 to 8.23
Ω_{arag} level range	0.88 to 4.93	0.08 to 4.89	0.89 to 4.79	0.33 to 1.66

Table 4.3 Biodiversity metrics (species per site, species richness, biomass, diversity and evenness ± SE). Offshore where CCA was present was compared to inshore where CCA was absent.

	Algae				
	Species per site	Species Richness cm2	Biomass mg*cm2	Shannon Diversity cm2	Evenness cm2
Offshore	6	1.266 (0.22)	46.6 (16.8)	0.239 (0.08)	0.213 (0.05)
Inshore	10	3.266 (.04)	169.8 (39.3)	0.488 (0.08)	0.131 (0.02)
		**	**	**	
	Invertebrates				
	Species per site	Species Richness cm2	Biomass mg*cm2	Shannon Diversity cm2	Evenness cm2
Offshore	11	2.266 (0.40)	1.6 (0.5)	0.312 (0.10)	0.153 (0.04)
Inshore	13	3.200 (0.44)	46.8 (3.8)	0.372 (0.09)	0.093 (0.02)
			**		

** denotes significant differences

FIGURES

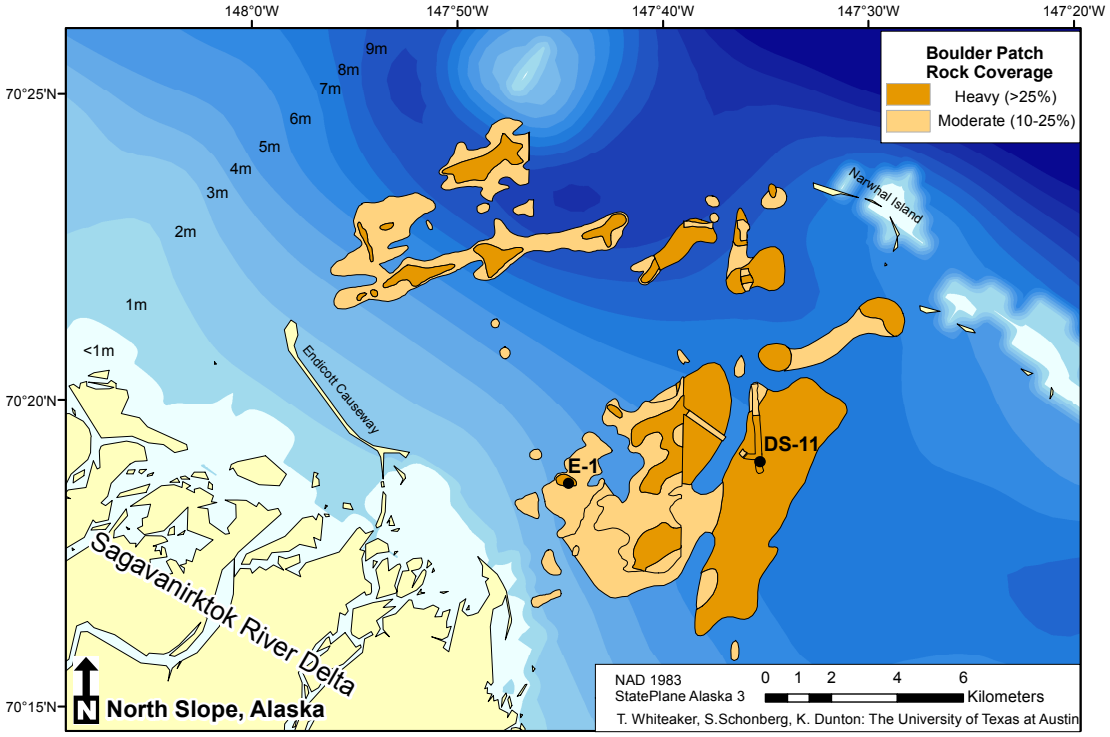

Figure 4.1 The Stefansson Sound Boulder Patch. Instrument deployment and benthic assessment sites include E-1 (inshore; CCA absent) and DS-11 (offshore; CCA present). The sites differed in proximity to the Sagavanirktok River, creating different salinity and chemistry regimes (adapted from Bonsell & Dunton 2018).

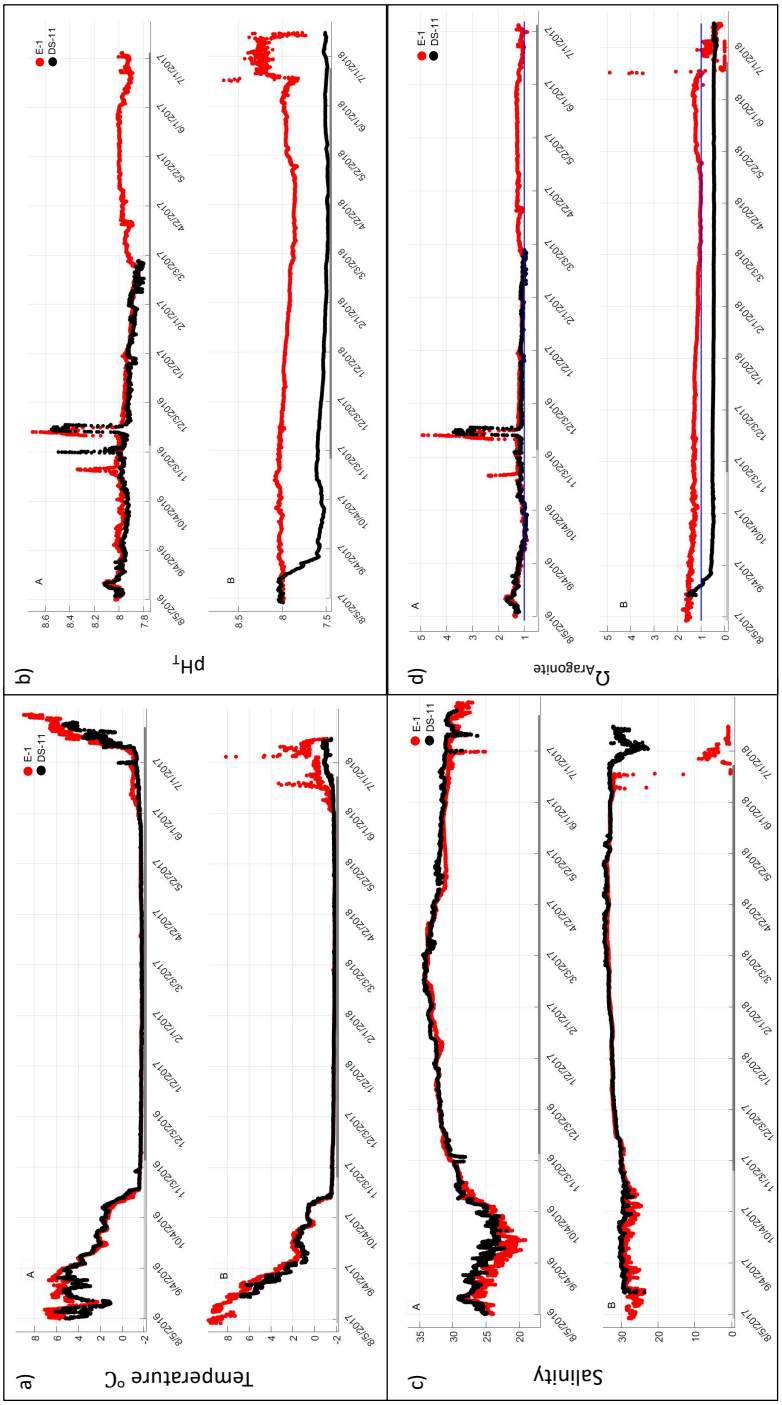

Figure 4.2 Timeseries of abiotic factors recorded for each site, for 2016-2017 (top graph of each section) and 2017-2018 deployments (bottom graph of each section). The inshore site (E-1; CCA absent) is in red and the offshore site (DS-11; CCA present) is in black. Data adapted from Muth et al. 2020a.

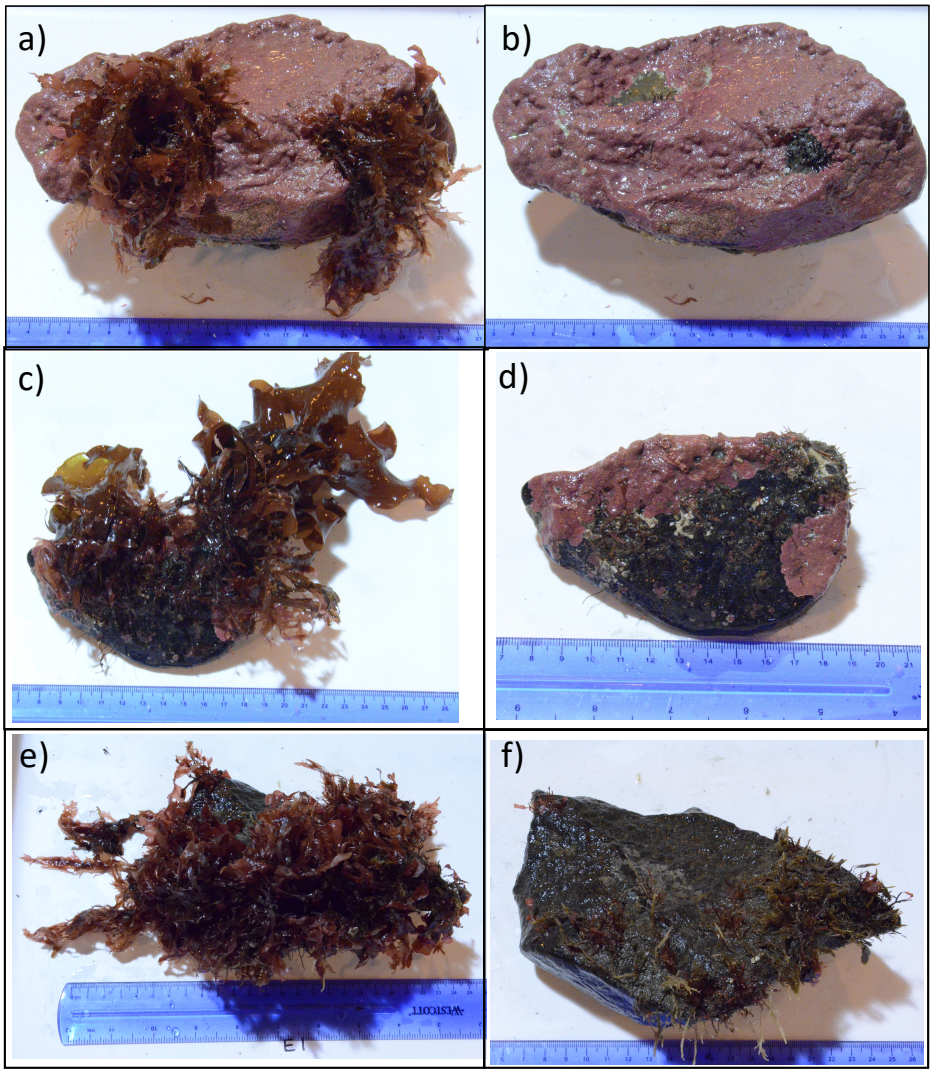

Figure 4.3 Cobble analysis pictures. a-d) images from cobbles collected at the offshore site (DS-11) where CCA were present, b and d are photographs of a and c with turf algae removed for CCA analysis. e and f) images from a cobble collected at the inshore site (E-1), without CCA present, f is an image of the cobble in e with all turf algae removed for CCA analysis.

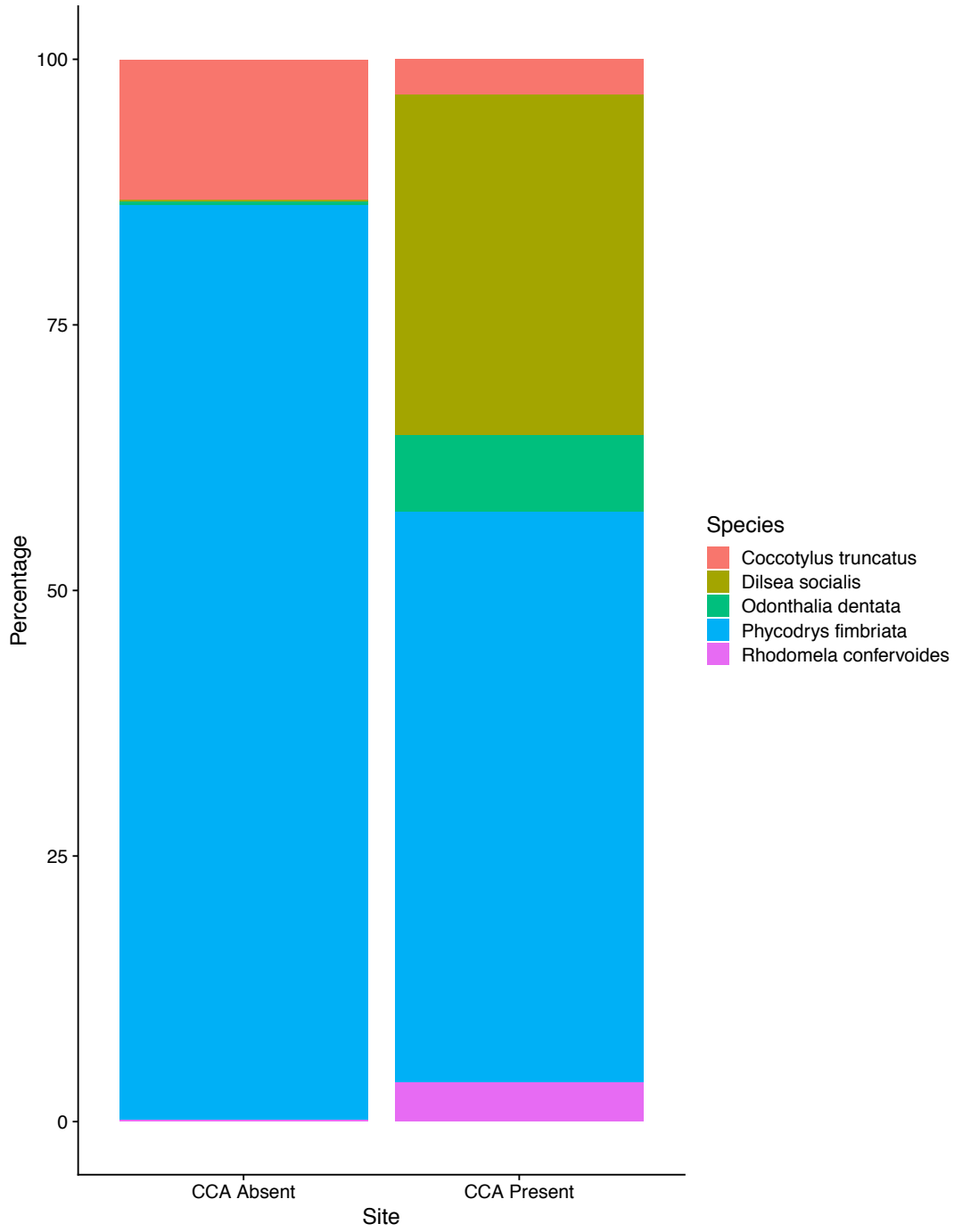

Figure 4.4 Red algal biomass composition of the assemblages when CCA were absent (E-1) and present (DS-11). *Phycodrys fimbriata* was dominant at both sites, but more species contributed to the overall biomass when CCA were present (not significant $F_{1,28}$=2.08, p=0.16)

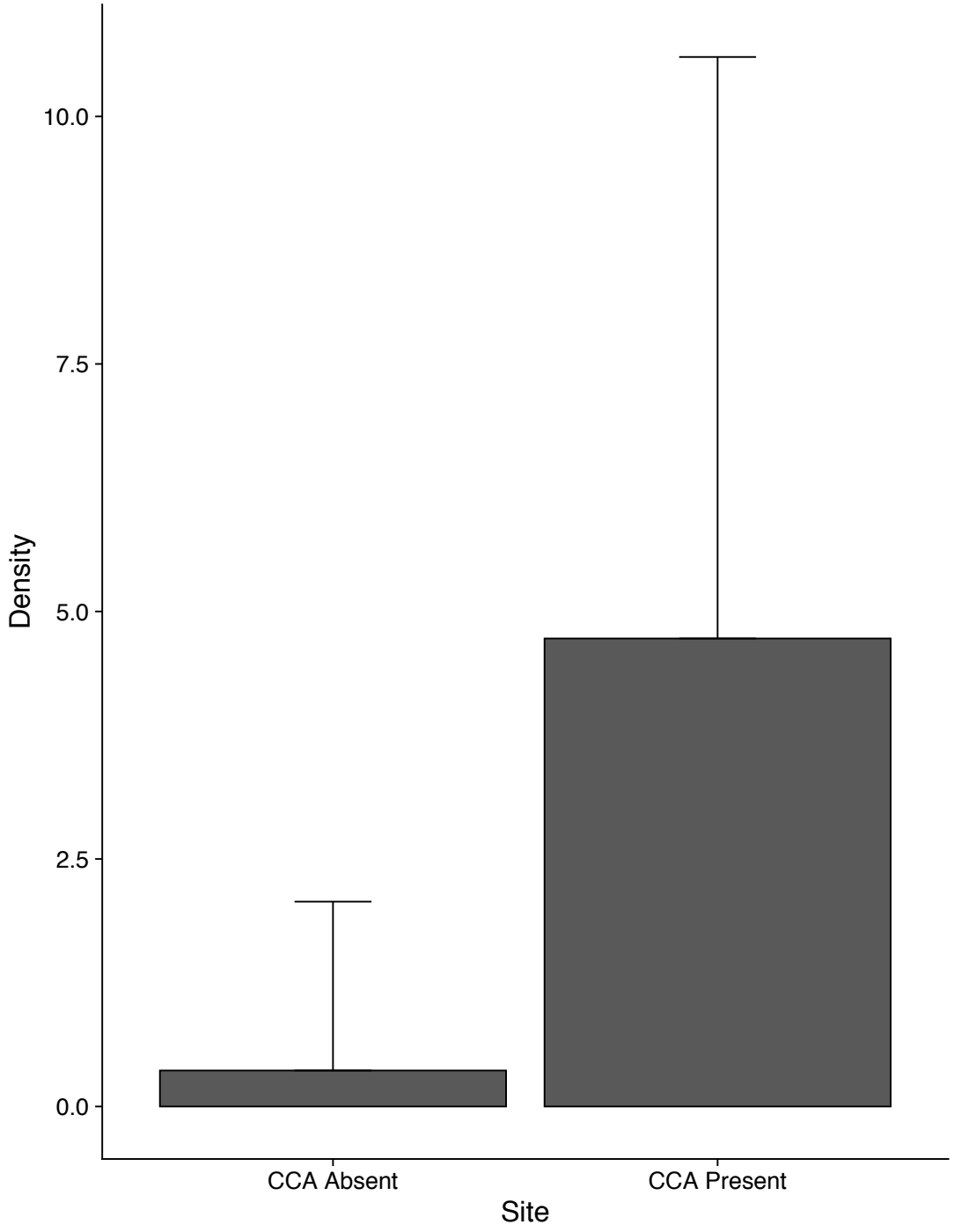

Figure 4.5 *Laminaria solidungula* densities m^{-2} at DS-11 where CCA were present and E-1 where CCA were absent.

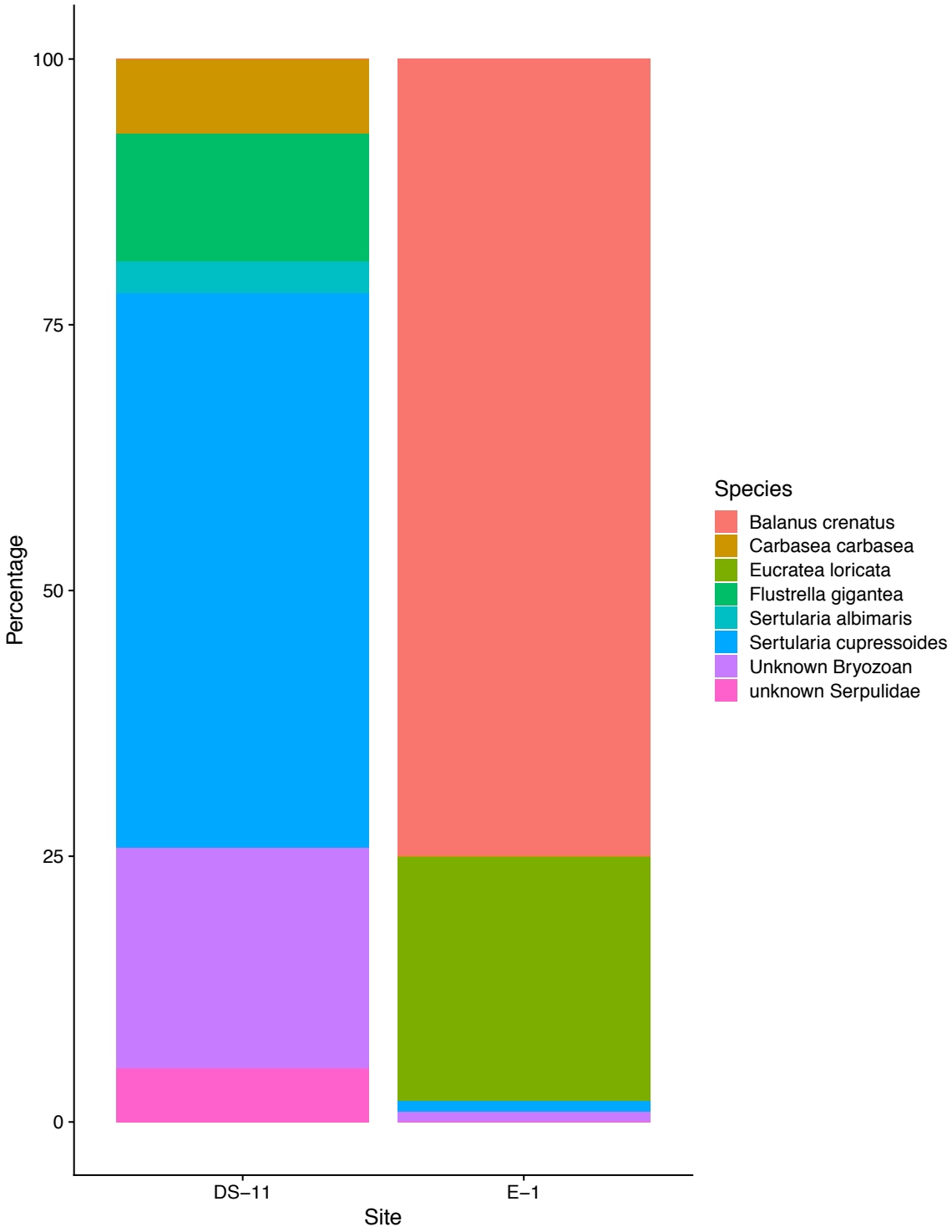

Figure 4.6 Invertebrate biomass composition of the assemblages when CCA were absent (E-1) and present (DS-11).

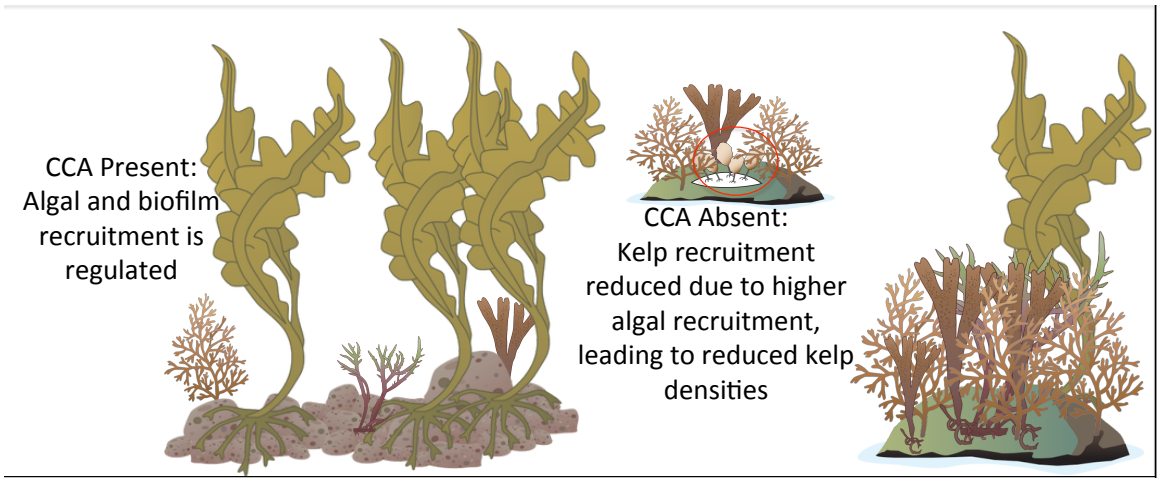

Figure 4.7 Conceptual model of facilitation and competition among kelps, CCA and turf and fleshy algae when CCA are present and absent. CCA outcompete turfs and sessile invertebrates, allowing for increased space and successful kelp recruitment and survivorship, thus CCA facilitate kelp recruitment in this scenario. Without CCA, algal turfs and invertebrates dominate the substrate, and competition with these species decreases kelp population densities (see area within red circle).

References

Airoldi, L. (2000). Effects of Disturbance , Life Histories , and Overgrowth on Coexistence of Algal Crusts and Turfs. *Ecology*, *81*(3), 798–814.

Asnaghi, V., Thrush, S. F., Hewitt, J. E., Mangialajo, L., Cattaneo-Vietti, R., & Chiantore, M. (2015). Colonisation processes and the role of coralline algae in rocky shore community dynamics. *Journal of Sea Research*, *95*, 132–138. https://doi.org/10.1016/j.seares.2014.07.012

Barner, Allison K. and Muth, A. F. (2020). Facilitation in marine forests. *Submitted*.

Bates, N. R., Garley, R., Frey, K. E., Shake, K. L., & Mathis, J. T. (2014). Sea-ice melt CO2-carbonate chemistry in the western Arctic Ocean: Meltwater contributions to air-sea CO2 gas exchange, mixed-layer properties and rates of net community production under sea ice. *Biogeosciences*, *11*(23), 6769–6789. https://doi.org/10.5194/bg-11-6769-2014

Bates, N. R., Mathis, J. T., & Cooper, L. W. (2009). Ocean acidification and biologically induced seasonality of carbonate mineral saturation states in the western Arctic Ocean. *Journal of Geophysical Research: Oceans*, *114*(11), 1–21. https://doi.org/10.1029/2008JC004862

Beatty, S. W. (1984). Influence of Microtopography and Canopy Species on Spatial Patterns of Forest Understory Plants. *Ecology*, *65*(5), 1406–1419. https://doi.org/10.2307/1939121

Bertness, M. D., & Callaway, R. (1994). Positive interactions in communities. *Trends in Ecology & Evolution*, *9*(5), 27–29.

Bertness, M. D., & Hacker, S. D. (1994). Physical Stress and Positive Associations Among Marsh Plants. *The American Naturalist*, *144*(3), 363–372. https://doi.org/10.1086/285681

Bertness, M. D., & Leonard, G. H. (1997). The role of positive interactions in communities:

Lessons from intertidal habitats. *Ecology*, *78*(7), 1976–1989. https://doi.org/10.1890/0012-9658(1997)078[1976:TROPII]2.0.CO;2

Bintanja, R., & Andry, O. (2017). Towards a rain-dominated Arctic. *Nature Climate Change*, *7*(4), 263–267. https://doi.org/10.1038/nclimate3240

Bonsell, C., & Dunton, K. H. (2018). Long-term patterns of benthic irradiance and kelp production in the central Beaufort sea reveal implications of warming for Arctic inner shelves. *Progress in Oceanography*, *162*(February), 160–170. https://doi.org/10.1016/j.pocean.2018.02.016

Bonsell, C. E. (2019). *Factors that influence the distribution of the Arctic endemic kelp , Laminaria solidungula (J . Agardh 1868). Dissertation, University of Texas at Austin. https://repositories.lib.utexas.edu/handle/2152/75764*.

Bonsell, C. E. and Dunton, K. H. (2020). Location and slow succession shapes benthic community structure in an Arctic kelp bed. *Frontiers in Marine Science*

Brown, J. H., & Kodric-Brown, A. (1977). Turnover rates in insular biogeography: effect of immigration on extinction. *Ecology*, *58*(2), 445–449. https://doi.org/10.2307/1935620

Büdenbender, J., Riebesell, U., & Form, A. (2011). Calcification of the Arctic coralline red algae *Lithothamnion glaciale* in response to elevated CO 2. *Marine Ecology Progress Series*, *441*, 79–87. https://doi.org/10.3354/meps09405

Bulleri, F., Bertocci, I., & Micheli, F. (2002). Interplay of encrusting coralline algae and sea urchins in maintaining alternative habitats. *Marine Ecology Progress Series*, *243*, 101–109. https://doi.org/10.3354/meps243101

Burdett, H. L., Hatton, A. D., & Kamenos, N. A. (2015). Effects of reduced salinity on the photosynthetic characteristics and intracellular DMSP concentrations of the red coralline

alga, *Lithothamnion glaciale*. *Marine Biology*, *162*(5), 1077–1085. https://doi.org/10.1007/s00227-015-2650-8

Burek, K. E., O'Brien, J. M., & Scheibling, R. E. (2018). Wasted effort: Recruitment and persistence of kelp on algal turf. *Marine Ecology Progress Series*, *600*, 3–19. https://doi.org/10.3354/meps12677

Callaway, R. M., Brooker, R. W., Choler, P., Kikvidze, Z., Lortie, C. J., Michalet, R., … Cook, B. J. (2002). Positive interactions among alpine plants increase with stress. *Nature*, *417*(6891), 844–848. https://doi.org/10.1038/nature00812

Carstensen, J., & Duarte, C. M. (2019). Drivers of pH Variability in Coastal Ecosystems [Review-article]. *Environmental Science and Technology*, *53*(8), 4020–4029. https://doi.org/10.1021/acs.est.8b03655

Chierici, M., & Fransson, A. (2009). Calcium carbonate saturation in the surface water of the Arctic Ocean: undersaturation in freshwater influenced shelves. *Biogeosciences Discussions*, *6*(3), 4963–4991. https://doi.org/10.5194/bgd-6-4963-2009

Chierici, Melissa, Fransson, A., Lansard, B., Miller, L. A., Mucci, A., Shadwick, E., … Papakyriakou, T. N. (2011). Impact of biogeochemical processes and environmental factors on the calcium carbonate saturation state in the Circumpolar Flaw Lead in the Amundsen Gulf, Arctic Ocean. *Journal of Geophysical Research: Oceans*, *116*(12), 1–12. https://doi.org/10.1029/2011JC007184

Cooper, L. W., McClelland, J. W., Holmes, R. M., Raymond, P. A., Gibson, J. J., Guay, C. K., & Peterson, B. J. (2008a). Flow-weighted values of runoff tracers (δ18O, DOC, Ba, alkalinity) from the six largest Arctic rivers. *Geophysical Research Letters*, *35*(18), 3–7. https://doi.org/10.1029/2008GL035007

Cooper, L. W., McClelland, J. W., Holmes, R. M., Raymond, P. A., Gibson, J. J., Guay, C. K., & Peterson, B. J. (2008). Flow-weighted values of runoff tracers (δ18O, DOC, Ba, alkalinity) from the six largest Arctic rivers. *Geophysical Research Letters*, *35*(18), 3–7. https://doi.org/10.1029/2008GL035007

Core Team, (Beaufort Lagoon Ecosystems LTER). (2020). Beaufort Lagoon Ecosystems LTER. Time series of water column pH; 2018-ongoing ver 1. Environmental Data Initiative. https://doi.org/10.6073/pasta/9305328d0f1ed28fbb2d7cf56c686786.

Craig, P. C., & McCart, P. J. (1975). Classification of Stream Types in Beaufort Sea Drainages between Prudhoe Bay , Alaska , and the Mackenzie Delta, N. W. T., Canada. *Arctic and Alpine Research*, *7*(2), 183–198.

DeGrandpre, M. D., Lai, C. Z., Timmermans, M. L., Krishfield, R. A., Proshutinsky, A., & Torres, D. (2019). Inorganic Carbon and pCO2 Variability During Ice Formation in the Beaufort Gyre of the Canada Basin. *Journal of Geophysical Research: Oceans*, *124*(6), 4017–4028. https://doi.org/10.1029/2019JC015109

Dethier, M. N., & Steneck, R. S. (2001). Growth and persistence of diverse intertidal crusts : survival of the slow in a fast-paced world. *Marine Ecology Progress Series 223*, 89–100.

Diaz-Pulido, G., Anthony, K. R. N., Kline, D. I., Dove, S., & Hoegh-Guldberg, O. (2012). Interactions between ocean acidification and warming on the mortality and dissolution of coralline algae. *Journal of Phycology*, *48*(1), 32–39. https://doi.org/10.1111/j.1529-8817.2011.01084.x

Dickinson, G. H., Ivanina, A. V., Matoo, O. B., Portner, H. O., Lannig, G., Bock, C., … Sokolova, I. M. (2012). Interactive effects of salinity and elevated CO2 levels on juvenile eastern oysters, *Crassostrea virginica*. *Journal of Experimental Biology*, *215*(1), 29–43.

https://doi.org/10.1242/jeb.061481

Dickson, A G, & Millero, F. J. (1987). A comparison of the equilibrium constants for the dissociation of carbonic acid in seawater media. *Deep Sea Research Part A. Oceanographic Research Papers*, *34*(10), 1733–1743. https://doi.org/https://doi.org/10.1016/0198-0149(87)90021-5

Dickson, Andrew G., Sabine, C. L., & Christian, J. R. (2007). *Guide to Best Practices for Ocean CO 2 Measurements*. (8).

Drake, T. W., Tank, S. E., Zhulidov, A. V., Holmes, R. M., Gurtovaya, T., & Spencer, R. G. M. (2018). Increasing Alkalinity Export from Large Russian Arctic Rivers [Research-article]. *Environmental Science and Technology*, *52*(15), 8302–8308. https://doi.org/10.1021/acs.est.8b01051

Dunton, K. H., & Schell, D. M. (1987). Dependence of consumers on macroalgal (*Laminaria solidungula*) carbon in an arctic kelp community: δ13C evidence. *Marine Biology*, *93*(4), 615–625. https://doi.org/10.1007/BF00392799

Dunton, K., & Schell, D. (1986). Seasonal carbon budget and growth of *Laminaria solidungula* in the Alaskan High Arctic. *Marine Ecology Progress Series*, *31*(1977), 57–66. https://doi.org/10.3354/meps031057

Dunton, Kenneth H, Reimnitz, E. R. K., & Schonberg, S. (1982). An Arctic Kelp Community in the Alaskan Beaufort Sea. *Arctic*, *35*(4), 465–484. https://doi.org/10.14430/arctic2355

Dunton, Kenneth H, Reimnitz, E., Schonberg, S., Dunton, K. H., Reimnitz, E. R. K., & Schonberg, S. (1982). An Arctic Kelp Community in the Alaskan Beaufort Sea. *Arctic*, *35*(4), 465–484.

Dupont, S., Ortega-Martínez, O., & Thorndyke, M. (2010). Impact of near-future ocean

acidification on echinoderms. *Ecotoxicology*, *19*(3), 449–462. https://doi.org/10.1007/s10646-010-0463-6

Evans, W., Mathis, J. T., & Cross, J. N. (2014). Calcium carbonate corrosivity in an Alaskan inland sea. *Biogeosciences*, *11*(2), 365–379. https://doi.org/10.5194/bg-11-365-2014

Fabricius, K. E., Cooper, T. F., Humphrey, C., Uthicke, S., De'ath, G., Davidson, J., … Thompson, A. (2012). A bioindicator system for water quality on inshore coral reefs of the Great Barrier Reef. *Marine Pollution Bulletin*, *65*(4–9), 320–332. https://doi.org/10.1016/J.MARPOLBUL.2011.09.004

Fabry, V. J., McClintok, J. B., Mathis, J. T., & Grebmeier, J. M. (2009). Ocean Acidification at High Latitudes: The Bellwether. *Oceanography*, *22*(4), 160–171. Retrieved from http://www.jstor.org/stable/24861032

Farrell, T. M. (1991). Models and Mechanisms of Succession: An Example From a Rocky Intertidal Community. *Ecological Monographs*, *61*(1), 95–113. https://doi.org/10.2307/1943001

Filbee-Dexter, K., & Wernberg, T. (2018). Rise of Turfs: A New Battlefront for Globally Declining Kelp Forests. *BioScience*, Vol. 68, pp. 64–76. https://doi.org/10.1093/biosci/bix147

Frieder, C. A., Gonzalez, J. P., Bockmon, E. E., Navarro, M. O., & Levin, L. A. (2014). Can variable pH and low oxygen moderate ocean acidification outcomes for mussel larvae? *Global Change Biology*, *20*(3), 754–764. https://doi.org/10.1111/gcb.12485

Gangstø, R., Gehlen, M., Schneider, B., Bopp, L., Aumont, O., & Joos, F. (2008). Modeling the marine aragonite cycle: Changes under rising carbon dioxide and its role in shallow water CaCO3dissolution. *Biogeosciences*, *5*(4), 1057–1072. https://doi.org/10.5194/bg-5-1057-

2008

Grime, J. P. (1977). Evidence for the Existence of Three Primary Strategies in Plants and Its Relevance to Ecological and Evolutionary Theory. *The American Naturalist*, *111*(982), 1169–1194. https://doi.org/10.1086/283244

Hall-Spencer, J. M., Rodolfo-Metalpa, R., Martin, S., Ransome, E., Fine, M., Turner, S. M., … Buia, M. C. (2008). Volcanic carbon dioxide vents show ecosystem effects of ocean acidification. *Nature*, *454*(7200), 96–99. https://doi.org/10.1038/nature07051

Harley, C. D. G., Anderson, K. M., Demes, K. W., Jorve, J. P., Kordas, R. L., Coyle, T. A., & Graham, M. H. (2012). EFfects Of Climate Change On Global Seaweed Communities. *Journal of Phycology*, *48*(5), 1064–1078. https://doi.org/10.1111/j.1529-8817.2012.01224.x

Hofmann, G. E., Smith, J. E., Johnson, K. S., Send, U., Levin, L. A., Micheli, F., … Martz, T. R. (2011). High-frequency dynamics of ocean pH: A multi-ecosystem comparison. *PLoS ONE*, *6*(12). https://doi.org/10.1371/journal.pone.0028983

Irving, A. D., Connell, S. D., & Elsdon, T. S. (2004). Effects of kelp canopies on bleaching and photosynthetic activity of encrusting coralline algae. *Journal of Experimental Marine Biology and Ecology*, *310*(1), 1–12. https://doi.org/10.1016/j.jembe.2004.03.020

Jiang, L., Feely, R. A., Carter, B. R., Greeley, D. J., Gledhill, D. K., & Arzayus, K. M. (2015). Global Biogeochemical Cycles saturation state in the global oceans. *Global Biogeochemical Cycles*, *29*(10), 1656–1673. https://doi.org/10.1002/2015GB005198.Received

Johnson, C. R., & Mann, K. H. (1986). The crustose coralline alga, Phymatolithon Foslie, inhibits the overgrowth of seaweeds without relying on herbivores. *Journal of Experimental Marine Biology and Ecology*, *96*(2), 127–146. https://doi.org/10.1016/0022-0981(86)90238-8

Kapsenberg, L., Alliouane, S., Gazeau, F., Mousseau, L., Kapsenberg, L., Alliouane, S., … Gattuso, J. (2017). *Coastal ocean acidification and increasing total alkalinity in the northwestern Mediterranean Sea To cite this version : HAL Id : hal-01534516 Coastal ocean acidification and increasing total alkalinity in the northwestern Mediterranean Sea*. https://doi.org/10.5194/os-13-411-2017

Kapsenberg, L., & Cyronak, T. (2019). Ocean acidification refugia in variable environments. *Global Change Biology*, (December 2018), 1–14. https://doi.org/10.1111/gcb.14730

Karsten, U. (2007). Research note: Salinity tolerance of Arctic kelps from Spitsbergen. *Phycological Research*, *55*(4), 257–262. https://doi.org/10.1111/j.1440-1835.2007.00468.x

Kelley, A. L., & and Lunden, J. J. (2017a). Meta-analysis identifies metabolic sensitivities to ocean acidificationRunning title: Ocean acidification impacts metabolic function. *AIMS Environmental Science*, *4*(5), 709–729. https://doi.org/10.3934/environsci.2017.5.709

Kelley, A. L., & and Lunden, J. J. (2017b). Meta-analysis identifies metabolic sensitivities to ocean acidificationRunning title: Ocean acidification impacts metabolic function. *AIMS Environmental Science*, *4*(5), 709–729. https://doi.org/10.3934/environsci.2017.5.709

King, R. J., & Schramm, W. (1982). Calcification in the Maerl Coralline Alga Phymatolithon-Calcareum - Effects of Salinity and Temperature. *Marine Biology*, *70*(2), 197–204. https://doi.org/10.1007/BF00397685

Konar, B., & Iken, K. (2005). Competitive dominance among sessile marine organisms in a high Arctic boulder community. *Polar Biology*, *29*(1), 61–64. https://doi.org/10.1007/s00300-005-0055-8

Kroeker, K. J., Gambi, M. C., & Micheli, F. (2013). Community dynamics and ecosystem simplification in a high-CO2 ocean. *Proceedings of the National Academy of Sciences*,

110(31), 12721–12726. https://doi.org/10.1073/pnas.1216464110

Kroeker, Kristy J., Kordas, R. L., Crim, R. N., & Singh, G. G. (2010). Meta-analysis reveals negative yet variable effects of ocean acidification on marine organisms. *Ecology Letters*, *13*(11), 1419–1434. https://doi.org/10.1111/j.1461-0248.2010.01518.x

Kroeker, K. J., Micheli, F., & Gambi, M. C. (2012). Ocean acidification causes ecosystem shifts via altered competitive interactions. *Nature Climate Change*, *2*(10), 1–4. https://doi.org/10.1038/nclimate1680

Kuklinski, P., Gulliksen, B., Lønne, O. J., & Weslawski, J. M. (2005). Composition of bryozoan assemblages related to depth in Svalbard fjords and sounds. *Polar Biology*, *28*(8), 619–630. https://doi.org/10.1007/s00300-005-0726-5

Lonthair, J., Ern, R., & Esbaugh, A. J. (2017). The early life stages of an estuarine fish, the red drum (Sciaenops ocellatus), are tolerant to high pCO2. *ICES Journal of Marine Science*, *74*(4), 1042–1050. https://doi.org/10.1093/icesjms/fsw225

Lubchenco, J. (1980). Algal Zonation in the New England Rocky Intertidal Community: An Experimental Analysis. *Ecology*, *61*(2), 333–344. https://doi.org/10.2307/1935192

Lüning, K., & Kadel, P. (1993). Daylength range for circannual rhythmicity in Pterygophora californica (Alariaceae, Phaeophyta) and synchronization of seasonal growth by daylength cycles in several other brown algae. *Phycologia*, *32*(5), 379–387. https://doi.org/10.2216/i0031-8884-32-5-379.1

Mathis, J., Cross, J., Evans, W., & Doney, S. (2015). Ocean Acidification in the Surface Waters of the Pacific-Arctic Boundary Regions. *Oceanography*, *25*(2), 122–135. https://doi.org/10.5670/oceanog.2015.36

Mathis, J. T., Cross, J. N., & Bates, N. R. (2011). Coupling primary production and terrestrial

runoff to ocean acidification and carbonate mineral suppression in the eastern Bering Sea. *Journal of Geophysical Research: Oceans*, *116*(2), 1–24. https://doi.org/10.1029/2010JC006453

Matson, P. G., Washburn, L., Martz, T. R., & Hofmann, G. E. (2014). *Abiotic versus Biotic Drivers of Ocean pH Variation under Fast Sea Ice in McMurdo Sound , Antarctica*. *9*(9). https://doi.org/10.1371/journal.pone.0107239

Mcclelland, J. W., Holmes, R. M., & Dunton, K. H. (2012). *The Arctic Ocean Estuary*. 353–368. https://doi.org/10.1007/s12237-010-9357-3

McClelland, J. W., Townsend-Small, A., Holmes, R. M., Pan, F., Stieglitz, M., Khosh, M., & Peterson, B. J. (2014). River export of nutrients and organic matter from the North Slope of Alaska to the Beaufort Sea. *Water Resources Research*, *50*(2), 1823–1839. https://doi.org/10.1002/2013WR014722

Mccoy, S. J. (2013). Morphology of the crustose coralline alga *Pseudolithophyllum muricatum* (Corallinales, Rhodophyta) responds to 30 years of ocean acidification in the Northeast Pacific. *Journal of Phycology*, *49*(5), 830–837. https://doi.org/10.1111/jpy.12095

Mccoy, S. J., & Kamenos, N. A. (2015). Coralline algae (Rhodophyta) in a changing world: Integrating ecological, physiological, and geochemical responses to global change. *Journal of Phycology*, *51*(1), 6–24. https://doi.org/10.1111/jpy.12262

Meier, W. N., Hovelsrud, G. K., van Oort, B. E. H., Key, J. R., Kavacs, K. M., Michel, C., Haas, C., Grankskog, M. A., Gerland, S., Perovich, D. K., Makshtas, A., and Reist, J. D. (2014). Arctic sea ice in transformation: a review of recent observed changes and impacts on biology and human activity. *Reviews of Geophysics*, *52*(3), 185–217. https://doi.org/10.1002/2013RG000431.Received

Miller, C. A., Pocock, K., Evans, W., & Kelley, A. L. (2018). *An evaluation of the performance of Sea-Bird Scientific ' s SeaFET ™ autonomous pH sensor : considerations for the broader oceanographic community*. 751–768.

Miller, L. A., Burgers, T. M., Burt, W. J., Granskog, M. A., & Papakyriakou, T. N. (2019). Air-Sea CO2 Flux Estimates in Stratified Arctic Coastal Waters: How Wrong Can We Be? *Geophysical Research Letters*, *46*(1), 235–243. https://doi.org/10.1029/2018GL080099

Miller, T. E. (1994). Direct and Indirect Species Interactions in an Early Old-Field Plant Community. *The American Naturalist*, *143*(6), 1007–1025. https://doi.org/10.1086/285646

Morison, J., Kwok, R., Peralta-Ferriz, C., Alkire, M., Rigor, I., Andersen, R., & Steele, M. (2012). Changing Arctic Ocean freshwater pathways. *Nature*, *481*(7379), 66–70. https://doi.org/10.1038/nature10705

Muth, A. F., Bonsell, C. E., and Dunton, K. H. (2020). Life history stage tolerance to seasonal variability in light and salinity in an Arctic kelp (*Laminaria solidungula*). *Submitted*.

Muth, A. F., Esbaugh, A., and Dunton, K. H. (2020). Physiological responses of an Arctic crustose coralline alga (Leptophytum foecundum) to variations in salinity. *Frontiers in Plant Science*

Muth, Arley F., Kelley, A. L., and Dunton, K. H. (2020). High-frequency pH time-series on the nearshore Arctic Ocean reveals pronounced seasonality. *Limnology and Oceanography*

Muth, A. F. (2012). Effects of Zoospore Aggregation and Substrate Rugosity on Kelp Recruitment Success. *Journal of Phycology*, *48*(6), 1374–1379. https://doi.org/10.1111/j.1529-8817.2012.01211.x

Muth, A. F., Graham, M. H., Lane, C. E., & Harley, C. D. G. (2019). Recruitment tolerance to increased temperature present across multiple kelp clades. *Ecology*, *100*(3), 1–7.

https://doi.org/10.1002/ecy.2594

Muth, A. F., Henríquez-Tejo, E. A., & Buschmann, A. H. (2017). Influence of sedimentation in the absence of macrograzers on recruitment of an annual population of *Macrocystis pyrifera* in Metri Bay, Chile. *Austral Ecology*, *42*(7), 783–789. https://doi.org/10.1111/aec.12496

Nelson, W. A. (2009). Calcified macroalgae – critical to coastal ecosystems and vulnerable to change : a review. *Marine and Freshwater Research* 787–801.

Network, M. I. (2016). *On reduced salinity tide-swept circalittoral mixed substrata*. 1–34.

Ortlieb, L., Barrientos, S., & Guzman, N. (1996). Coseismic coastal uplift and coralline algae record in Northern Chile: The 1995 Antofagasta earthquake case. *Quaternary Science Reviews*, *15*(8–9), 949–960. https://doi.org/10.1016/S0277-3791(96)00056-X

Perry, H., Trigg, C., Larsen, K., Freeman, J., Erickson, M., & Henry, R. (2001). Calcium concentration in seawater and exoskeletal calcification in the blue crab, Callinectes sapidus. *Aquaculture*, *198*(3–4), 197–208. https://doi.org/10.1016/S0044-8486(00)00603-7

Raven, J., Caldeira, K., Elderfield, H., Hoegh-Guldberg, O., Liss, P., Riebesell, U., … Watson, A. (2005). Ocean acidification due to increasing. *Coral Reefs*, *12/05*(June), 68. Retrieved from http://eprints.ifm-geomar.de/7878/1/965_Raven_2005_OceanAcidificationDueToIncreasing_Monogr_pubid13120.pdf

Rawlins, M. A., Cai, L., Stuefer, S. L., & Nicolsky, D. (2019). Changing characteristics of runoff and freshwater export from watersheds draining northern Alaska. *Cryosphere*, *13*(12), 3337–3352. https://doi.org/10.5194/tc-13-3337-2019

Rember, R. D., & Trefry, J. H. (2004). Increased concentrations of dissolved trace metals and organic carbon during snowmelt in rivers of the alaskan arctic. *Geochimica et*

Cosmochimica Acta, *68*(3), 477–489. https://doi.org/10.1016/S0016-7037(03)00458-7

Robbins, L. L., Hansen, M. E., Kleypas, J. A., & Meylan, S. C. (2010). CO2calc: A User-Friendly Seawater Carbon Calculator for Windows, Mac OS X, and iOS (iPhone). In *Open-File Report*. https://doi.org/10.3133/ofr20101280

Schneider, A., Wallace, D. W. R., & Körtzinger, A. (2007). Alkalinity of the Mediterranean Sea. *Geophysical Research Letters*, *34*(15), 1–5. https://doi.org/10.1029/2006GL028842

Schoenrock, K. M., Bacquet, M., Pearce, D., Rea, B. R., Schofield, J. E., Lea, J., … Kamenos, N. (2018). Influences of salinity on the physiology and distribution of the Arctic coralline algae, *Lithothamnion glaciale* (Corallinales, Rhodophyta). *Journal of Phycology*, *54*(5), 690–702. https://doi.org/10.1111/jpy.12774

Schoenrock, K., Vad, J., Muth, A., Pearce, D. M., Rea, B. R., Schofield, J. E., & Kamenos, N. A. (2018). Biodiversity of Kelp Forests and Coralline Algae Habitats in Southwestern Greenland. *Diversity*, 1–20. https://doi.org/10.3390/d10040117

Sellmann, P. V., Delaney, A. J., Chamberlain, E. J., & Dunton, K. H. (1992). Seafloor temperature and conductivity data from Stefansson Sound, Alaska. *Cold Regions Science and Technology*, *20*(3), 271–288. https://doi.org/10.1016/0165-232X(92)90034-R

Semiletov, I., Pipko, I., Gustafsson, Ö., Anderson, L. G., Sergienko, V., Pugach, S., … Shakhova, N. (2016). Acidification of East Siberian Arctic Shelf waters through addition of freshwater and terrestrial carbon. *Nature Geoscience*, *9*(5), 361–365. https://doi.org/10.1038/ngeo2695

Sievers, J., Sørensen, L. L., Papakyriakou, T., Else, B., Sejr, M. K., Søgaard, D. H., & Barber, D. (2015). Winter observations of CO 2 exchange between sea ice and the atmosphere in a coastal fjord environment. *The Cryosphere* 1701–1713. https://doi.org/10.5194/tc-9-1701-

2015

Takeshita, Y., Frieder, C. A., Martz, T. R., Ballard, J. R., Feely, R. A., Kram, S., … Smith, J. E. (2015). Including high-frequency variability in coastal ocean acidification projections. *Biogeosciences*, *12*(19), 5853–5870. https://doi.org/10.5194/bg-12-5853-2015

Tank, S. E., Raymond, P. A., Striegl, R. G., McClelland, J. W., Holmes, R. M., Fiske, G. J., & Peterson, B. J. (2012). A land-to-ocean perspective on the magnitude, source and implication of DIC flux from major Arctic rivers to the Arctic Ocean. *Global Biogeochemical Cycles*, *26*(4), 1–15. https://doi.org/10.1029/2011GB004192

Tynan, E., Clarke, J. S., Humphreys, M. P., Ribas-Ribas, M., Esposito, M., Rérolle, V. M. C., … Achterberg, E. P. (2016). Physical and biogeochemical controls on the variability in surface pH and calcium carbonate saturation states in the Atlantic sectors of the Arctic and Southern Oceans. *Deep-Sea Research Part II: Topical Studies in Oceanography*, *127*, 7–27. https://doi.org/10.1016/j.dsr2.2016.01.001

Wai, T. C., & Williams, G. A. (2006). Effect of grazing on coralline algae in seasonal, tropical, low-shore rock pools: Spatio-temporal variation in settlement and persistence. *Marine Ecology Progress Series*, *326*, 99–113. https://doi.org/10.3354/meps326099

Weingartner, T. J., Danielson, S. L., Potter, R. A., Trefry, J. H., Mahoney, A., Savoie, M., … Sousa, L. (2017). Circulation and water properties in the landfast ice zone of the Alaskan Beaufort Sea. *Continental Shelf Research*, *148*(March), 185–198. https://doi.org/10.1016/j.csr.2017.09.001

Wernberg, T., Bennett, S., Babcock, R. C., Bettignies, T. De, Cure, K., Depczynski, M., … Tuya, F. (2015). Temperate Marine Ecosystem. *Science*, *353*(6295), 169–172. https://doi.org/10.1126/science.aad8745

Wickett, K., & Caldiera. (2003). Anthropogenic carbon and ocean pH. *Nature*, *425*(September), 365. https://doi.org/10.1038/425365a

Wiencke, C., Clayton, M. N., Gómez, I., Iken, K., Lüder, U. H., Amsler, C. D., … Dunton, K. (2006). Life strategy, ecophysiology and ecology of seaweeds in polar waters. *Reviews in Environmental Science and Bio/Technology*, *6*(1–3), 95–126. https://doi.org/10.1007/s11157-006-9106-z

Wilce, R. T., & Dunton, K. H. (2014). The boulder Patch (North Alaska, Beaufort Sea) and its benthic algal flora. *Arctic*, *67*(1), 43–56. https://doi.org/10.14430/arctic4360

Wilson, S., Blake, C., Berges, J. A., & Maggs, C. A. (2004). Environmental tolerances of free-living coralline algae (maerl): implications for European marine conservation. *Biological Conservation*, *120*(2), 279–289. https://doi.org/https://doi.org/10.1016/j.biocon.2004.03.001

Yamamoto-Kawai, M., McLaughlin, F. A., Carmack, E. C., Nishino, S., & Shimada, K. (2009). Aragonite Undersaturation in the Arctic. *Science*, *326*(November), 1098–1100. https://doi.org/10.1126/science.1174190

Yamamoto-kawai, M., & Tanaka, N. (2005). *Freshwater and brine behaviors in the Arctic Ocean deduced from historical data of D 18 O and alkalinity (1929 – 2002 A . D .)*. *110*, 1–16. https://doi.org/10.1029/2004JC002793

Zhang, J. (2005). Warming of the arctic ice-ocean system is faster than the global average since the 1960s. *Geophysical Research Letters*, *32*(19), 1–4. https://doi.org/10.1029/2005GL024216